SYMPLECTIC ELASTICITY APPROACH FOR EXACT BENDING SOLUTIONS OF RECTANGULAR THIN PLATES

CUI SHUANG

MASTER OF PHILOSOPHY
CITY UNIVERSITY OF HONG KONG
November 2007

CUI SHUANG

SYMPLECTIC ELASTICITY APPROACH FOR EXACT BENDING SOLUTIONS OF RECTANGULAR THIN PLATES

MPhil
2007

CityU

CITY UNIVERSITY OF HONG KONG
香港城市大學

SYMPLECTIC ELASTICITY APPROACH FOR EXACT BENDING SOLUTIONS OF RECTANGULAR THIN PLATES
辛彈性力學方法在矩形薄板的彎曲精確解上的應用

Submitted to
Department of Building and Construction
建築學系
in Partial Fulfillment of the Requirements
for the Degree of Master of Philosophy
哲學碩士學位

by

Cui Shuang
崔爽

November 2007
二零零七年十一月

Abstract

This thesis presents a bridging analysis for combining the modeling methodology of quantum mechanics/relativity with that of elasticity. Using the symplectic method that is commonly applied in quantum mechanics and relativity, a new symplectic elasticity approach is developed for deriving exact analytical solutions to some basic problems in solid mechanics and elasticity that have long been stumbling blocks in the history of elasticity. Specifically, the approach is applied to the bending problem of rectangular thin plates the exact solutions for which have been hitherto unavailable. The approach employs the Hamiltonian principle with Legendre's transformation. Analytical bending solutions are obtained by eigenvalue analysis and the expansion of eigenfunctions. Here, bending analysis requires the solving of an eigenvalue equation, unlike the case of classical mechanics in which eigenvalue analysis is required only for vibration and buckling problems. Furthermore, unlike the semi-inverse approaches of classical plate analysis that are employed by Timoshenko and others in which a trial deflection function is predetermined, such as Navier's solution, Levy's solution, or the Rayleigh-Ritz method, this new symplectic plate analysis is completely rational and has no guess functions, yet it renders exact solutions beyond the scope of the semi-inverse approaches. In short, the symplectic plate analysis that is developed in this paper presents a breakthrough in analytical mechanics, and access into an area unaccountable by Timoshenko's plate theory and other, similar theories. Here,

examples for rectangular plates with 21 boundary conditions are solved, and the exact solutions are discussed. Specially, a chapter on benchmarks of uniformly loaded corner-supported rectangular plate is also presented. Comparison of the solutions with the classical solutions shows excellent agreement. As the derivation of this new approach is fundamental, further research can be conducted not only for other types of boundary conditions, but also for thick plates, vibration, buckling, wave propagation, and so forth. Remarks and directions for future work are given in the conclusion.

Acknowledgements

I would like to express my great gratitude and respect to my supervisor, Dr. C. W., Lim, for his patient guidance and encouragement throughout the course of my research. I would also like to thank Dr. Lim for his close monitoring on the progress of my research and his intensive training on my critical and philosophical thinking. It is not only beneficial to the works of this thesis but also widened my eyes to the world of knowledge and trained me the positive attitude to problem solving. It is definitely important for my future research work. Without his encouragement and directions, it is not possible for me to complete this thesis.

I would like to give my sincere thanks to Professor Yao Weian for his invaluable suggestions, discussions and criticisms on my works which are the most important factors to the success of this research. His knowledge in the field of Simplectic Elasticity was definitely important in the inspiration of my ideas on the extension of the Simplectic Elasticity approach to thin plate bending problems.

I am also greatly grateful to my friend Walter Sun and the departmental colleague for their moral support to me. With these supports, I can overcome the frustrations in my research.

I would also thank Dr. Mike Poole for his assistance in proof reading.

Finally, I would like to acknowledge with thanks to City University of Hong Kong and the University Grants Committee (UGC) of Hong Kong SAR for providing the Postgraduate Studentship during my study period.

Table of Contents

List of Figures

List of Tables

Chapter 1 Introduction

1.1 Background

Rectangular thin plates are initially flat structural members that are bounded by two parallel planes. The load-carrying action of a plate is similar, to a certain extent, to that of a beam or cable. Thus, plates can be approximated by a grid work of an infinite number of beams or by a network of an infinite number of cables, depending on the flexural rigidity of the structures. The two-dimensional structural action of plates results in lighter structures, and therefore offers numerous economic advantages. The plate, originally flat, develops shear force and bending and twisting moments to resist transverse loads. Because the loads are generally carried in both directions and because the twisting rigidity in isotropic plates is quite significant, a plate is considerably stiffer than is a beam of comparable span and thickness. Therefore, thin plates combine a light weight and an efficient form with a high load-carrying capacity, economy, and technological effectiveness.

Because of the distinct advantages that are discussed above, thin plates are extensively used in all fields of engineering. Plates are used in, for example, architectural structures, bridges, hydraulic structures, pavements, containers, airplanes, missiles, ships, instruments, and machine parts.

1.2 History of research on thin plate bending

As plates have such important applications, research on plates is abundant and plate bending has been a subject of study in solid mechanics for more than a century. Here gives a brief review of the history of research on thin plate bending. This section will be divided into two parts. In part one: previous research work is reviewed for the plates with different boundary condition. While the approximation methods for solving the bending problems of the plates are introduced in part two.

1.2.1 Thin plates with various boundary conditions

Firstly, analytical and numerical methods that have been developed to solve the bending problems of a rectangular thin plate under various boundary conditions are reviewed, and are shown in the following sub-sections.

1.2.1.1 Plates with two opposite sides simply supported

Early in 19th century, Navier (1823) used the double trigonometric series to obtain the first solution to the problem of the bending of simply supported rectangular plates. Lévy (1899) suggested an alternative solution for the bending of rectangular plates that have two opposite edges simply supported. The transformation of the double series of the Navier solution (Navier, 1823) into the simple series of Lévy's solution (Lévy, 1899) was presented by Estanave (1900). Later, Nádai (1925) simplified Levy's solution (Lévy, 1899) for uniformly loaded and simply supported rectangular plates. A more convenient form to satisfy some particular boundary conditions was suggested by Papkovitch (1941). The deflection

of plates by a concentrated load was investigated experimentally by Bergsträsser (1928), which can also be found from the work of Newmark and Lepper (1939). The bending problems of a plate with simply supported opposite sides are the easiest problems to solve, and exact solutions are available for this type of plate.

1.2.1.2 Plates with all sides built in

The first numerical results for calculating stresses and deflections in clamped rectangular plates were obtained by Koialovich (1902) in his doctorate dissertation. Later, Boobnoff (1902, 1914) obtained the deflections and moments in uniformly loaded rectangular plates with clamped edges. Approximately during the same period of 1913 to 1915 the problem of bending of the clamped rectangular plate was addressed in the remarkable dissertation by Hencky (1913) and in papers by Happel (1914) and Galerkin (1915 b). In these three works rectangular plates with both the uniform load and the concentrated load at the centre were considered.

All authors in above mentioned literature used the superposition method. But with the systems of the trigonometric functions that complete different from Koialovich (1902) and Boobnoff (1902, 1914), the justification of the traditional way of solving the infinite system by the method of reduction was obtained later by Leitz (1917) and March (1925). Hencky's solution (Hencky, 1913) was independently obtained later by Sezawa (1923), Marcus (1932) and Inglis (1925). It appeared that even one term in each of Fourier series with only integral satisfaction of the boundary condition for the slope can provide a reasonable value for the deflection at the centre. Hencky's method (Hencky, 1913) was well known to converge quickly but does pose some slightly tricky issues with regard to programming due to over/underflow problems in the evaluation of hyperbolic trigonometric functions

with large arguments. While Szilard (1974) developed the double cosine series method which is devoid of the over/underflow issue but is known to converge very slowly. An experimental investigation for that problem was also done by Laws (1937).

Other solutions for the plate with all edges clamped under various cases of loading are due to Nádai (1925), Evans (1939), Young (1940), Weinstein and Rock (1944), Funk and Berger (1950), Grinberg (1951), Girkmann and Tungl (1953).

More recently, Meleshko (1997) addresses the fascinating long history of the classical problem of bending of a thin rectangular elastic plate with clamped edges by uniform pressure and reviewed various mathematical and engineering approaches for that problem. Although research on the clamped plate is numerous, only numerical approaches have been developed up to now.

1.2.1.3 Corner supported rectangular plates

Some earliest attempts on corner supported rectangular thin plates were due to Nádai (1922) and Marcus (1932), respectively in the 1920s and 1930s, who presented their solutions by means of numerical methods for a specific Poisson's ratio. A couple of decades later, Galerkin (1953) attempted to solve a rectangular plate with four edges elastically supported. By taking the stiffness of support to approach zero, he presented asymptotic bending solutions for corner supported plates with free edges. The earliest comprehensive analyses was presented by Lee and Ballesteros (1960) who adopted a semi-inverse approach by using a predetermined trial function to approximate the plate deflection which similar to that of Timoshenko and Woinowsky-Krieger (1959) while the unknown constants were

determined by the boundary conditions. The trial functions satisfied the geometric boundary conditions at the outset while the natural boundary conditions were enforced in an integral sense along the boundary. Subsequently, Pan (1961) proved that the results of Lee and Ballesteros (1960) were in reasonable agreement with that of Galerkin (1953).

Later in the end of 1980s, Shanmugam *et al*. (1988, 1989) used the polynomial deflection function to solve the corner supported plates with rhombic (Shanmugam *et al*.1988) and triangular shapes (Shanmugam *et al*.1989). The vibration of corner supported thick Mindlin plate was investigated by Kitipornchai *et al*. (1994) who employed a hybrid numerical approach combining the Rayleigh-Ritz method and the Lagrange multiplier in order to impose zero lateral deflection constraints at plate corners. More recently, Wang *et al.* (2002) discussed the problems and remedy of the Ritz method in solving the corner supported rectangular plates under transverse uniformly distributed load. They showed that the Ritz method fails to predict accurate stress resultants and, in particular, the twisting moment and shear forces. Because the natural boundary conditions are not completely satisfied, they proposed to use the Lagrange multiplier method to ensure the satisfaction of the natural boundary conditions and a surface-smoothing technique to post-process the solution to eliminate the oscillations in the distribution of stress resultants. This type of plate is the most difficult one to deal with and no exact solutions exit.

1.2.1.4 Cantilever plates

Cantilever plates are another important structural element. Holl (1937) firstly used the method of finite difference to obtain a solution of a cantilever plate with concentrated load acting at the middle of the long free edge. The ratio of the clamped

edge to the adjacent free edge of the plate is equal to four. Later, Jaramillo (1950) made further calculations of an infinite cantilever plate by placing the concentrated load respectively at distance 1/4, 1/2, 3/4 of the depth of the plate. With the finite difference method, Nash (1952) extended the bending solutions for rectangular cantilever plate with uniformly loaded condition. This problem is also solved by Barton (1948), Macneal (1951), Livesly and Birchall (1956) separately with the finite difference method. Besides the finite difference method, point-matching is another popular approach which was developed by Nash (1952) for the bending problem of the cantilever plate. Algebraic polynomial and hyperbolic-trigonometric series were used by Nash (1952) for the cantilever plate. Leissa and Niedenfuhr (1962 a) presented the solution for the uniformly loaded cantilevered square plate using two approaches in their paper: point matching, using an algebraic-trigonometric polynomial, and a Rayleigh-Ritz minimal-energy formulation.

Besides the approaches mentioned above, Shu and Shih (1957) were the first to use the generalized variational principle for the elastic thin plate. They attempted to get a solution of the same problem solved by Nash (1952). Later, this variational principle was also used by Plass *et al.* (1962) to work out a solution for a uniformly loaded square cantilever plate. Recently, with the advent of computer the method of finite elements was used to track this old problem. Different from the above approximate methods, Chang (1979, 1980) derived the analytical exact solution for bending of both the uniformly loaded and concentrated loaded cantilever rectangular plates by using the idea of generalized simply supported edge together with the method of superposition. Both analytical exact solution and numerical approximate solution are available for the cantilever plates.

1.2.1.5 Other types of plates

The problem of the uniformly loaded square plate with two adjacent edges free and the others clamped was solved by Huang and Conway (1952). This involved a skillful superposition of five problems and the partial solution of an infinite set of simultaneous equations. Yeh (1954) employed the Rayleigh-Ritz method to generalize this same problem by including the reaction due to an elastic foundation. Leissa and Niedenfuhr (1962 b) established the solutions for the problems of a square plate with two adjacent edges free and the others clamped or simply supported subjected to either a uniform transverse loading or a concentrated force at the free corner by the point-matching approach. Exact solution is unavailable for the plates with such boundary conditions.

A plate with some edges simply supported and the others clamped can be solved by superposing appropriate Lévy's solutions (Lévy, 1899) for a simply supported plate: one corresponding to the given load and the others corresponding to fixed end moments which are adjusted such that the net normal slopes are zero. Many such solutions were presented in elaborate detail by Timoshenko and Woinowsky-Krieger (1959)

In recent years, with the popularity of the approximate methods, these types of plates are always solved by boundary collection method (Timoshenko and Woinowsky-Krieger, 1959; Finlayson, 1972; Kolodziej, 1987; Johnson, 1987; Hutchinson, 1991), finite element method (Courant, 1943; Turner *et al.*, 1956; Argyris *et al.*, 1964; Gallagher, 1975; Zienkiewicz, 1977;Hughes, 1987), Ritz method (Ritz, 1909; Washizu, 1968; Szilard, 1974) etc. Details of these methods and their limitations will be presented in the next session.

1.2.2 Approximate methods for the solution of plate bending

According to the above literature review, the analytical exact solutions are only applicable to some simple cases. If these conditions are more complicated, the classical analytical methods become increasingly tedious or even impossible, in such cases, approximate methods are the only approaches that can be employed for the solution of practically important plate bending problems. These approximate methods may be divided into two groups: indirect methods and direct methods.

Indirect methods enable us to obtain numerical values of unknown functions by direct discretization of the governing differential equation of the corresponding boundary value problem. Well-known methods such as the finite difference method, the method of boundary collocations, the boundary element method, and the Galerkin method are belong to that category.

Direct methods use the variational principle for determining numerical fields of unknown functions, avoiding the differential equations of the plate. Ritz method and finite element method are the direct methods.

1.2.2.1 Finite difference method (FDM)

This is a method of the solution of boundary value problems for differential equations (Salvadori and Baron, 1967; Wang, 1969). A set of linear algebraic equations written for every nodal point within the plate are obtained.

The limitations of this method:

- It requires mathematically trained operators;
- It requires more work to achieve complete automation of the procedure in

program writing;

- The matrix of the approximating system of linear algebraic equations if asymmetric, causing some difficulties in numerical solution of this system;
- An application of the FDM to domains of complicated geometry may run into serious difficulties.

1.2.2.2 The boundary collocation method (BCM)

The BCM solution (Finlayson, 1972; Hutchinson, 1991; Timoshenko and Woinowsky-Krieger, 1959; Kolodziej, 1987; Johnson, 1987) is expressed as a sum of known solutions of the governing differential equation, and boundary conditions are satisfied at selected collocation points on the boundary. Thus, the obtained solution satisfies the governing differential equation exactly and the prescribed boundary conditions only approximately.

The limitations of the BCM:

- It is limited to linear problems;
- A complete set of solutions to the differential equations must be known;
- The matrix is full and sometimes ill-conditioned, and a known arbitrariness exists in the selection of the collocation points.

1.2.2.3 The boundary element method (BEM)

The BEM (Tottenham, 1979; Hartmann, 1991; Brebbia *et al.*,1984; Banerjee and Butterfield, 1981; Ventsel, 1997; Krishnasamy *et al.*, 1990) reduces a given boundary value problem for a plate, in the form of partial differential equations to

the integral equations over the boundary of the plate. Then, the BEM proceeds to obtain an approximate solution by solving these integral equations.

The limitations of BEM:

- The method requires that a fundamental solution of a governing differential equation or Green's function be represented in the explicit analytical form. For the plate bending problems discussed, the fundamental solution is of the very simple analytical form. If the above mentioned fundamental solution is more awkward than for plate bending problems, the BEM formulation and numerical approximation becomes less efficient.
- The matrix of the approximating system of linear algebraic equations is full matrix, which causes some difficulties in its numerical implementation.

1.2.2.4 The Galerkin method

Galerkin method (Galerkin, 1915a) is a class of methods for converting a differential equation to a discrete problem. In principle, it is the equivalent of applying the method of variation to a function space, by converting the equation to a weak formulation.

The limitation of the Galerkin method:

- It is difficult to find the trial functions for some boundary conditions.

1.2.2.5 The Ritz method

The Ritz method (Ritz, 1909; Washizu, 1968; Szilard, 1974) is among the variational methods that are commonly used as approximate methods for the solutions of various boundary value problems in mechanics.

The limitation of the Ritz method:

- The Ritz method can be applicable only to simple configurations of plates (rectangular, circular, etc.), because of the complexity of selecting the Ritz trial functions for domains of complex geometry.
- The Ritz method approximation results in the full matrix of linear algebraic equations that produces some difficulties in its numerical implementation.

1.2.2.6 The finite element method (FEM)

According to the FEM (Courant, 1943; Turner *et al.*, 1956; Argyris *et al.*, 1964; Gallagher, 1975; Zienkiewicz, 1977; Hughes, 1987), a plate is discretized into a finite number of elements which connected at their nodes and along interelement boundaries. The equilibrium and compatibility conditions must be satisfied at each node and along the boundaries between finite elements. To determine the above-mentioned unknown functions at nodal points, variational principle is applied. As a result, a system of algebraic equations is obtained. Its solution determines the state of stress and strain in a given plate.

The limitation of FEM:

- The FEM requires the use of powerful computers of considerable speed and storage capacity.
- It is difficult to ascertain the accuracy of numerical results when large structural systems are analyzed.
- The method is poorly adapted to a solution of the so-called singular problems (e.g., plates and shells with cracks, corner points, discontinuity internal actions, etc.), and of problems for unbounded domains,

- The method presents many difficulties associated with problems of C^1 continuity and nonconforming elements in plate (and shell) bending analysis.

1.2.2.7 Closure

Although the numerical methods developed well in the history, analytical exact solutions are essential to develop. In addition, analytical exact solutions enable one to gain insight view into the variation of stresses and strains with basic shape and property changes, and provide an understanding of the physical plate behavior under an applied loading. And they can be used as a basis for incisively evaluating the results of approximate solutions through quantitative comparisons and order-of-magnitude bounds. In this study, the symplectic method is used to derive the exact solution. It is applicable to different kinds of rectangular thin plates and the procedure is identical with all the 21 boundary conditions.

1.3 History of symplectic method

Symplecticity is a mathematical concept of geometry. A symplectic group is a classical group and it was first used and defined by Weyl (1939) by borrowing a term from the Greek. The theory on symplectic geometry can be referred to Koszul and Zou (1986). Since then, the use of symplectic space has been exploited in a number of fields in physics and mathematics for many years particularly in relativity and gravitation (Kauderer, 1994), and classical and quantum mechanics (De Gosson, 2001) including the famous Yang-Mills field theory (Krauth and Staudacher, 2000), etc. In elasticity and Hamiltonian mechanics, the computational approach for

symplectic Hamiltonian systems including fluid dynamics was first developed by Feng and his associates. (Feng, 1985, 1986a, 1986b; Qin, 1990; Feng and Qin, 1991). Beginning from 1984, Feng proposed symplectic algorithms based on symplectic geometry for Hamiltonian systems with finite and infinite dimensions, and on dynamical systems with Lie algebraic structures, such as contact systems, source free systems, etc, via the corresponding geometry and Lie group. These algorithms are superior to conventional algorithms in many practical applications, such as celestial mechanics, molecular dynamics, etc. The contribution of Feng and his associates (Feng, 1985, 1986a, 1986b; Qin, 1990; Feng and Qin, 1991) in symplectic algorithm was particularly significant and important as stated in a memorial article dedicated to him by Lax (1993).

Unlike Feng and his associates who emphasized on computational algorithm, Zhong, Yao and their colleagues (zhong, 1991,1992; Yao and Yang, 2001; Yao *et al.* 2007) developed a new analytical symplectic elasticity approach for deriving exact analytical solutions to some basic problems in solid mechanics and elasticity since the early 1990s. These problems have long been bottlenecks in the development of elasticity. It is based on Hamiltonian principle with Legendre's transformation and analytical solutions could be obtained by expansion of eigenfunctions. It is rational and systematic with a clearly defined, step-by-step derivation procedure. The advantage of symplectic approach with respect to the classical approach by semi-inverse method is at least three-fold. First, the symplectic approach alters the classical practice and concept of solution methodology and many basic problems previously unsolvable or too complicated to be solved can hence be resolved accordingly. For instance, the conventional approach in plate and shell theories by Timoshenko has been based on the semi-inverse method with trial 1D or 2D

displacement functions, such as Navier's method (Navier,1823) and the Lévy's (Lé vy, 1899) method for plates. The trial functions, however, do not always exist except in some very special cases of boundary conditions such as plates with two opposite sides simply supported. Using the symplectic approach, trial functions are not required. Second, it consolidates the many seemingly scattered and unrelated solutions of rigid body movement and elastic deformation by mapping with a series of zero and nonzero eigenvalues. Last but not least, the Saint-Venant problems for plain elasticity and elastic cylinders can be described in a new system of equations and solved. The difficulty of satisfying end boundary conditions in conventional problems which could only be covered using the Saint-Vanent principle can also be solved.

1.4 Objective of study

The research on bending solutions of rectangular thin plates by symplectic elasticity approach is mainly contributed by Yao *et al.* (2007). In that book, the eigenvalue, eigenvector and the general expression for the bending solution have been established for plates with opposite sides simply supported, opposite sides clamped and opposite sides free. However, the illustration of the symplectic treatment on the x direction is not enough and the plates with other types of boundary conditions such as plates with opposite sides unsymmetrical are not mentioned in this book. In addition, exact bending results are available only for two cases of plates (plates with all edges simply supported and plates with all edges clamped) in that book. In order to further complete the research on symplectic approach for rectangular thin plate bending, this thesis establishes the exact bending

solutions for 21 boundary conditions with numerous results listed in the tables. Convergence and comparison studies are conducted to test the stability and reliability of this approach.

1.5 Scope of study

The thesis begins with a brief review of some of the previous works on the rectangular thin plate bending problems and the development of symplectic method. In Chapter 2, the basic formulation of symplectic method and Hamiltonian system is introduced; general symplectic solution for rectangular thin plates is established (Yao *et al.*, 2007). There are totally 21 boundary conditions for rectangular plates with different combinations of clamped, fixed and free edges. The plates are divided into four categories: plates with two opposite sides simply supported, plates with two opposite sides clamped, plates with two opposite sides unsymmetrical and corner supported plates. These cases will be discussed in Chapter 3 to Chapter 6 consequently. Based on the research work of Yao *et al.* (2007), the exact bending solutions are newly developed.

In Chapter 3, the problems considered are plates with two opposite sides simply supported. It is a well developed subject and symplectic solution is presented here to verify the validity of the method.

The symplectic solutions for plates with two opposite sides clamped, plates with two opposite sides unsymmetrical are derived in Chapter 4 and Chapter 5 respectively. The convergence study for symplectic method is performed for these

two cases and the results are compared with those calculated by finite element software ABAQUS®.

The corner supported rectangular plate presented in Chapter 6 is a very popular structural element and its bending problem is the most difficult one among these 21cases. More treatments are carried out on the boundary with symplectic method. Convergency and comparison studies are conducted and the contour plots are presented to give a bird view of the overall results.

Chapter 7 summarizes the results and explores the possibilities of future researches and applications in the related problems.

Chapter 2 Fundamental Formulation of Symplectic Elasticity

2.1 Introduction

In this chapter, a set of fundamental equations for the classical bending theory of thin plate is presented. The Pro-Hellinger-Reissner variational principle and the multi-variational principle are then established for bending of thin plates. The Hamiltonian system and its symplectic geometry theory are directly applied to the thin plate bending problem to derive a system of Hamiltonian symplectic solution. Consequently the thin plate bending problem can be analyzed using a rational Hamiltonian approach. This part of research is from Yao *et al*. (2007) and shown here for the completeness of the current study.

2.2 Symplectic formulation

Thin plate is a plate with a ratio of thickness to minimum characteristic dimension smaller than 1/100 in general. The neutral plane is normally assigned as the xy-plane with the positive direction of the z-axis pointing downwards. If the deflection of the plate is considerably smaller than the plate thickness, it is a small deflection problem.

The basic assumption of small deflection theory of thin plate was first established by Kirchhoff and hence it is called the Kirchhoff Hypothesis. It states that a straight line normal to the neutral plane remains straight and normal to the deflected plane after deformation. Besides, the length of line is invariant before and after deformation which is commonly known as transverse inextensibility.

According to this hypothesis, it can be derived that

$$\gamma_{xz} = \gamma_{yz} = \varepsilon_z = 0 \tag{2.1}$$

Where γ_{xz} γ_{yz} are shear train and ε_z is the normal strain. It can also be deduced that there is only transverse displacement w during bending for every point on the neutral plane. Bending occurs without displacements along the x-direction and y-direction on the neutral plane.

Hence

$$(u)_{z=0} = (v)_{z=0} = 0, \quad (w)_{z=0} = w(x, y) \tag{2.2}$$

Where u, v are the displacement at the x and y directions respectively. As $\varepsilon_z = 0$, the displacement w is independent of the transverse z-coordinate and it is only a function of the in-plane coordinates x and y, or

$$w = w(x, y) \tag{2.3}$$

As we have known

$$\gamma_{xz} = \gamma_{yz} = 0 \tag{2.4}$$

And the train-displacement relationship is given by

$$\left.\begin{aligned} &\varepsilon_x = \frac{\partial u}{\partial x}; \qquad \varepsilon_y = \frac{\partial v}{\partial y}; \qquad \varepsilon_z = \frac{\partial w}{\partial z}; \\ &\gamma_{xy} = \frac{\partial u}{\partial y} + \frac{\partial v}{\partial x}; \quad \gamma_{xz} = \frac{\partial u}{\partial z} + \frac{\partial w}{\partial x}; \quad \gamma_{yz} = \frac{\partial v}{\partial z} + \frac{\partial w}{\partial y}; \end{aligned}\right\} \tag{2.5}$$

Where It can be deduced that

$$\frac{\partial u}{\partial z} = -\frac{\partial w}{\partial x}, \quad \frac{\partial v}{\partial z} = -\frac{\partial w}{\partial y} \tag{2.6}$$

From Eq. (2.2) and Eq. (2.6)

$$u = -z\frac{\partial w}{\partial x}, \quad v = -z\frac{\partial w}{\partial y} \tag{2.7}$$

Applying the geometric relations (2.5) yields

$$\varepsilon_x = -z\kappa_x, \quad \varepsilon_y = -z\kappa_y, \quad \gamma_{xy} = 2z\kappa_{xy} \tag{2.8}$$

Where γ_{xz} γ_{yz} and γ_{xy} are the shear stains, ε_x ε_y and ε_z are the normal stresses.

$$\kappa_x = \frac{\partial^2 w}{\partial x^2}, \quad \kappa_y = \frac{\partial^2 w}{\partial y^2}, \quad \kappa_{xy} = -\frac{\partial^2 w}{\partial x \partial y} \tag{2.9}$$

are curvature and twisting curvature of the plate, respectively. Eq. (2.9) shows the relationship between the curvature and deflection.

Since the normal stress perpendicular to the neutral plane is considerably small and negligible as compared with σ_x, σ_y and τ_{xy}, the stress-strain relations can be simplified as

$$\left.\begin{aligned} \sigma_x &= \frac{E}{1-\nu^2}\left(\varepsilon_x + \nu\varepsilon_y\right) \\ \sigma_y &= \frac{E}{1-\nu^2}\left(\varepsilon_y + \nu\varepsilon_x\right) \\ \tau_{xy} &= \frac{E}{2\left(1+\nu\right)}\gamma_{xy} \end{aligned}\right\} \tag{2.10}$$

Where σ_x, σ_y, σ_z are the normal stresses, ν is Poisson's ratio, τ_{xy} is the shear stress E is the Yong's modulus and G is the shear modulus. Substituting Eq. (2.8) into Eq. (2.10) yields

$$\left.\begin{aligned}\sigma_x &= -\frac{Ez}{1-\nu^2}\left(\kappa_x + \nu\kappa_y\right)\\ \sigma_y &= -\frac{Ez}{1-\nu^2}\left(\kappa_y + \nu\kappa_x\right)\\ \tau_{xy} &= \frac{Ez}{1+\nu}\kappa_{xy}\end{aligned}\right\} \tag{2.11}$$

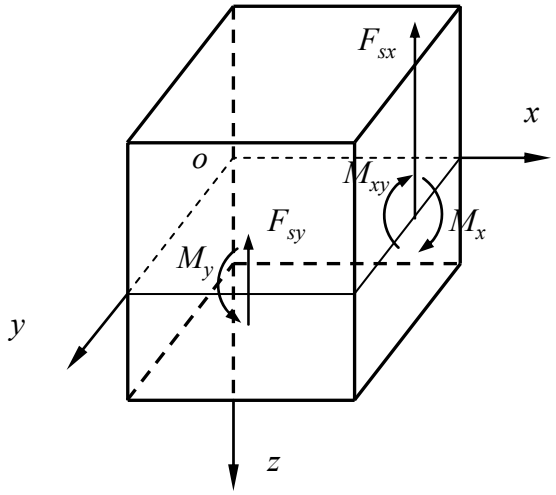

Fig. 2.1 Directions of positive internal forces on plate

The normal stresses on the side of element result in a couple of forces (i.e. bending moment). Figure 2.1 shows the direction of positive internal forces.

The moment per unit length is

$$\left.\begin{aligned}M_x &= \int_{-h/2}^{h/2}\left(-\sigma_x z\right)dz = D\left(\kappa_x + \nu\kappa_y\right)\\ M_y &= \int_{-h/2}^{h/2}\left(-\sigma_y z\right)dz = D\left(\kappa_y + \nu\kappa_x\right)\end{aligned}\right\} \tag{2.12}$$

where D is the flexural rigidity (bending stiffness) of the plate and can be expressed as

$$D = \frac{Eh^3}{12\left(1-\nu^2\right)} \tag{2.13}$$

Where h is the plate thickness. The shear stresses τ_{xy} also result in a couple (i.e. torsional moment) and the moment per unit length is

$$M_{xy} = \int_{-h/2}^{h/2} \tau_{xy} z dz = D(1-\nu)\kappa_{xy} \tag{2.14}$$

Projecting all forces acting on the element onto the z-axis, we obtain the following equation of equilibrium

$$\frac{\partial F_{sx}}{\partial x} + \frac{\partial F_{sy}}{\partial y} - q = 0 \tag{2.15}$$

Taking moments of all forces acting on the element with respect to the y-axis and neglecting higher-order small quantities, we obtain the following equation of equilibrium

$$\frac{\partial M_x}{\partial x} - \frac{\partial M_{xy}}{\partial y} - F_{sx} = 0 \tag{2.16}$$

Similarly

$$\frac{\partial M_y}{\partial y} - \frac{\partial M_{xy}}{\partial x} - F_{sy} = 0 \tag{2.17}$$

Since there are no forces in the x- and y-directions and no moments with respect to the z-axis on the element, Eqs. (2.15), (2.16) and (2.17) completely define the state of equilibrium of the element, or they are the equilibrium equations of internal forces for plate bending. Substituting Eqs. (2.16) and (2.17) into Eq. (2.15), we obtain the equilibrium equation in terms of bending moment and torsional moment as

$$\frac{\partial^2 M_x}{\partial x^2} - 2\frac{\partial^2 M_{xy}}{\partial x \partial y} + \frac{\partial^2 M_y}{\partial y^2} = q \tag{2.18}$$

Finally, substituting the moment-curvature relation (2.12) and the curvature-deflection relation (2.9) into the Eq. (2.18), we obtain the basic governing equation in terms of displacement for bending of thin plates as

$$\nabla^2 \nabla^2 w = \frac{q}{D} \tag{2.19}$$

where ∇^2 is the two-dimensional Laplacian operator

$$\nabla^2 = \frac{\partial^2}{\partial x^2} + \frac{\partial^2}{\partial y^2} \tag{2.20}$$

The various boundary conditions for thin plate are discussed here. We consider a rectangular plate as an example and assume the x- and y-axes are parallel to the sides of plate. We focus on the side AB of plate at $y = b$.

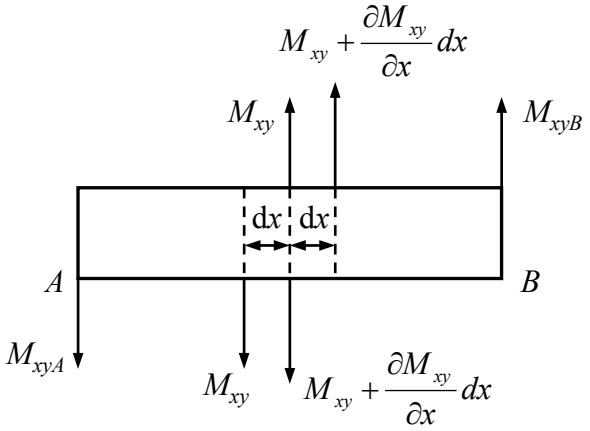

Fig. 2.2 Static equivalence for torsional moment on side AB of plate

From statics viewpoint, the distributed torsional moment is equivalent to shearing force. Hence the torsional moment $M_{xy}dx$ acting on one side with differential length dx can be replaced equivalently by two forces of magnitude M_{xy} acting on two opposite sides as shown in Fig. 2.2. The torsional moment $\left[M_{xy} + \left(\partial M_{xy} / \partial x\right) dx\right] dx$ acting on the adjacent side with differential length dx can be replaced equivalently be two forced of magnitude $M_{xy} + \left(\partial M_{xy} / \partial x\right) dx$ acting on two opposite sides. On the intersection boundary the resultant force is $\left(\partial M_{xy} / \partial x\right) dx$ which can be replaced by distributed shear force $\partial M_{xy} / \partial x$ along dx. When it is

combined with the original transverse shear force F_{sy} we obtain the total equivalent shear force on side AB as

$$F_{Vy} = F_{Sy} - \frac{\partial M_{xy}}{\partial x} \tag{2.21}$$

The positive direction of equivalent distributed shear force F_{Vy} coincides with that of F_{Sy}. It should be noted that there are two concentrated forces $\left(M_{xy}\right)_A$ and $\left(M_{xy}\right)_B$ at the ends A and B of side AB. As there are also concentrated forces on the adjacent sides, there will be a resultant concentrated force at each corner, $2\left(M_{xy}\right)_B$ at point B for instance.

Thus we obtain the various boundary conditions along $y = b$ of the plate. In general, we have

(1) For a clamped edge, the deflection and rotation must be zero, i.e.

$$\left(w\right)_{y=b} = 0, \quad \left(\frac{\partial w}{\partial y}\right)_{y=b} = 0 \tag{2.22}$$

(2) For a simply supported edge, the deflection and bending moment must be zero, i.e.

$$\left(w\right)_{y=b} = 0, \quad \left(M_y\right)_{y=b} = 0 \tag{2.22}$$

(3) For a free edge, the bending moment and total equivalent shear force must be zero, i.e.

$$\left(M_y\right)_{y=b} = 0, \quad \left(F_{Vy}\right)_{y=b} = 0 \tag{2.23}$$

If two adjacent sides are both free, there should be a further corner condition. Assuming point B is the corner of two adjacent free sides without support, there is

$$2\left(M_{xy}\right)_B = 0 \tag{2.24}$$

while there is

$$\left(w\right)_B = 0 \tag{2.25}$$

If there is a support at point B, the boundary conditions for other edges can be obtained in a similar way.

According to the analogy, we introduce the bending moment functions for thin plate bending corresponding to the displacement u, v of plane elasticity. Hence, there exist the following relations between moment and bending moment function for thin plate bending corresponding to the geometric relation of plane elasticity

$$M_y = \frac{\partial \phi_x}{\partial x}, \quad M_x = \frac{\partial \phi_y}{\partial y}, \quad 2M_{xy} = \frac{\partial \phi_x}{\partial y} + \frac{\partial \phi_y}{\partial x} \tag{2.26}$$

The strain energy density in terms of curvature is

$$v_\varepsilon(\boldsymbol{\kappa}) = \frac{1}{2}\boldsymbol{\kappa}^{\mathrm{T}}\boldsymbol{C}\boldsymbol{\kappa} = \frac{1}{2}D[\kappa_x^2 + \kappa_y^2 + 2\nu\kappa_x\kappa_y + 2(1-\nu)\kappa_{xy}^2] \tag{2.27}$$

$$\boldsymbol{\kappa} = \begin{Bmatrix} \kappa_y \\ \kappa_x \\ \kappa_{xy} \end{Bmatrix} = \begin{Bmatrix} \dfrac{\partial^2 w}{\partial y^2} \\ \dfrac{\partial^2 w}{\partial x^2} \\ -\dfrac{\partial^2 w}{\partial x \partial y} \end{Bmatrix} \text{ and } \boldsymbol{C} = D\begin{bmatrix} 1 & \nu & 0 \\ \nu & 1 & 0 \\ 0 & 0 & 2(1-\nu) \end{bmatrix} \tag{2.28}$$

are the curvature vector and elasticity coefficient matrix of material, respectively.

In accordance with the Hellinger-Reissner variational principle for plane elasticity, the Pro-Hellinger-Reissner variational principle for thin plate bending is introduced as

$$\begin{aligned} \delta\Pi_2 = \delta\Big\{ \iint_V \left[\boldsymbol{\kappa}^{\mathrm{T}}\hat{\boldsymbol{E}}(\nabla)\boldsymbol{\phi} - v_\varepsilon(\boldsymbol{\kappa})\right] \mathrm{d}x\mathrm{d}y - \int_{\Gamma_u} (\phi_s\bar{\kappa}_{ns} + \phi_n\bar{\kappa}_s)\mathrm{d}s \\ - \int_{\Gamma_\sigma} [\kappa_{ns}(\phi_s - \bar{\phi}_s) + \kappa_s(\phi_n - \bar{\phi}_n)]\mathrm{d}s \Big\} = 0 \end{aligned} \tag{2.29}$$

where

$$\hat{\boldsymbol{E}}(\nabla)=\begin{bmatrix}\dfrac{\partial}{\partial x} & 0\\ 0 & \dfrac{\partial}{\partial y}\\ \dfrac{\partial}{\partial y} & \dfrac{\partial}{\partial x}\end{bmatrix},\ \boldsymbol{\phi}=\begin{Bmatrix}\phi_x\\ \phi_y\end{Bmatrix}\ \text{and}\ \begin{Bmatrix}M_y\\ M_x\\ M_{xy}\end{Bmatrix}=\begin{Bmatrix}\dfrac{\partial\phi_x}{\partial x}\\ \dfrac{\partial\phi_y}{\partial y}\\ \dfrac{1}{2}\left(\dfrac{\partial\phi_x}{\partial y}+\dfrac{\partial\phi_y}{\partial x}\right)\end{Bmatrix} \tag{2.30}$$

are the operator matrix, bending moment function and bending moment, respectively. Subscripts n and s in Eq. (2.29) indicate directions normal and tangential to the boundary, while Γ_u and Γ_σ are the boundaries with specified geometric conditions (displacements, gradients, etc.) and natural conditions (forces, moments, etc.), respectively. Details of the derivation of this principle can be referred to the book of Yao (Yao *et al*. 2007). Known constants on the boundaries are denoted by $\overline{\kappa}_s$ $\overline{\kappa}_{ns}$ $\overline{\phi}_s$ and $\overline{\phi}_n$. Substituting (2.27) (2.28) and (2.30) into Eq. (2.29) and using $M_x=D\left(\kappa_x+\nu\kappa_y\right)$ to eliminate κ_x yields

$$\delta\left\{\int_{x_0}^{x_f}\int_{b_1}^{b_2}\left[\kappa_y\dot{\phi}_x+\kappa_{xy}\dot{\phi}_y-\nu\kappa_y\frac{\partial\phi_y}{\partial y}+\kappa_{xy}\frac{\partial\phi_x}{\partial y}+\frac{1}{2D}\left(\frac{\partial\phi_y}{\partial y}\right)^2-D(1-\nu)\kappa_{xy}^2-\frac{D(1-\nu^2)}{2}\kappa_y^2\right]\mathrm{d}y\,\mathrm{d}x\right.$$
$$\left.-\int_{\Gamma_\sigma}\left[\kappa_{ns}\left(\phi_s-\overline{\phi}_s\right)+\kappa_s\left(\phi_n-\overline{\phi}_n\right)\right]\mathrm{d}s-\int_{\Gamma_u}\left(\phi_s\overline{\kappa}_{ns}+\phi_n\overline{\kappa}_s\right)\mathrm{d}s\right\}=0 \tag{2.31}$$

where an overdot denotes differentiation with respect to x. The state variables in Eq. (2.31) are ϕ_x, ϕ_y, κ_y and κ_{xy}. The variation of Eq. (2.31) yields the Hamiltonian dual equation as

$$\dot{\boldsymbol{v}}=\boldsymbol{H}\boldsymbol{v} \tag{2.32}$$

where the Hamiltonian operator matrix $\boldsymbol{H}$ is defined as

$$\boldsymbol{H}=\begin{bmatrix} 0 & \nu\dfrac{\partial}{\partial y} & D(1-\nu^2) & 0 \\ -\dfrac{\partial}{\partial y} & 0 & 0 & 2D(1-\nu) \\ 0 & 0 & 0 & -\dfrac{\partial}{\partial y} \\ 0 & -\dfrac{1}{D}\dfrac{\partial}{\partial y} & \nu\dfrac{\partial}{\partial y} & 0 \end{bmatrix} \tag{2.33}$$

and $\boldsymbol{v}=\left\{\phi_{x,}\,\phi_{y,}\,\kappa_{y,}\,\kappa_{xy}\right\}^T$ is the state vector for variables.

Applying the method of separation of variables to $\boldsymbol{v}$ yields

$$\boldsymbol{v}(x,y)=\xi(x)\boldsymbol{\psi}(y) \tag{2.34}$$

Substituting the above expression into Eq. (2.32) gives

$$\xi(x)=e^{\mu x} \tag{2.35}$$

and the eigenvalue equation

$$\boldsymbol{H}\boldsymbol{\psi}(y)=\mu\boldsymbol{\psi}(y) \tag{2.36}$$

where μ is the eigenvalue and $\boldsymbol{\psi}(y)$ is the corresponding eigenvector. The eigen-solutions of nonzero eigenvalues in Eq. (2.36) may be obtained by expanding the eigenvalue equation. First, the eigenvalues λ in the y-direction can be obtained by substituting

$$\phi_x=e^{\lambda y}\quad \phi_y=e^{\lambda y}\quad \kappa_y=e^{\lambda y}\quad \kappa_{xy}=e^{\lambda y} \tag{2.37}$$

into Eq. (2.36). Expanding the determinant yields the eigenvalue equation

$$\left(\lambda^2+\mu^2\right)^2=0 \tag{2.38}$$

with repeated roots $\lambda=\pm\mu i$ as the eigenvalues. Hence, the general solutions of nonzero eigenvalues are

$$\begin{aligned}
\phi_x &= A_1\cos(\mu y)+B_1\sin(\mu y)+C_1 y\sin(\mu y)+D_1 y\cos(\mu y)\\
\phi_y &= A_2\sin(\mu y)+B_2\cos(\mu y)+C_2 y\cos(\mu y)+D_2 y\sin(\mu y)\\
\kappa_y &= A_3\cos(\mu y)+B_3\sin(\mu y)+C_3 y\sin(\mu y)+D_3 y\cos(\mu y)\\
\kappa_{xy} &= A_4\sin(\mu y)+B_4\cos(\mu y)+C_4 y\cos(\mu y)+D_4 y\sin(\mu y)
\end{aligned} \tag{2.39}$$

The constants are not all independent. For convenience, A_2, B_2, C_2 and D_2 may be chosen as the independent constants. Substituting Eq. (2.39) into Eq. (2.36) yields the relations between these constants.

Further substituting the general solution (2.39) into the corresponding boundary conditions on both sides $y=b_1$ or b_2 yields the transcendental equation of nonzero eigenvalues and the corresponding eigenvectors. Then method of eigenvector expansion can be applied.

Eq. (2.39) is only valid for the basic eigenvectors with nonzero eigenvalues μ. If Jordan form eigen-solution exists, we should solve the following equation

$$\boldsymbol{H}\boldsymbol{\psi}^{(k)}=\mu\boldsymbol{\psi}^{(k)}+\boldsymbol{\psi}^{(k-1)} \qquad (k=1,2,\cdots) \tag{2.40}$$

where superscript k denotes the k-th order Jordan form eigen-solution. The Jordan form eigen-solution is formed by superposing a particular solution resulted from the inhomogeneous term $\boldsymbol{\psi}^{(k-1)}$ and the solution of Eq. (2.40).

2.3 Closure

This chapter introduces the basic elasticity formula for the thin plates. General symplectic bending solutions for rectangular thin plates are derived. The following chapters will discuss the treatment of different boundary conditions by the symplectic method.

Chapter 3 Plates with Opposite Sides Simply Supported

3.1 Introduction

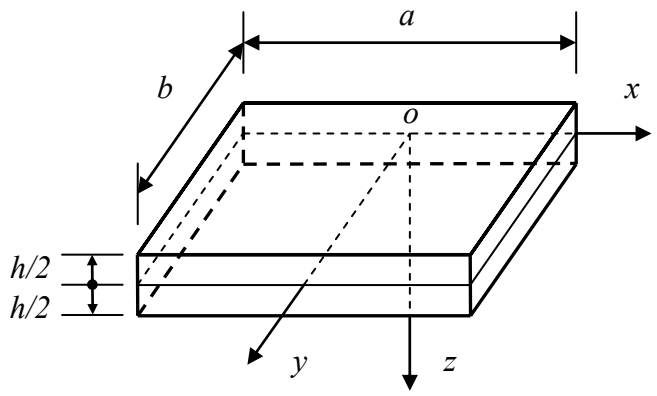

Fig. 3.1 Configuration and coordinate system of plates

Bending for plate simply supported on both opposite sides has been a well developed subject. This subject is chosen again here for solution because it is a classical case corresponding to the solution of Jordan form with nonzero eigenvalues. Besides, the methodology presented can be applied to plates with different boundary conditions for which the classical semi-inverse solution methodology fails. The expression of general solution has been formulated by Yao *et al*. (2007). Based on that formulation, the exact bending solutions for plates with two opposite sides simply supported have been derived and shown in this chapter. Fig. 3.1 shows the configuration and coordinate system of plates which discussed in this chapter.

3.2 Symplectic formulation

Consider a plate with two opposite sides simply supported at $y=0$ and $y=b$, the boundary conditions are

$$M_y\big|_{y=0,b}=0 \quad ; \quad w\big|_{y=0,b}=0 \tag{3.1}$$

Knowing that $M_y=\dfrac{\partial \phi_x}{\partial x}$ and $\kappa_x=\dfrac{1}{D}\dfrac{\partial \phi_y}{\partial y}-\nu\kappa_y=\dfrac{\partial^2 w}{\partial x^2}$, the boundary conditions in Eq. (3.1) can be replaced by

$$\begin{aligned} &\phi_x\big|_{y=0}=0 \quad ; \quad \left(\frac{1}{D}\frac{\partial \phi_y}{\partial y}-\nu\kappa_y\right)\Bigg|_{y=0}=0 \\ &\phi_x\big|_{y=b}=a_1 \quad ; \quad \left(\frac{1}{D}\frac{\partial \phi_y}{\partial y}-\nu\kappa_y\right)\Bigg|_{y=b}=0 \end{aligned} \tag{3.2}$$

The unknown constant a_1 in the boundary conditions should be solved first because it is an inhomogeneous term. After obtaining the expression for deflection w with respect to boundary condition a_1, it appears that this solution does not satisfy the boundary condition $w=0$ on both sides in Eq. (3.1). It is a spurious solution and thus should be abandoned. (Yao *et al*., 2007). The emergence of this spurious solution of the original problem is due to the replacement of $w=0$ by $\kappa_x=0$ in the boundary conditions (3.2). Therefore with respect to bending of a plate simply supported on two opposite sides, the homogeneous boundary conditions are

$$\phi_x\big|_{y=0,b}=0 \quad ; \quad \left(\frac{1}{D}\frac{\partial \phi_y}{\partial y}-\nu\kappa_y\right)\Bigg|_{y=0,b}=0 \tag{3.3}$$

For a zero eigenvalue, the eigen-solutions are all equal to zero. These are trivial solutions and they do not have physical interpretation. (Yao *et al*., 2007).For

nonzero eigenvalues, substituting the general eigen-solutions expressed by Eq. (2.39) into the homogeneous boundary conditions (3.3), and equating the determinant of coefficient matrix to zero yield the transcendental equation of nonzero eigenvalues for bending of simply supported plate on opposite sides along $y=0$ and $y=b$ as

$$\sin^2(\mu b)=0 \tag{3.4}$$

which gives real repeated double roots as

$$\mu_n=\frac{n\pi}{b}\quad (n=\pm1,\pm2,\cdots) \tag{3.5}$$

The corresponding basic eigenvector is

$$\boldsymbol{\psi}_n^{(0)}=\begin{pmatrix}\phi_x\\ \phi_y\\ \kappa_y\\ \kappa_{xy}\end{pmatrix}=\begin{pmatrix}\dfrac{D(1-\nu)}{\mu_n}\sin(\mu_n y)\\ \dfrac{D(1-\nu)}{\mu_n}\cos(\mu_n y)\\ \sin(\mu_n y)\\ \cos(\mu_n y)\end{pmatrix} \tag{3.6}$$

Then the solution to eigenvalue equation (2.32) is

$$\boldsymbol{v}_n^{(0)}=e^{\mu_n x}\boldsymbol{\psi}_n^{(0)} \tag{3.7}$$

From the curvature-deflection relation (2.9), the deflection of plate can be expressed as

$$w_n^{(0)}=-\frac{1}{\mu_n^2}e^{\mu_n x}\sin(\mu_n y) \tag{3.8}$$

where the constants of integration are determined as zero by imposing the boundary conditions $w=0$ on both sides.

Because the eigenvalue μ_n is a double root, the first-order Jordan form eigen-solution can be solved via

$$\boldsymbol{H}\boldsymbol{\psi}^{(1)}=\boldsymbol{\psi}^{(0)}+\mu\boldsymbol{\psi}^{(1)} \tag{3.9}$$

Imposing the boundary conditions (3.3) yields

$$\boldsymbol{\psi}_n^{(1)} = \begin{pmatrix} \phi_x \\ \phi_y \\ \kappa_y \\ \kappa_{xy} \end{pmatrix} = \begin{pmatrix} -\dfrac{3+\nu}{2\mu_n^{\,2}} D\sin(\mu_n y) \\ \dfrac{3+\nu}{2\mu_n^{\,2}} D\cos(\mu_n y) \\ -\dfrac{1}{2\mu_n}\sin(\mu_n y) \\ \dfrac{1}{2\mu_n}\cos(\mu_n y) \end{pmatrix} \tag{3.10}$$

Hence the solution to Eq. (2.32) is

$$\boldsymbol{v}_n^{(1)} = e^{\mu_n x}\left(x\boldsymbol{\psi}_n^{(0)} + \boldsymbol{\psi}_n^{(1)}\right) \tag{3.11}$$

Again from the curvature-deflection relation (2.9), the deflection of plate can be expressed as

$$w_n^{(1)} = \frac{1-2x\mu_n}{2\mu_n^{\,3}} e^{\mu_n x}\sin(\mu_n y) \tag{3.12}$$

The eigenvectors in Eqs. (3.12) and (3.10) are adjoint symplectic orthogonal because $\boldsymbol{H}$ is a Hamiltonian operator matrix. The eigenvector symplectic adjoint with $\boldsymbol{\psi}_n^{(0)}$ should be $\boldsymbol{\psi}_{-n}^{(1)}$, i.e.

$$\left\langle \boldsymbol{\psi}_n^{(0)}, \boldsymbol{\psi}_{-n}^{(1)} \right\rangle = -\frac{2Db}{\mu_n^2} \neq 0 \quad \text{for} \quad n = \pm 1, \pm 2, \cdots \tag{3.13}$$

while the other eigenvectors are symplectic orthogonal to each other. The symplectic inner product for any two vectors $\boldsymbol{\alpha}$, $\boldsymbol{\beta}$ in a $2n$-dimensional phase space W in a real number field R is denoted as $<\boldsymbol{\alpha}, \boldsymbol{\beta}>$ and it satisfies four basic properties (Yao et al., 2007).

From the eigenvalues and eigenvectors with adjoint symplectic orthogonality property, the general solution for plate bending simply supported on both opposite sides can be expressed as

$$\boldsymbol{v} = \sum_{n=1}^{\infty}\left[f_n^{(0)}\boldsymbol{v}_n^{(0)} + f_n^{(1)}\boldsymbol{v}_n^{(1)} + f_{-n}^{(0)}\boldsymbol{v}_{-n}^{(0)} + f_{-n}^{(1)}\boldsymbol{v}_{-n}^{(1)}\right] \tag{3.14}$$

according to the expansion theorem. The equation above strictly satisfies the homogeneous differential equation in the domain and the homogeneous boundary conditions (3.3) while $f_n^{(k)}\ \left(k = 0,1; n = \pm 1, \pm 2, \cdots\right)$ are unknown constants which can be determined by imposing the remaining two boundary conditions at $x = -a/2$ and $x = a/2$.

After determining the constants $f_n^{(k)}$, the solution of the original problem for bending deflection of a thin plate governed by Eq. (2.19) is

$$w = \bar{w} + \sum_{n=1}^{\infty}\left[f_n^{(0)}w_n^{(0)} + f_n^{(1)}w_n^{(1)} + f_{-n}^{(0)}w_{-n}^{(0)} + f_{-n}^{(1)}w_{-n}^{(1)}\right] \tag{3.15}$$

where $\bar{w}$ is a particular solution with respect to the transverse load q.

For example, the particular solution for a plate with two opposite sides simply supported at $y = 0$, $y = b$ and with uniformly distributed load q is

$$\bar{w} = \frac{q}{24D}\left(y^4 - 2by^3 + b^3 y\right) \tag{3.16}$$

and the corresponding curvatures and bending moments are

$$\begin{aligned} &\bar{\kappa}_y = \frac{q}{2D}y\left(y-b\right) \quad ; \quad \bar{\kappa}_x = 0 \quad ; \quad \bar{\kappa}_{xy} = 0 \\ &\bar{M}_x = \frac{1}{2}q\nu y\left(y-b\right) \quad ; \quad \bar{M}_y = \frac{1}{2}qy\left(y-b\right) \quad ; \quad \bar{M}_{xy} = 0 \end{aligned} \tag{3.17a-f}$$

The expressions of $\bar{M}_x$ and $\bar{\kappa}_y$ above can be represented in Fourier series as

$$\bar{M}_x = \sum_{n=1}^{\infty}\frac{2\sin\left(\dfrac{n\pi y}{b}\right)}{b}\int_0^b \frac{1}{2}q\nu y\left(y-b\right)\sin\left(\frac{n\pi y}{b}\right)dy = -\frac{4b^2 q\nu}{\pi^3}\sum_{n=1,3,5,\ldots}^{\infty}\frac{1}{n^3}\sin\left(\frac{n\pi y}{b}\right) \tag{3.18a}$$

$$\bar{\kappa}_y = \sum_{n=1}^{\infty} \frac{2\sin\left(\frac{n\pi y}{b}\right)}{b} \int_0^b \frac{q}{2D} y(y-b) \sin\left(\frac{n\pi y}{b}\right) dy = -\frac{4b^2 q}{\pi^3 D} \sum_{n=1,3,5,\ldots}^{\infty} \frac{1}{n^3} \sin\left(\frac{n\pi y}{b}\right)$$

(3.18b)

which are required to determine the other four constants when the boundary conditions at the remaining two sides are considered.

3.3 Exact plate bending solutions and numerical examples

The formulation derived in Sec. 3.2 is valid for bending of a thin plate with two opposite sides simply supported at $y = 0$ and $y = b$ and no restriction is imposed on the remaining two boundaries. Exact bending solutions for various examples of such plates are presented as follows.

3.3.1 Fully simply supported plate (SSSS)

A fully simply supported plate denoted as SSSS is solved first because it is a classical problem with well-established exact solution for comparison. The plate is bounded within a domain $-a/2 \le x \le a/2$ and $0 \le y \le b$. In addition to the two simply supported boundary conditions at $y = 0, b$ expressed in Eq. (3.3), the additional boundary conditions are

$$M_x\big|_{x=\pm a/2} = 0 \quad ; \quad \kappa_y\big|_{x=\pm a/2} = 0 \qquad (3.19a,b)$$

in which $w\big|_{x=\pm a/2} = 0$ is replaced by $\kappa_y\big|_{x=\pm a/2} = 0$. From Eqs. (3.17, 3.19), we obtain

$$M_x\big|_{x=\pm a/2} = -\bar{M}_x = -\frac{1}{2}q\nu y\left(y-b\right) \quad ; \quad \kappa_y\big|_{x=\pm a/2} = -\bar{\kappa}_y = -\frac{q}{2D}y\left(y-b\right) \quad \text{(3.20a,b)}$$

Furthermore, from Eqs. (3.14) and (2.30), we have

$$M_x = \frac{\partial \phi_y}{\partial y} = \sum_{n=1}^{\infty} D\left\{-f_n^{(0)}e^{\mu_n x}\left(1-\nu\right) - f_n^{(1)}e^{\mu_n x}\left[x\left(1-\nu\right)+\frac{3+\nu}{2\mu_n}\right] + f_{-n}^{(0)}e^{-\mu_n x}\left(1-\nu\right) + f_{-n}^{(1)}e^{-\mu_n x}\left[x\left(1-\nu\right)-\frac{3+\nu}{2\mu_n}\right]\right\}\sin\left(\mu_n y\right) \tag{3.21a}$$

$$\kappa_y = \sum_{n=1}^{\infty}\left[f_n^{(0)}e^{\mu_n x} + f_n^{(1)}e^{\mu_n x}\left(x-\frac{1}{2\mu_n}\right) - f_{-n}^{(0)}e^{-\mu_n x} - f_{-n}^{(1)}e^{-\mu_n x}\left(x+\frac{1}{2\mu_n}\right)\right]\sin\left(\mu_n y\right) \quad \text{(3.21b)}$$

Substituting $x = \pm a/2$ into Eqs. (3.21a, b) for the left-hand-side of Eqs. (3.20a,b) and using the Fourier series representations of $\bar{M}_x$ and $\bar{\kappa}_y$ in Eqs. (3.18a,b) on the right-hand-side, four set of equations can be derived. The constants $f_n^{(0)}$, $f_n^{(1)}$, $f_{-n}^{(0)}$, $f_{-n}^{(1)}$ can be solved by comparing the coefficients of $\sin\left(\mu_n y\right)$, which are

$$\begin{aligned} f_n^{(0)} &= f_{-n}^{(0)} = f_n^{(1)} = f_{-n}^{(1)} = 0 && \text{for} \quad n = 2,4,6,\cdots \\ f_n^{(0)} &= -f_{-n}^{(0)} = \frac{q\left(3+2\alpha_n\tanh\alpha_n\right)}{2Db{\mu_n}^3\cosh\alpha_n} && \text{for} \quad n = 1,3,5,\cdots \\ f_n^{(1)} &= f_{-n}^{(1)} = -\frac{q}{Db{\mu_n}^2\cosh\alpha_n} && \text{for} \quad n = 1,3,5,\cdots \end{aligned} \tag{3.22}$$

Where

$$\alpha_n = \frac{\alpha n\pi}{2b} \qquad \text{for} \quad n = 1,3,5,\cdots \tag{3.23}$$

From Eqs. (3.8), (3.12), (3.15), (3.16) and (3.22), the bending deflection of a thin plate under uniformly distributed load is

$$w = \frac{q}{24D}\left(y^4 - 2by^3 + b^3y\right) + \frac{2q}{Db}\sum_{n=1}^{\infty}\frac{\left[\mu_n x\sinh\left(\mu_n x\right) - \cosh\left(\mu_n x\right)\left(2+\alpha_n\tanh\alpha_n\right)\right]\sin\left(\mu_n y\right)}{{\mu_n}^5\cosh\alpha_n} \tag{3.24}$$

In addition, the general solutions for bending moments and stress resultants of a SSSS plate related to the state vector $\boldsymbol{v} = \left\{ \phi_{x,}\, \phi_{y,}\, \kappa_{y,}\, \kappa_{xy} \right\}^T$ can be derived accordingly. The numerical results are shown below.

Table 3.1 Deflection and bending moment factors α, β, γ for a uniformly loaded SSSS rectangular plate with $\upsilon = 0.3$

Aspect ratio a/b	Deflection factor α where $w_{max}=\alpha qb^4/D$		Bending moment factor β where $(M_y)_{max}=\beta qb^2$		Bending moment factor γ where $(M_x)_{max}=\gamma qb^2$	
	[1]	Present	[1]	Present	[1]	Present
1.0	0.00406	0.00406235	0.0479	0.0478864	0.0479	0.0478864
1.2	0.00564	0.00565053	0.0627	0.0626818	0.0501	0.0500809
1.5	0.00772	0.00772402	0.0812	0.0811601	0.0498	0.0498427
1.7	0.00883	0.00883800	0.0908	0.0907799	0.0486	0.0486149
2.0	0.01013	0.01012870	0.1017	0.101683	0.0464	0.0463503

[1]: (Timoshenko and Woinowsky-Krieger, 1959)

3.3.2 Plate with two opposite sides simply supported and the others free (SFSF)

A SFSF plate bounded within a domain $-a/2 \le x \le a/2$ and $0 \le y \le b$ is considered here. In addition to the two simply supported boundary conditions at $y = 0, b$ expressed in Eq. (3.3), the additional boundary conditions are

$$M_x\big|_{x=\pm a/2} = 0 \quad ; \quad \phi_x\big|_{x=\pm a/2} = 0 \qquad (3.25a,b)$$

where the free shear force condition $F_{\mathrm{V}x}\big|_{x=\pm a/2} = 0$ is replaced by $\phi_x\big|_{x=\pm a/2} = 0$. From Eqs. (3.17,3.25), we obtain

$$M_x\big|_{x=\pm a/2} = -\bar{M}_x = -\frac{1}{2}q\nu y\left(y-b\right) \quad ; \quad \phi_x\big|_{x=\pm a/2} = -\bar{\phi}_x = 0 \tag{3.26a,b}$$

Furthermore, from Eqs. (3.14) and (2.30), we have

$$M_x = \frac{\partial \phi_y}{\partial y} = \sum_{n=1}^{\infty} D\left\{-f_n^{(0)}e^{\mu_n x}\left(1-\nu\right) - f_n^{(1)}e^{\mu_n x}\left[x\left(1-\nu\right)+\frac{3+\nu}{2\mu_n}\right] + f_{-n}^{(0)}e^{-\mu_n x}\left(1-\nu\right) + f_{-n}^{(1)}e^{-\mu_n x}\left[x\left(1-\nu\right)-\frac{3+\nu}{2\mu_n}\right]\right\}\sin\left(\mu_n y\right) \tag{3.27a}$$

$$\phi_x = \sum_{n=1}^{\infty} D\left\{f_n^{(0)}e^{\mu_n x}\left(1-\nu\right) + f_n^{(1)}e^{\mu_n x}\left[x\left(1-\nu\right)-\frac{\left(3+\nu\right)}{2\mu_n}\right] + f_{-n}^{(0)}e^{-\mu_n x}\left(1-\nu\right) + f_{-n}^{(1)}e^{-\mu_n x}\left[x\left(1-\nu\right)+\frac{\left(3+\nu\right)}{2\mu_n}\right]\right\}\frac{\sin\left(\mu_n y\right)}{\mu_n} \tag{3.27b}$$

Substituting $x = \pm a/2$ into Eqs. (3.27a,b) for the left-hand-side of Eqs. (3.26a,b) and using the Fourier series representations of $\bar{M}_x$ in Eqs. (3.18a) on the right-hand-side, four set of equations can be derived. The constants $f_n^{(0)}$, $f_n^{(1)}$, $f_{-n}^{(0)}$, $f_{-n}^{(1)}$ can be solved by comparing the coefficients of $\sin\left(\mu_n y\right)$, which are

$$\begin{aligned}
f_n^{(0)} &= f_{-n}^{(0)} = f_n^{(1)} = f_{-n}^{(1)} = 0 && \text{for} \quad n = 2,4,6\cdots \\
f_n^{(0)} &= -f_{-n}^{(0)} = -\frac{2q\nu\left[\left(3+\nu\right)\sinh\alpha_n - 2\left(1-\nu\right)\alpha_n\cosh\alpha_n\right]}{Db{\mu_n}^3\left(1-\nu\right)\left[\left(3+\nu\right)\sinh\left(2\alpha_n\right)-2\left(1-\nu\right)\alpha_n\right]} && \text{for} \quad n = 1,3,5\cdots \\
f_n^{(1)} &= f_{-n}^{(1)} = -\frac{4q\nu\sinh\alpha_n}{Db{\mu_n}^2\left[\left(3+\nu\right)\sinh\left(2\alpha_n\right)-2\left(1-\nu\right)\alpha_n\right]} && \text{for} \quad n = 1,3,5\cdots
\end{aligned} \tag{3.28}$$

where α_n is given in Eq. (3.23).

From Eqs. (3.8), (3.12), (3.15), (3.16) and (3.28), the bending deflection of a thin plate under uniformly distributed load is

$$w=\frac{q}{24D}\left(y^4-2by^3+b^3y\right)+\frac{4q}{(1-\nu)bD}\times$$
$$\sum_{n=1}^{\infty}\frac{\left\{\nu\cosh(\mu_n x)\left[\alpha_n(1-\nu)\cosh\alpha_n-(1+\nu)\sinh\alpha_n\right]-\mu_n x(1-\nu)\nu\sinh\alpha_n\sinh(\mu_n x)\right\}\sin(\mu_n y)}{\mu_n{}^5\left[\alpha_n(1-\nu)-(3+\nu)\cosh\alpha_n\sinh\alpha_n\right]} \tag{3.29}$$

In addition, the general solutions for bending moments and stress resultants of a SFSF plate related to the state vector $\boldsymbol{v}=\left\{\phi_{x,}\,\phi_{y,}\,\kappa_{y,}\,\kappa_{xy}\right\}^T$ can be derived accordingly. The numerical results are shown below.

Table 3.2 Deflection and bending moment factors α, β, γ for a uniformly loaded SFSF rectangular plate with $\upsilon = 0.3$

Aspect ratio	Deflection factor α where $w_{max}=\alpha qb^4/D$		Bending moment factor β where $(M_y)_{max}=\beta qb^2$		Bending moment factor γ where $(M_x)_{max}=\gamma qb^2$	
a/b	[1]	Present	[1]	Present	[1]	Present
0.5	0.01377	0.0137131	0.1235	0.123642	0.0102	0.0121476
1.0	0.01309	0.0130937	0.1225	0.122545	0.0271	0.0270782
2.0	0.01289	0.0128873	0.1235	0.123468	0.0364	0.0363888

[1]: (Timoshenko and Woinowsky-Krieger, 1959)

3.3.3 Plate with two opposite sides simply supported and the others clamped (SCSC)

A SCSC plate bounded within a domain $-a/2 \le x \le a/2$ and $0 \le y \le b$ is considered here. In addition to the two opposite sides simply supported, the additional boundary conditions are

$$\kappa_y\big|_{x=\pm a/2}=0 \quad ; \quad \kappa_{xy}\big|_{x=\pm a/2}=0 \tag{3.30}$$

where $w\big|_{x=\pm a/2}=0$ is replaced by $\kappa_y\big|_{x=\pm a/2}=0$ and $\left.\frac{\partial w}{\partial x}\right|_{x=\pm a/2}=0$ is replaced by $\kappa_{xy}\big|_{x=\pm a/2}=0$. From Eqs. (3.17,3.30), we obtain

$$\kappa_y\big|_{x=\pm a/2}=-\bar{\kappa}_y=-\frac{q}{2D}y\left(y-b\right) \quad ; \quad \kappa_{xy}\big|_{x=\pm a/2}=-\bar{\kappa}_{xy}=0 \tag{3.31}$$

Furthernore, from Eqs. (3.14), we have

$$\kappa_y=\sum_{n=1}^{\infty}\left[f_n^{(0)}e^{\mu_n x}+f_n^{(1)}e^{\mu_n x}\left(x-\frac{1}{2\mu_n}\right)-f_{-n}^{(0)}e^{-\mu_n x}-f_{-n}^{(1)}e^{-\mu_n x}\left(x+\frac{1}{2\mu_n}\right)\right]\sin\left(\mu_n y\right) \tag{3.32a}$$

$$\kappa_{xy}=\sum_{n=1}^{\infty}\left[f_n^{(0)}e^{\mu_n x}+f_n^{(1)}e^{\mu_n x}\left(x+\frac{1}{2\mu_n}\right)-f_{-n}^{(0)}e^{-\mu_n x}+f_{-n}^{(1)}e^{-\mu_n x}\left(x-\frac{1}{2\mu_n}\right)\right]\cos\left(\mu_n y\right) \tag{3.32b}$$

Substituting $x=\pm a/2$ into Eqs. (3.32a,b) for the left-hand-side of Eqs. (3.31a,b) and using the Fourier series representations of $\bar{\kappa}_y$ in Eqs. (3.18b) on the right-hand-side, four set of equations can be derived. The constants $f_n^{(0)}$, $f_n^{(1)}$, $f_{-n}^{(0)}$, $f_{-n}^{(1)}$ can be solved by comparing the coefficients of $\sin\left(\mu_n y\right)$, which are

$$\begin{aligned}
&f_n^{(0)}=f_{-n}^{(0)}=f_n^{(1)}=f_{-n}^{(1)}=0 && \text{for} \quad n=2,4,6\cdots \\
&f_n^{(0)}=-f_{-n}^{(0)}=-\frac{2q\left(2\alpha_n\cosh\alpha_n+\sinh\alpha_n\right)}{Db{\mu_n}^3\left[2\alpha_n+\sinh\left(2\alpha_n\right)\right]} && \text{for} \quad n=1,3,5\cdots \\
&f_n^{(1)}=f_{-n}^{(1)}=-\frac{4q\sinh\alpha_n}{Db{\mu_n}^2\left[2\alpha_n+\sinh\left(2\alpha_n\right)\right]} && \text{for} \quad n=1,3,5\cdots
\end{aligned} \tag{3.33}$$

where α_n is given in Eq. (3.23).

From Eqs. (3.8), (3.12), (3.15), (3.16) and (3.33), the bending deflection of a thin plate under uniformly distributed load is

$$w=\frac{q}{24D}\left(y^4-2by^3+b^3y\right)+$$
$$\frac{4q}{bD}\sum_{n=1}^{\infty}\left\{\left\{e^{4\alpha_n}\sin\left(\mu_n y\right)\left[-2\left(3\alpha_n+\mu_n x\right)\cosh\left(\alpha_n-\mu_n x\right)+\left(\alpha_n+\mu_n x\right)\cosh\left(3\alpha_n-\mu_n x\right)\right.\right.$$
$$-5\alpha_n\cosh\left(\alpha_n+\mu_n x\right)+3\mu_n x\cosh\left(\alpha_n+\mu_n x\right)+2\alpha_n\cosh\left(3\alpha_n+\mu_n x\right)-2\mu_n x\cosh\left(3\alpha_n+\mu_n x\right)$$
$$\left.+8\cosh\left(2\alpha_n\right)\cosh\left(\mu_n x\right)\sinh\alpha_n-4\alpha_n\left(\alpha_n-\mu_n x\right)\sinh\left(\alpha_n+\mu_n x\right)\right]\}$$
$$/\,\mu_n^{\,5}\left(1+8\alpha_n e^{4\alpha_n}-e^{8\alpha_n}\right)\Big\} \tag{3.34}$$

In addition, the general solutions for bending moments and stress resultants of a SCSC plate related to the state vector $\boldsymbol{v}=\left\{\phi_{x,}\,\phi_{y,}\,\kappa_{y,}\,\kappa_{xy}\right\}^T$ can be derived accordingly. Below are the numerical results.

Table 3.3 Deflection and bending moment factors α, β, γ for a uniformly loaded SCSC rectangular plate with $\upsilon = 0.3$ ($l = b$ for $a \geq b$ and $l = a$ for $a < b$)

Aspect ratio a/b	Deflection factor α where $w_{max}=\alpha qb^4/D$		Bending moment factor β where $(M_y)_{max}=\beta qb^2$		Bending moment factor γ where $(M_x)_{max}=\gamma qb^2$	
	[1]	Present	[1]	Present	[1]	Present
1/2	0.00260	0.00261079	0.0142	0.0141716	0.0420	0.0420629
2/3	0.00247	0.0024757	0.0179	0.0178003	0.0406	0.0406276
1	0.00192	0.00191714	0.0244	0.0243874	0.0332	0.0332449
3/2	0.00531	0.00532645	0.0585	0.0584803	0.0460	0.0459444
2	0.00844	0.00844500	0.0869	0.0868681	0.0474	0.0473622

[1]: (Timoshenko and Woinowsky-Krieger, 1959)

3.3.4 Plate with two opposite sides simply supported, one clamped and one free. (SFSC)

A SFSC plate bounded within a domain $-a/2 \le x \le a/2$ and $0 \le y \le b$ is considered here. In addition to the two opposite sides simply supported, the additional boundary conditions are

$$\begin{aligned} M_x\big|_{x=-a/2} &= 0 \quad ; \quad \phi_x\big|_{x=-a/2} = 0 \\ \kappa_y\big|_{x=a/2} &= 0 \quad ; \quad \kappa_{xy}\big|_{x=a/2} = 0 \end{aligned} \tag{3.35a-d}$$

where the free shear force condition $F_{\mathrm{V}x}\big|_{x=\pm a/2} = 0$ is replaced by $\phi_x\big|_{x=\pm a/2} = 0$, $w\big|_{x=\pm a/2} = 0$ is replaced by $\kappa_y\big|_{x=\pm a/2} = 0$ and $\left.\dfrac{\partial w}{\partial x}\right|_{x=\pm a/2} = 0$ is replaced by $\kappa_{xy}\big|_{x=\pm a/2} = 0$.

From Eqs. (3.17, 3.35), we obtain

$$\begin{aligned} M_x\big|_{x=-a/2} &= -\bar{M}_x = -\frac{1}{2} q\nu y\left(y-b\right) \quad ; \quad \phi_x\big|_{x=-a/2} = -\bar{\phi}_x = 0 \\ \kappa_y\big|_{x=a/2} &= -\bar{\kappa}_y = -\frac{q}{2D} y\left(y-b\right) \quad ; \quad \kappa_{xy}\big|_{x=a/2} = -\bar{\kappa}_{xy} = 0 \end{aligned} \tag{3.36a-d}$$

Furthermore, from Eqs. (3.14) and (2.30), we have

$$\begin{aligned} \phi_x = \sum_{n=1}^{\infty} D\Bigg\{ & f_n^{(0)} e^{\mu_n x}\left(1-\nu\right) + f_n^{(1)} e^{\mu_n x}\left[x\left(1-\nu\right) - \frac{\left(3+\nu\right)}{2\mu_n} \right] + f_{-n}^{(0)} e^{-\mu_n x}\left(1-\nu\right) + \\ & f_{-n}^{(1)} e^{-\mu_n x}\left[x\left(1-\nu\right) + \frac{\left(3+\nu\right)}{2\mu_n} \right] \Bigg\} \frac{\sin\left(\mu_n y\right)}{\mu_n} \end{aligned} \tag{3.37a}$$

$$\kappa_y = \sum_{n=1}^{\infty} \left[f_n^{(0)} e^{\mu_n x} + f_n^{(1)} e^{\mu_n x}\left(x - \frac{1}{2\mu_n} \right) - f_{-n}^{(0)} e^{-\mu_n x} - f_{-n}^{(1)} e^{-\mu_n x}\left(x + \frac{1}{2\mu_n} \right) \right] \sin\left(\mu_n y\right) \tag{3.37b}$$

$$\kappa_{xy} = \sum_{n=1}^{\infty} \left[f_n^{(0)} e^{\mu_n x} + f_n^{(1)} e^{\mu_n x}\left(x + \frac{1}{2\mu_n} \right) - f_{-n}^{(0)} e^{-\mu_n x} + f_{-n}^{(1)} e^{-\mu_n x}\left(x - \frac{1}{2\mu_n} \right) \right] \cos\left(\mu_n y\right) \tag{3.37c}$$

Substituting $x = \pm a/2$ into Eqs. (3.37a-c) for the left-hand-side of Eqs. (3.36a-d) and using the Fourier series representations of $\overline{\kappa}_y$ in Eqs. (3.18b) on the right-hand-side, four set of equations can be derived. The constants $f_n^{(0)}$, $f_n^{(1)}$, $f_{-n}^{(0)}$, $f_{-n}^{(1)}$ can be solved by comparing the coefficients of $\sin(\mu_n y)$, which are

$$
\begin{aligned}
&f_n^{(0)} = f_{-n}^{(0)} = f_n^{(1)} = f_{-n}^{(1)} = 0 \qquad \text{for } n = 2,4,6\cdots \\
&f_n^{(0)} = \Big\{2qe^{\alpha_n}\Big\{e^{6\alpha_n}(1+2\alpha_n)(\nu-1)(3+\upsilon) - e^{2\alpha_n}\Big[-2\alpha_n(\nu-1)^2 + 8\alpha_n{}^2(-1+\nu)^2 + (3+\nu)^2\Big] \\
&\quad -e^{4\alpha_n}\nu\Big\{-1+\nu+2\alpha_n\Big[3+4\alpha_n(\nu-1)+\nu\Big]\Big\}\Big\}\Big\} \\
&\quad / Db\mu_n{}^3\Big\{(\nu-1)(3+\nu) + e^{8\alpha_n}(\nu-1)(3+\nu) - 2e^{4\alpha_n}\Big[5+8\alpha_n{}^2(\nu-1)^2 + \nu(2+\nu)\Big]\Big\} \\
&\qquad\qquad \text{for } n = 1,3,5\cdots \\
&f_{-n}^{(0)} = -\Big\{2e^{\alpha_n}q\Big\{-(-1+2\alpha_n)(-1+\nu)(3+\nu) + e^{6\alpha_n}\nu\Big[3+\nu+2\alpha_n(-1+\nu)\Big] \\
&\quad -e^{4\alpha_n}\Big[2\alpha_n(-1+\nu)^2 + 8\alpha_n{}^2(-1+\nu)^2 + (3+\nu)^2\Big] - e^{2\alpha_n}\nu\Big\{-1+\nu+2\alpha_n\Big[-3+4\alpha_n(\nu-1)-\nu\Big]\Big\}\Big\} \\
&\quad / Db\mu_n{}^3\Big\{(\nu-1)(3+\nu) + e^{8\alpha_n}(\nu-1)(3+\nu) - 2e^{4\alpha_n}\Big[5+8\alpha_n{}^2(\nu-1)^2 + \nu(2+\nu)\Big]\Big\} \\
&\qquad\qquad \text{for } n = 1,3,5\cdots \\
&f_n^{(1)} = \Big\{4qe^{\alpha_n}\Big\{-e^{2\alpha_n}(-1+4\alpha_n)(-1+\nu)^2 - (-1+\nu)\nu - e^{6\alpha_n}(-1+\nu)(3+\nu) + e^{4\alpha_n}\nu\Big[3+4\alpha_n(-1+\nu)+\nu\Big]\Big\}\Big\} \\
&\quad / Db\mu_n{}^2\Big\{(\nu-1)(3+\nu) + e^{8\alpha_n}(\nu-1)(3+\nu) - 2e^{4\alpha_n}\Big[5+8\alpha_n{}^2(\nu-1)^2 + \nu(2+\nu)\Big]\Big\} \\
&\qquad\qquad \text{for } n = 1,3,5\cdots \\
&f_{-n}^{(1)} = -\Big\{4e^{\alpha_n}q\Big\{-e^{4\alpha_n}(1+4\alpha_n)(-1+\nu)^2 + e^{2\alpha_n}\Big[-3+4\alpha_n(-1+\nu)-\nu\Big]\nu + e^{6\alpha_n}(-1+\nu)\nu + (-1+\nu)(3+\nu)\Big\}\Big\} \\
&\quad / Db\mu_n{}^2\Big\{(\nu-1)(3+\nu) + e^{8\alpha_n}(\nu-1)(3+\nu) - 2e^{4\alpha_n}\Big[5+8\alpha_n{}^2(\nu-1)^2 + \nu(2+\nu)\Big]\Big\} \\
&\qquad\qquad \text{for } n = 1,3,5\cdots
\end{aligned}
\tag{3.38}
$$

where α_n is given in Eq. (3.23).

From Eqs. (3.8), (3.12), (3.15), (3.16) and (3.38), the bending deflection of a thin plate under uniformly distributed load is

$$w=\frac{q}{24D}\left(y^4-2by^3+b^3y\right)+$$
$$\frac{8q}{bD}\sum_{n=1}^{\infty}\left\{\left\{e^{4\alpha_n}\sin(\mu_n y)\left\{\left[5+4\alpha_n{}^2\left(\nu-1\right)^2+\nu\left(2+\nu\right)\right]\cosh\left(\alpha_n-\mu_n x\right)+3\cosh\left(3\alpha_n+\mu_n x\right)\right.\right.\right.$$
$$+\nu\cosh\left(\mu_n x\right)\left\{\left[1+4\alpha_n{}^2\left(\nu-1\right)+\nu\right]\cosh\alpha_n+\left(-3+\alpha_n-2\nu\right)\cosh\left(3\alpha_n\right)\right.$$
$$\left.+\mu_n x\left[-5\sinh\alpha_n-\left(\nu-1\right)\sinh\left(3\alpha_n\right)\right]\right\}+\nu\left\{-\mu_n x\left(1+2\nu\right)\cosh\alpha_n+\mu_n x\left(\nu-1\right)\cosh\left(3\alpha_n\right)\right.$$
$$\left.+\left[1+4\alpha_n{}^2\left(\nu-1\right)+\nu\right]\sinh\alpha_n+\left(\alpha_n-1\right)\sinh\left(3\alpha_n\right)\right\}\sinh\left(\mu_n x\right)-\alpha_n\left\{\cosh\left(\mu_n x\right)\right.$$
$$\left\{4\mu_n x\left(\nu-1\right)\cosh\alpha_n-3\sinh\alpha_n+\nu\left\{\cosh\left(3\alpha_n\right)+\left[5-4\nu+4\nu\cosh\left(2\alpha_n\right)\right]\sinh\alpha_n\right\}\right\}$$
$$\left.+\left[\left(3-7\nu\right)\cosh\alpha_n+2\nu\cosh\left(3\alpha_n\right)+4\mu_n x\left(\nu-1\right)\left(2\nu-1\right)\sinh\alpha_n+\nu\sinh\left(3\alpha_n\right)\right]\sinh\left(\mu_n x\right)\right\}$$
$$\left.+\mu_n x\sinh\left(\alpha_n-\mu_n x\right)-\left[\alpha_n\left(\nu-3\right)-\mu_n x\left(\nu-1\right)\left(\nu+3\right)\right]\sinh\left(3\alpha_n+\mu_n x\right)\right\}\Big/$$
$$\left.\left\{\mu_n{}^5\left\{\left(\nu-1\right)\left(\nu+3\right)+e^{8\alpha_n}\left(\nu-1\right)\left(\nu+3\right)-2e^{4\alpha_n}\left[5+8\alpha_n{}^2\left(\nu-1\right)^2+\nu\left(2+\nu\right)\right]\right\}\right\}\right\} \tag{3.39}$$

Table 3.4 Deflection and bending moment factors α, β, γ for a uniformly loaded SCSC rectangular plate with $\upsilon = 0.3$ ($l = b$ for $a \geq b$ and $l = a$ for $a < b$).

Aspect ratio a/b	Deflection factor α at $x = a/2, y = b/2$ where $w_{max}=\alpha qb^4/D$		Bending moment factor β at $x = a/2, y = b/2$ where $(M_y)_{max}= \beta qb^2$		Bending moment factor γ at $x = 0, y = b/2$ where $(M_x)_{max}= \gamma qb^2$	
	[1]	Present	[1]	Present	[1]	Present
1/3	0.0940	0.0939792	0.0078	0.00782003	0.428	0.427944
1/2	0.0582	0.0582267	0.0293	0.0292631	0.319	0.318975
1	0.0113	0.0112359	0.0972	0.0971846	0.119	0.118407
2	0.0150	0.0149491	0.131	0.130529	0.125	0.124666
3	0.0152	0.0152035	0.133	0.132814	0.125	0.124975

[1]: (Timoshenko and Woinowsky-Krieger, 1959)

In addition, the general solutions for bending moments and stress resultants of a SFSC plate related to the state vector $\boldsymbol{v} = \left\{ \phi_{x,}\, \phi_{y,}\, \kappa_{y,}\, \kappa_{xy} \right\}^T$ can be derived accordingly. Table 3.4 shows the numerical results for the SFSC plate.

3.3.5 Plate with three sides simply supported and the other free (SSSF)

A SSSF plate bounded within a domain $-a/2 \le x \le a/2$ and $0 \le y \le b$ is considered here. In addition to the two opposite sides simply supported, the additional boundary conditions are

$$\begin{aligned} M_x\big|_{x=-a/2} &= 0 \quad ; \quad \kappa_y\big|_{x=-a/2} = 0 \\ M_x\big|_{x=a/2} &= 0 \quad ; \quad \phi_x\big|_{x=a/2} = 0 \end{aligned} \tag{3.40a-d}$$

in which $w\big|_{x=\pm a/2} = 0$ is replaced by $\kappa_y\big|_{x=\pm a/2} = 0$ and the free shear force condition $F_{\mathrm{V}x}\big|_{x=\pm a/2} = 0$ is replaced by $\phi_x\big|_{x=\pm a/2} = 0$. From Eqs. (3.17, 3.40) we obtain

$$\begin{aligned} M_x\big|_{x=-a/2} &= -\bar{M}_x = -\frac{1}{2} q\nu y\left(y-b\right) \quad ; \quad \kappa_y\big|_{x=-a/2} = -\bar{\kappa}_y = -\frac{q}{2D} y\left(y-b\right) \\ M_x\big|_{x=a/2} &= -\bar{M}_x = -\frac{1}{2} q\nu y\left(y-b\right) \quad ; \quad \phi_x\big|_{x=a/2} = -\bar{\phi}_x = 0 \end{aligned} \tag{3.41a-d}$$

Furthermore, from Eqs. (3.14) and (2.30), we have

$$\begin{aligned} M_x = \frac{\partial \phi_y}{\partial y} = \sum_{n=1}^{\infty} D \Bigg\{ & -f_n^{(0)} e^{\mu_n x}\left(1-\nu\right) - f_n^{(1)} e^{\mu_n x}\left[x\left(1-\nu\right) + \frac{3+\nu}{2\mu_n} \right] + f_{-n}^{(0)} e^{-\mu_n x}\left(1-\nu\right) \\ & + f_{-n}^{(1)} e^{-\mu_n x}\left[x\left(1-\nu\right) - \frac{3+\nu}{2\mu_n} \right] \Bigg\} \sin\left(\mu_n y\right) \end{aligned} \tag{3.42a}$$

$$\phi_x = \sum_{n=1}^{\infty} D\left\{ f_n^{(0)} e^{\mu_n x}(1-\nu) + f_n^{(1)} e^{\mu_n x}\left[x(1-\nu) - \frac{(3+\nu)}{2\mu_n} \right] + f_{-n}^{(0)} e^{-\mu_n x}(1-\nu) + f_{-n}^{(1)} e^{-\mu_n x}\left[x(1-\nu) + \frac{(3+\nu)}{2\mu_n} \right] \right\} \frac{\sin(\mu_n y)}{\mu_n} \tag{3.42b}$$

$$\kappa_y = \sum_{n=1}^{\infty} \left[f_n^{(0)} e^{\mu_n x} + f_n^{(1)} e^{\mu_n x}\left(x - \frac{1}{2\mu_n} \right) - f_{-n}^{(0)} e^{-\mu_n x} - f_{-n}^{(1)} e^{-\mu_n x}\left(x + \frac{1}{2\mu_n} \right) \right] \sin(\mu_n y) \tag{3.42c}$$

Substituting $x = \pm a/2$ into Eqs. (3.42a-c) for the left-hand-side of Eqs. (3.41a-d) and using the Fourier series representations of $\bar{M}_x$ and $\bar{\kappa}_y$ in Eqs. (3.18a,b) on the right-hand-side, four set of equations can be derived. The constants $f_n^{(0)}$, $f_n^{(1)}$, $f_{-n}^{(0)}$, $f_{-n}^{(1)}$ can be solved by comparing the coefficients of $\sin(\mu_n y)$, which are

$$\begin{aligned}
f_n^{(0)} &= f_{-n}^{(0)} = f_n^{(1)} = f_{-n}^{(1)} = 0 && ; \quad \text{for } n = 2,4,6\cdots \\
f_n^{(0)} &= \Big\{ e^{-3\alpha_n} q \Big\{ -2e^{2\alpha_n}\left[-3 + 6\alpha_n(-1+\nu) - \nu \right]\nu + (-3+2\alpha_n)(-1+\nu)(3+\nu) + \\
&\quad 2e^{6\alpha_n}\nu\left[3 + 2\alpha_n(-1+\nu) + \nu \right] - e^{4\alpha_n}\left[6\alpha_n(-1+\nu)^2 + 8{\alpha_n}^2(-1+\nu)^2 + (3+\nu)^2 \right] \Big\} \Big\} && ; \quad \text{for } n = 1,3,5\cdots \\
&\quad / 2Db{\mu_n}^3(-1+\nu)\left[-4\alpha_n(-1+\nu) + (3+\nu)\sinh(4\alpha_n) \right] \\
f_{-n}^{(0)} &= \Big\{ e^{-3\alpha_n} q \Big\{ -e^{6\alpha_n}(-1+\nu)(3+\nu)(3+2\alpha_n) + 2\nu\left[3 + 2\alpha_n(-1+\nu) + \nu \right] + \\
&\quad 2e^{4\alpha_n}\nu\left[3 + 6\alpha_n(-1+\nu) + \nu \right] - e^{2\alpha_n}\left[-6\alpha_n(-1+\nu)^2 + 8{\alpha_n}^2(-1+\nu)^2 + (3+\nu)^2 \right] \Big\} && ; \quad \text{for } n = 1,3,5\cdots \\
&\quad / 2Db{\mu_n}^3(-1+\nu)\left[-4\alpha_n(-1+\nu) + (3+\nu)\sinh(4\alpha_n) \right] \\
f_n^{(1)} &= \frac{2qe^{\alpha_n}\left\{ 3+\nu+e^{4\alpha_n}\left[(3+4\alpha_n)(-1+\nu) - 4\nu\cosh(2\alpha_n) \right] \right\}}{Db{\mu_n}^2\left[3 + 8\alpha_n e^{4\alpha_n}(-1+\nu) + \nu - e^{8\alpha_n}(3+\nu) \right]} && ; \quad \text{for } n = 1,3,5\cdots \\
f_{-n}^{(1)} &= \frac{2e^{\alpha_n} q\left[-e^{2\alpha_n}(-3+4\alpha_n)(-1+\nu) - 2\nu - 2e^{4\alpha_n}\nu + e^{6\alpha_n}(3+\nu) \right]}{Db{\mu_n}^2\left[3 + 8\alpha_n e^{4\alpha_n}(-1+\nu) + \nu - e^{8\alpha_n}(3+\nu) \right]} && ; \quad \text{for } n = 1,3,5\cdots
\end{aligned} \tag{3.43}$$

where α_n is given in Eq. (3.23).

From Eqs. (3.8), (3.12), (3.15), (3.16) and (3.43), the bending deflection of a thin plate under uniformly distributed load is

$$w=\frac{q}{24D}\left(y^4-2by^3+b^3y\right)+$$
$$\frac{2q}{bD}\sum_{n=1}^{\infty}\left\{\left\{e^{\alpha_n-\mu_n x}\left\{-2e^{2(\alpha_n+\mu_n x)}\left[-1+3\alpha_n(\nu-1)+\mu_n x(\nu-1)-\nu\right]\nu+e^{2\mu_n x}\left(-2+\alpha_n+\mu_n x\right)(\nu-1)\right.\right.\right.$$
$$(3+\nu)-2e^{4\alpha_n}\nu\left[1+3\alpha_n(\nu-1)+\mu_n x(\nu-1)+\nu\right]+2\nu\left[-1-\alpha_n+\mu_n x+\left(-1+\alpha_n-\mu_n x\right)\nu\right]+$$
$$e^{2\alpha_n}\left[6+4{\alpha_n}^2(\nu-1)^2+3\mu_n x(\nu-1)^2-\alpha_n(5+4\mu_n x)(\nu-1)^2+2\nu^2\right]+2e^{6\alpha_n+2\mu_n x}\nu$$
$$\left[1+\alpha_n(\nu-1)+\nu-\mu_n x(\nu-1)\right]+e^{4\alpha_n+2\mu_n x}\left[-4{\alpha_n}^2(\nu-1)^2+3\mu_n x(\nu-1)^2+\alpha_n(-5+4\mu_n x)(\nu-1)^2\right.$$
$$\left.\left.\left.-2(3+\nu)^2\right]\right\}\sin(\mu_n y)\right\}\Big/\left\{{\mu_n}^5(\nu-1)\left[8\alpha_n e^{4\alpha_n}(\nu-1)+\left(1-e^{8\alpha_n}\right)(3+\nu)\right]\right\}\Bigg\} \tag{3.44}$$

In addition, the general solutions for bending moments and stress resultants of a SSSF plate related to the state vector $\boldsymbol{v}=\left\{\phi_{x,}\,\phi_{y,}\,\kappa_{y,}\,\kappa_{xy}\right\}^T$ can be derived accordingly. Below are numerical results for the SSSF plates.

Table 3.5 Deflection and bending moment factors α, β, γ for a uniformly loaded SSSF rectangular plate with $\upsilon = 0.3$.

Aspect ratio a/b	Deflection factor α at $x = 0, y = b$ where $w_{max}=\alpha qb^4/D$		Bending moment factor β at $x = 0, y = b$ where $(M_y)_{max}=\beta qb^2$		Bending moment factor γ at $x = 0, y = b/2$ where $(M_x)_{max}=\gamma qb^2$	
	[1]	Present	[1]	Present	[1]	Present
1/2	0.00710	0.00709414	0.060	0.0601585	0.022	0.0223242
2/3	0.00968	0.00967944	0.083	0.0832446	0.030	0.0302317
1	0.01286	0.0128524	0.112	0.111701	0.039	0.0389809
2	0.01507	0.0150692	0.132	0.131608	0.041	0.0414129
3	0.01520	0.0152107	0.133	0.132878	0.039	0.0390640

[1]: (Timoshenko and Woinowsky-Krieger, 1959)

3.3.6 Plate with three sides simply supported and the other clamped (SSSC)

A SSSC plate bounded within a domain $-a/2 \le x \le a/2$ and $0 \le y \le b$ is considered here. In addition to the two opposite sides simply supported, the additional boundary conditions are

$$\begin{aligned} M_x\big|_{x=-a/2} &= 0 \quad ; \quad \kappa_y\big|_{x=-a/2} = 0 \\ \kappa_y\big|_{x=a/2} &= 0 \quad ; \quad \kappa_{xy}\big|_{x=a/2} = 0 \end{aligned} \tag{3.45a-d}$$

in which $w\big|_{x=\pm a/2} = 0$ is replaced by $\kappa_y\big|_{x=\pm a/2} = 0$ and $\left.\dfrac{\partial w}{\partial x}\right|_{x=\pm a/2} = 0$ is replaced by $\kappa_{xy}\big|_{x=\pm a/2} = 0$. From Eqs. (3.17) and (3.45), we obtain

$$\begin{aligned} M_x\big|_{x=-a/2} &= -\bar{M}_x = -\frac{1}{2} q\nu y(y-b) \quad ; \quad \kappa_y\big|_{x=-a/2} = -\bar{\kappa}_y = -\frac{q}{2D} y(y-b) \\ \kappa_y\big|_{x=a/2} &= -\bar{\kappa}_y = -\frac{q}{2D} y(y-b) \quad ; \quad \kappa_{xy}\big|_{x=a/2} = -\bar{\kappa}_{xy} = 0 \end{aligned} \tag{3.46a-d}$$

Furthermore, from Eqs. (3.14), we have

$$M_x = \frac{\partial \phi_y}{\partial y} = \sum_{n=1}^{\infty} D\left\{ -f_n^{(0)} e^{\mu_n x}(1-\nu) - f_n^{(1)} e^{\mu_n x}\left[x(1-\nu) + \frac{(3+\nu)}{2\mu_n} \right] + f_{-n}^{(0)} e^{-\mu_n x}(1-\nu) + f_{-n}^{(1)} e^{-\mu_n x}\left[x(1-\nu) - \frac{(3+\nu)}{2\mu_n} \right] \right\} \sin(\mu_n y) \tag{3.47a}$$

$$\kappa_y = \sum_{n=1}^{\infty} \left[f_n^{(0)} e^{\mu_n x} + f_n^{(1)} e^{\mu_n x}\left(x - \frac{1}{2\mu_n} \right) - f_{-n}^{(0)} e^{-\mu_n x} - f_{-n}^{(1)} e^{-\mu_n x}\left(x + \frac{1}{2\mu_n} \right) \right] \sin(\mu_n y) \tag{3.47b}$$

$$\kappa_{xy} = \sum_{n=1}^{\infty} \left[f_n^{(0)} e^{\mu_n x} + f_n^{(1)} e^{\mu_n x}\left(x + \frac{1}{2\mu_n} \right) - f_{-n}^{(0)} e^{-\mu_n x} + f_{-n}^{(1)} e^{-\mu_n x}\left(x - \frac{1}{2\mu_n} \right) \right] \cos(\mu_n y) \tag{3.47c}$$

Substituting $x = \pm a/2$ into Eqs. (3.47a-c) for the left-hand-side of Eqs. (3.46a-d) and using the Fourier series representations of $\overline{M}_x$ and $\overline{\kappa}_y$ in Eqs. (3.18a,b) on the right-hand-side, four set of equations can be derived. The constants $f_n^{(0)}$, $f_n^{(1)}$, $f_{-n}^{(0)}$, $f_{-n}^{(1)}$ can be solved by comparing the coefficients of $\sin(\mu_n y)$, which are

$$
\begin{aligned}
&f_n^{(0)} = f_{-n}^{(0)} = f_n^{(1)} = f_{-n}^{(1)} = 0 && \text{for} \quad n = 2,4,6\cdots \\
&f_n^{(0)} = \frac{e^{\alpha_n} q\left\{-3+2\alpha_n + e^{2\alpha_n}\left[2-12\alpha_n + e^{2\alpha_n}\left(-1+2e^{2\alpha_n}-4\alpha_n\right)\left(1+2\alpha_n\right)\right]\right\}}{Db{\mu_n}^3\left(-1+e^{8\alpha_n}-8\alpha_n e^{4\alpha_n}\right)} && \text{for} \quad n = 1,3,5\cdots \\
&f_{-n}^{(0)} = \frac{e^{\alpha_n} q\left[2-4\alpha_n - e^{6\alpha_n}\left(3+2\alpha_n\right) - e^{2\alpha_n}\left(-1+2\alpha_n\right)\left(-1+4\alpha_n\right) + e^{4\alpha_n}\left(2+12\alpha_n\right)\right]}{Db{\mu_n}^3\left(-1+e^{8\alpha_n}-8\alpha_n e^{4\alpha_n}\right)} && \text{for} \quad n = 1,3,5\cdots \\
&f_n^{(1)} = \frac{2e^{\alpha_n} q\left\{1+e^{4\alpha_n}\left[3+4\alpha_n - 4\cosh\left(2\alpha_n\right)\right]\right\}}{Db{\mu_n}^2\left(-1+e^{8\alpha_n}-8\alpha_n e^{4\alpha_n}\right)} && \text{for} \quad n = 1,3,5\cdots \\
&f_{-n}^{(1)} = -\frac{2e^{\alpha_n} q\left[-2+e^{2\alpha_n}\left(3-2e^{2\alpha_n}+e^{4\alpha_n}-4\alpha_n\right)\right]}{Db{\mu_n}^2\left(-1+e^{8\alpha_n}-8\alpha_n e^{4\alpha_n}\right)} && \text{for} \quad n = 1,3,5\cdots
\end{aligned}
\tag{3.48}
$$

where α_n is given in Eq. (3.23).

From Eqs. (3.8), (3.12), (3.15), (3.16) and (3.48), the bending deflection of a thin plate under uniformly distributed load is

$$
\begin{aligned}
w = {} & \frac{q}{24D}\left(y^4 - 2by^3 + b^3 y\right) + \\
& \frac{4q}{bD}\sum_{n=1}^{\infty}\left\{\left\{e^{4\alpha_n}\sin\left(\mu_n y\right)\left[-2\left(3\alpha_n+\mu_n x\right)\cosh\left(\alpha_n-\mu_n x\right) + \left(\alpha_n+\mu_n x\right)\cosh\left(3\alpha_n-\mu_n x\right) - \right.\right. \\
& 5\alpha_n\cosh\left(\alpha_n+\mu_n x\right) + 3\mu_n x\cosh\left(\alpha_n+\mu_n x\right) + 2\alpha_n\cosh\left(3\alpha_n+\mu_n x\right) - 2\mu_n x\cosh\left(3\alpha_n+\mu_n x\right) + \\
& \left.\left.8\cosh\left(2\alpha_n\right)\cosh\left(\mu_n x\right)\sinh\left(\alpha_n\right) - 4\alpha_n\left(\alpha_n-\mu_n x\right)\sinh\left(\alpha_n+\mu_n x\right)\right]\right\} \Big/ \left[\left(1+8e^{4\alpha_n}-e^{8\alpha_n}\right){\mu_n}^5\right]\Big\}
\end{aligned}
\tag{3.49}
$$

In addition, the general solutions for bending moments and stress resultants of a SSSC plate related to the state vector $\boldsymbol{v} = \left\{\phi_{x,}\, \phi_{y,}\, \kappa_{y,}\, \kappa_{xy}\right\}^T$ can be derived accordingly. Numerical results are shown below:

Table 3.6 Deflection and bending moment factors α, β, γ for a uniformly loaded SSSC rectangular plate with $\upsilon = 0.3$ ($l = b$ for $a \geq b$ and $l = a$ for $a < b$).

Aspect ratio a/b	Deflection factor α at centre $x = 0, y = b/2$ ($w = \alpha q l^4/D$)		Bending moment factor β at $x = a/2, y = b/2$ where ($M_y = \beta q b^2$)		Bending moment factor γ at $x = 0, y = b/2$ where ($M_x = \gamma q b^2$)	
	[1]	Present	[1]	Present	[1]	Present
1/2	0.0093	0.00927022	0.122	0.121513	0.047	0.0468662
2/3	0.0064	0.00644513	0.112	0.112132	0.048	0.0477637
1	0.0028	0.00278549	0.084	0.0838752	0.039	0.0391781
1.5	0.0042	0.00424944	0.111	0.111212	0.054	0.0543760
2	0.0049	0.00487850	0.122	0.0121190	0.060	0.0601393

[1]: (Timoshenko and Woinowsky-Krieger, 1959)

3.4 Closure

It is noted that exact analytical solutions for many of the cases above are not presented in the book (Timoshenko and Woinowsky-Krieger, 1959), only the maximum deflection w_{max} or deflection at specific locations are given. Using the approach presented here, the exact deflection solutions for the cases are expressed in Eqs. (3.24), (3.29), (3.34), (3.39), (3.44) and (3.49) for SSSS, SFSF, SCSC, SFSC, SSSF and SSSC, respectively. In addition, exact expressions for bending moments and stress resultants can be easily derived using basic relation of elasticity.

Comparison with the results in the book (Timoshenko and Woinowsky-Krieger, 1959) for the six cases above is presented in Tables 3.1 to 3.6, respectively. It is obvious that excellent comparison is observed in all cases thus indicating

applicability and validity of the symplectic approach for solving exact plate bending solutions. This part of the research has been published in the international journal (Lim *et al*., 2007 a). The analysis can be easily extended to bending of plates with other types of boundary conditions and it will constitute the scope of analysis in the following sessions of this thesis.

Chapter 4 Plates with Opposite Sides Clamped

4.1 Introduction

Although there are numerous research works on this type of plates, exact solution is still unavailable. The difference between the clamped one and the simply supported one is that: eigenvalue is complex number for the former. It means more mathematical treatment is required for plates with opposite sides clamped. The expression of general solution has been formulated by Yao *et al*. (2007). Based on that formulation, the exact bending solutions for plates with two opposite sides clamped have been derived and shown in this chapter. Below shows the configuration and coordinate system of plates which are discussed in this chapter.

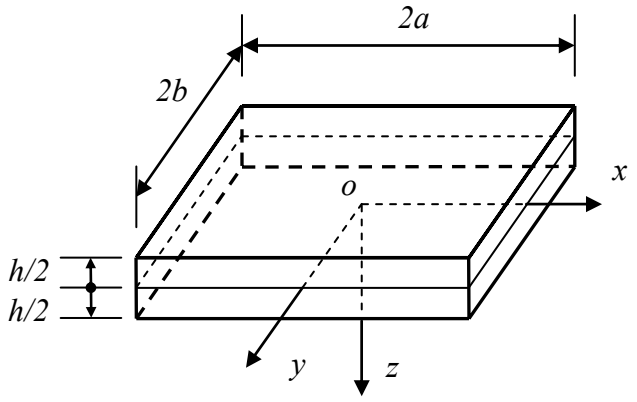

Fig. 4.1 Configuration and coordinate system of plates

4.2 Symplectic formulation

Consider a plate with two opposite sides clamped at $y=-b$ and $y=b$, the boundary conditions are

$$w\big|_{y=\pm b}=0,\quad \theta\big|_{y=\pm b}=\left.\frac{\partial w}{\partial y}\right|_{y=\pm b}=0 \tag{4.1a,b}$$

Knowing that $\kappa_x=\frac{1}{D}\frac{\partial \phi_y}{\partial y}-\nu\kappa_y=\frac{\partial^2 w}{\partial x^2}$ and $\kappa_{xy}=-\frac{\partial w^2}{\partial x\partial y}$, the boundary conditions in Eq. (4.1) can be replaced by

$$\left.\left(\frac{1}{D}\frac{\partial \phi_y}{\partial y}-\upsilon\kappa_y\right)\right|_{y=\pm b}=0,\quad \kappa_{xy}\big|_{y=\pm b}=0 \tag{4.2a,b}$$

There are six eigen-solutions with zero eigenvalue (including Jordan form eigen-solution) but they are all solutions without real physical interpretation. (Zhong and Yao, 1997).There are simply the spurious solutions of the original problem due to the replacement of $w=\frac{\partial w}{\partial y}=0$ by $\kappa_x=\kappa_{xy}=0$. Hence only the eigen-solutions of nonzero eigenvalues for plate with opposite sides clamped are discussed here. The solutions can be divided into two sets: the symmetric and the antisymmetric solutions with respect to x.

Substituting solutions with only A and C terms in general solutions into the homogeneous boundary conditions (4.2) and equating the determinant of coefficient matrix to zero yields a transcendental equation of nonzero eigenvalues for symmetric plate deformation with both opposite sides clamped as

$$2\mu b+\sin\left(2\mu b\right)=0 \tag{4.3}$$

Let eigenvalues μ_n be a solution to Eq. (4.3), the corresponding eigen-solution for symmetric deformation is

$$\psi_n = \begin{Bmatrix} -\left[\cos^2(\mu_n b)+\dfrac{1+\nu}{1-\nu}\right]\cos(\mu_n y)+\mu_n y\sin(\mu_n y) \\ \left[\cos^2(\mu_n b)-\dfrac{2}{1-\nu}\right]\sin(\mu_n y)+\mu_n y\cos(\mu_n y) \\ \dfrac{\mu_n}{D(1-\nu)}\left\{-\left[1+\cos^2(\mu_n b)\right]\cos(\mu_n y)+\mu_n y\sin(\mu_n y)\right\} \\ \dfrac{\mu_n}{D(1-\nu)}\left\{\cos^2(\mu_n b)\sin(\mu_n y)+\mu_n y\cos(\mu_n y)\right\} \end{Bmatrix} \tag{4.4}$$

And the solution for the corresponding problem

$$\dot{\nu} = \boldsymbol{H}\nu \tag{4.5}$$

is

$$\nu_n = \exp(\mu_n x)\psi_n \tag{4.6}$$

Further from the curvature-deflection relation, the deflection of plate after integration is

$$w_n = -\frac{\exp(\mu_n x)}{D\mu_n(1-\upsilon)}\left\{\sin^2(\mu_n b)\cos(\mu_n y)+\mu_n y\sin(\mu_n y)\right\} \tag{4.7}$$

The first several eigenvalues calculated by Mathematica for a plate with Poisson's ratio ν=0.3 are listed in Table 4.1

Table 4.1 Nonzero eigenvalue for symmetric deformation of thin plate with both opposite sides free (ν=0.3)

N	1	2	3	4	5
Re($\mu_n b$)	0.5π+0.5354	1.5π +0.6439	2.5π +0.6827	3.5π +0.7036	4.5π +0.7169
Im($\mu_n b$)	1.1254	1.5516	1.7755	1.9294	2.0469

Substituting solutions with only B and D terms in general solutions into the homogeneous boundary conditions (4.2) and equating the determinant of coefficient matrix to zero yield the transcendental equation of nonzero eigenvalues for antisymmetric plate deformation with both opposite sides free as

$$2\mu b = \sin\left(2\mu b\right) \tag{4.8}$$

The corresponding eigen-solution for antisymmetric deformation is

$$\bar{\psi}_n = \begin{Bmatrix} -\left[\sin^2\left(\bar{\mu}_n b\right)+\dfrac{1+\nu}{1-\nu}\right]\sin\left(\bar{\mu}_n y\right)-\bar{\mu}_n y\cos\left(\bar{\mu}_n y\right) \\ \left[\dfrac{2}{1-\nu}-\sin^2\left(\bar{\mu}_n b\right)\right]\cos\left(\bar{\mu}_n y\right)+\bar{\mu}_n y\sin\left(\bar{\mu}_n y\right) \\ -\dfrac{\bar{\mu}_n}{D\left(1-\nu\right)}\left\{\left[1+\sin^2\left(\bar{\mu}_n b\right)\right]\sin\left(\bar{\mu}_n y\right)+\bar{\mu}_n y\cos\left(\bar{\mu}_n y\right)\right\} \\ \dfrac{\bar{\mu}_n}{D\left(1-\nu\right)}\left\{-\sin^2\left(\bar{\mu}_n b\right)\cos\left(\bar{\mu}_n y\right)+\bar{\mu}_n y\sin\left(\bar{\mu}_n y\right)\right\} \end{Bmatrix} \tag{4.9}$$

And the solution for Eq. (4.5) is

$$\bar{\boldsymbol{v}}_n = \exp(\mu_n x)\bar{\boldsymbol{\psi}}_n \tag{4.10}$$

Further from the curvature-deflection relation, the deflection of plate after integration is

$$\bar{w}_n = \frac{\exp(\bar{\mu}_n x)}{D\bar{\mu}_n\left(1-\upsilon\right)}\left\{-\cos^2\left(\bar{\mu}_n b\right)\sin\left(\bar{\mu}_n y\right)+\bar{\mu}_n y\cos\left(\bar{\mu}_n y\right)\right\} \tag{4.11}$$

Table 4.2 Nonzero eigenvalue for antisymmetric deformation of thin plate with both opposite sides free (v=0.3)

N	1	2	3	4	5
Re($\bar{\mu}_n b$)	π+0.6072	2 π+0.6668	3 π+0.6954	4 π+0.7109	5π+0.7219
Im($\bar{\mu}_n b$)	1.3843	1.6761	1.8584	1.9916	2.0966

Similarly, the first several eigenvalues for a plate with Poisson's ratio ν=0.3, are listed in Table 4.2.

Based on the eigenvalues and eigenvectors, the general solution for plate with both opposite sides clamped can be solved from the expansion theorem. Thus analytical solution of the original problem can be obtained.

Consider bending of plate with both opposite sides clamped under uniformly distributed load q. As the problem is symmetric with respect to x-axis, the expanded expression can only be constructed from the symmetric eigen-solutions of nonzero eigenvalue (4.3), (4.4), (4.6) and (4.7) as

$$\boldsymbol{v} = \sum_{n=1}^{\infty} \left[f_n \boldsymbol{v}_n + \overline{f}_n \overline{\boldsymbol{v}}_n + f_{-n} \boldsymbol{v}_{-n} + \overline{f}_{-n} \overline{\boldsymbol{v}}_{-n} \right] \tag{4.12}$$

And the deflection of the plate is

$$w = w^* + \sum_{n=1}^{\infty} \left[f_n w_n + \overline{f}_n \overline{w}_n + f_{-n} w_{-n} + \overline{f}_{-n} \overline{w}_{-n} \right] \tag{4.13}$$

where $\boldsymbol{v}_n, \boldsymbol{v}_{-n}$ are eigenvalues corresponding to the eigenvalue μ_n listed in table 4.1 and their respective symplectic adjoint eigenvalue $-\mu_n$, while $\overline{\boldsymbol{v}}_n, \overline{\boldsymbol{v}}_{-n}$ are eigenvectors corresponding to the complex conjugate eigenvalues $\pm\mu_n$. A particular solution caused by distributed load q in the domain is

$$w^* = \frac{q}{24D}\left(y^2 - b^2\right)^2 \tag{4.14}$$

the corresponding curvatures and bending moments are

$$\begin{aligned} &\kappa_x^* = \kappa_{xy}^* = 0, \qquad \kappa_y^* = \frac{q}{6D}\left(3y^2 - b^2\right) \\ &\phi_x^* = 0, \qquad \phi_y^* = \frac{q\nu}{6}\left(y^3 - b^2 y\right) \\ &M_x^* = \frac{q\nu}{6}\left(3y^2 - b^2\right), \qquad M_y^* = \frac{q}{6}\left(3y^2 - b^2\right) \end{aligned} \tag{4.15a-f}$$

Eq. (4.12) satisfies the homogeneous differential equation in the domain and the homogeneous boundary conditions on two sides (4.2). $f_i, \overline{f}_i$ $(i = \pm 1, \pm 2, \cdots)$ are the unknown constants which can be determined by the boundary conditions at x direction.

Value of w, M_x, M_y can be obtained once the constant f can be determined through the boundary conditions at x direction.

4.3 Symplectic treatment for the boundary

The formulation derived in Sec. 4.2 is valid for bending of a thin plate with two opposite sides clamped at $y = -b$ and $y = b$ and no restriction is imposed on the remaining two boundaries. Exact bending solutions for various examples of such plates are presented as follows.

4.3.1 Fully clamped plate (CCCC)

The boundary condition at x direction is

$$\kappa_y\big|_{x=\pm a} = 0 \quad ; \quad \kappa_{xy}\big|_{x=\pm a} = 0 \tag{4.16}$$

Then the variational formula for the boundary conditions at two ends $x = \pm a$ is

$$\int_{-b}^{b} \left[\left(\kappa_y + \kappa_y^* \right) \delta\phi_x + \left(\kappa_{xy} + \kappa_{xy}^* \right) \delta\phi_y \right]_{x=-a}^{x=a} dy = 0 \tag{4.17}$$

Substitute Eqs. (4.4), (4.6), (4.12) and (4.15) into Eq. (4.17), since $\delta \boldsymbol{f}$ is arbitrary, the coefficient of it should always be zero and so a set of algebraic equations for solving $\boldsymbol{f}$ can be obtained.

$$\boldsymbol{pf} = \boldsymbol{q} \tag{4.18}$$

where $\boldsymbol{p}$ is the coefficient matrix of $\delta \boldsymbol{f}^T \boldsymbol{f}$ in $\int_{-b}^{b}\left[\kappa_y \delta\phi_x + \kappa_{xy}\delta\phi_y\right]_{x=-a}^{x=a} dy$, and $\boldsymbol{q}$ is the coefficient matrix of $\boldsymbol{f}$ in $-\int_{-b}^{b}\left[\kappa_y^* \delta\phi_x + \kappa_{xy}^*\delta\phi_y\right]_{x=-a}^{x=a} dy$.

Solve the first k terms in Eq (4.18) yields the value for $f_n, \overline{f}_n, f_{-n}, \overline{f}_{-n}$. Substitute that results of $f_n, \overline{f}_n, f_{-n}, \overline{f}_{-n}$,Eqs.(4.7) and (4.14) into Eq.(4.13), any point's value about w can be obtained. Others bending solutions such as bending moment and shear force can be derived by the relationships with the deflection. The larger is the k, the more accurate is the result. Actually, when $k = 4$, the solutions have shown excellent agreement with classical results(Timoshenko and Woinowsky-Krieger, 1959), while the latter are obtained by expansion of different series with many more terms （Timoshenko and Woinowsky-Krieger, 1959）and our solutions converge more quickly. The results are listed in table 4.8.

4.3.2 Plate with three sides clamped and one side simply supported (CCCS)

The boundary condition at x direction is

$$\begin{aligned} \kappa_y\big|_{x=-a} &= 0 \quad ; \quad \kappa_{xy}\big|_{x=-a} = 0 \\ \phi_y\big|_{x=a} &= 0 \quad ; \quad \kappa_y\big|_{x=a} = 0 \end{aligned} \tag{4.19}$$

The variational formula for the boundary conditions at two ends $x = \pm a$ is:

$$\int_{-b}^{b}\left[\left(\kappa_y + \kappa_y^*\right)\delta\phi_x + \left(\kappa_{xy} + \kappa_{xy}^*\right)\delta\phi_y\right]_{x=-a} dy + \int_{-b}^{b}\left[\left(\kappa_y + \kappa_y^*\right)\delta\phi_x + \left(\phi_y + \phi_y^*\right)\delta\kappa_{xy}\right]_{x=a} dy = 0 \tag{4.20}$$

Substitute the Eqs. (4.4), (4.6), (4.12) and (4.15) into Eq. (4.19), since $\delta \boldsymbol{f}$ is arbitrary, the coefficient of it should always be zero and so a set of algebraic equations for solving $\boldsymbol{f}$ can be obtained.

$$\boldsymbol{p}\boldsymbol{f} = \boldsymbol{q} \tag{4.21}$$

where $\boldsymbol{p}$ is the coefficient matrix of $\delta \boldsymbol{f}^T \boldsymbol{f}$ in expression $\int_{-b}^{b}\left[\kappa_y \delta\phi_x + \kappa_{xy}\delta\phi_y\right]_{x=-a} dy$ $+\int_{-b}^{b}\left[\kappa_y \delta\phi_x + \phi_y \delta\kappa_{xy}\right]_{x=a} dy$ and $\boldsymbol{q}$ is the coefficient matrix of $\boldsymbol{f}$ in expression $-\left\{\int_{-b}^{b}\left[\kappa_y^* \delta\phi_x + \kappa_{xy}^* \delta\phi_y\right]_{x=-a} dy + \int_{-b}^{b}\left[\kappa_y^* \delta\phi_x + \phi_y^* \delta\kappa_{xy}\right]_{x=a} dy\right\}$.

Solve the first k terms in Eq (4.21) yields the value for $f_n, \overline{f}_n, f_{-n}, \overline{f}_{-n}$. Substitute that results of $f_n, \overline{f}_n, f_{-n}, \overline{f}_{-n}$,Eqs.(4.7)and(4.14)into Eq.(4.13), any point's value about w can be obtained. Others bending solutions such as bending moment and shear force can be derived by the relationships with the deflection. The larger is the k , the more accurate is the result.

4.3.3 Plate with three sides clamped and one side free (CCCF)

The boundary condition at x direction is

$$\begin{aligned} \kappa_y\big|_{x=-a} &= 0 \quad ; \quad \kappa_{xy}\big|_{x=-a} = 0 \\ \phi_x\big|_{x=a} &= 0 \quad ; \quad \phi_y\big|_{x=a} = 0 \end{aligned} \tag{4.22}$$

In this case, the variational formula for the boundary conditions at two ends $x = \pm a$ is

$$\int_{-b}^{b}\left[\left(\kappa_y + \kappa_y^*\right)\delta\phi_x + \left(\kappa_{xy} + \kappa_{xy}^*\right)\delta\phi_y\right]_{x=-a} dy + \int_{-b}^{b}\left[\left(\phi_x + \phi_x^*\right)\delta\kappa_y + \left(\phi_y + \phi_y^*\right)\delta\kappa_{xy}\right]_{x=a} dy = 0 \tag{4.23}$$

Substitute the Eqs. (4.4), (4.6), (4.12) and (4.15) into Eq. (4.23), since $\delta \boldsymbol{f}$ is arbitrary, the coefficient of it should always be zero and so a set of algebraic equations for solving $\boldsymbol{f}$ can be obtained.

$$\boldsymbol{p}\boldsymbol{f} = \boldsymbol{q} \tag{4.24}$$

where $\boldsymbol{p}$ is the coefficient matrix of $\delta \boldsymbol{f}^T \boldsymbol{f}$ in expression $\int_{-b}^{b}\left[\kappa_y \delta\phi_x + \kappa_{xy}\delta\phi_y\right]_{x=-a} dy$ $+\int_{-b}^{b}\left[\phi_x \delta\kappa_y + \phi_y \delta\kappa_{xy}\right]_{x=a} dy$ and $\boldsymbol{q}$ is the coefficient matrix of $\boldsymbol{f}$ in $-\left\{\int_{-b}^{b}\left[\kappa_y^* \delta\phi_x + \kappa_{xy}^* \delta\phi_y\right]_{x=-a} dy + \int_{-b}^{b}\left[\phi_x^* \delta\kappa_y + \phi_y^* \delta\kappa_{xy}\right]_{x=a} dy\right\}$.

Solve the first k terms in Eq (4.24) yields the value for $f_n, \overline{f}_n, f_{-n}, \overline{f}_{-n}$. Substitute that results of $f_n, \overline{f}_n, f_{-n}, \overline{f}_{-n}$,Eqs.(4.7)and(4.14)into Eq.(4.13), any point's value about w can be obtained. Others bending solutions such as bending moment and shear force can be derived by the relationships with the deflection. The larger is the k , the more accurate is the result.

4.3.4 Plate with two opposite sides clamped, one side simply supported and the other side free (CSCF)

The boundary condition at x direction is

$$\begin{aligned} \phi_y\big|_{x=-a} &= 0 \quad ; \qquad \kappa_y\big|_{x=-a} = 0 \\ \phi_x\big|_{x=a} &= 0 \quad ; \qquad \phi_y\big|_{x=a} = 0 \end{aligned} \tag{4.25}$$

The variational formula for the boundary conditions at two ends $x = \pm a$ is

$$\int_{-b}^{b}\left[\left(\kappa_y + \kappa_y^*\right)\delta\phi_x + \left(\phi_y + \phi_y^*\right)\delta\kappa_{xy}\right]_{x=-a} dy + \int_{-b}^{b}\left[\left(\phi_x + \phi_x^*\right)\delta\kappa_y + \left(\phi_y + \phi_y^*\right)\delta\kappa_{xy}\right]_{x=a} dy = 0 \tag{4.26}$$

Substitute the Eqs. (4.4), (4.6), (4.12) and (4.15) into Eq. (4.26), since $\delta \boldsymbol{f}$ is arbitrary, the coefficient of it should always be zero and so a set of algebraic equations for solving $\boldsymbol{f}$ can be obtained.

$$\boldsymbol{p}\boldsymbol{f} = \boldsymbol{q} \tag{4.27}$$

where $\boldsymbol{p}$ is the coefficient matrix of $\delta \boldsymbol{f}^T \boldsymbol{f}$ in the expression of $\int_{-b}^{b}\left[\kappa_y \delta\phi_x + \phi_y \delta\kappa_{xy}\right]_{x=-a} dy + \int_{-b}^{b}\left[\phi_x \delta\kappa_y + \phi_y \delta\kappa_{xy}\right]_{x=a} dy$ and $\boldsymbol{q}$ is the coefficient matrix of $\boldsymbol{f}$ in expression $-\left\{\int_{-b}^{b}\left[\kappa_y^* \delta\phi_x + \phi_y^* \delta\kappa_{xy}\right]_{x=-a} dy + \int_{-b}^{b}\left[\phi_x^* \delta\kappa_y + \phi_y^* \delta\kappa_{xy}\right]_{x=a} dy\right\}$.

Solve the first k terms in Eq. (4.27) yields the value for $f_n, \overline{f}_n, f_{-n}, \overline{f}_{-n}$ can be solved. Substitute those results of $f_n, \overline{f}_n, f_{-n}, \overline{f}_{-n}$, Eqs. (4.7) and (4.14) into Eq. (4.13), any point's value about w can be obtained. Others bending solutions such as bending moment and shear force can be derived by the relationships with the deflection. The larger is the k, the more accurate is the result.

4.3.5 Plate with two opposite sides clamped, the other sides free (CFCF)

The boundary condition at x direction is

$$\phi_x\big|_{x=\pm a} = 0 \quad ; \qquad \phi_y\big|_{x=\pm a} = 0 \tag{4.28}$$

The variational formula for the boundary conditions at two ends $x = \pm a$ is

$$\int_{-b}^{b}\left[\left(\phi_x + \phi_x^*\right)\delta\kappa_y + \left(\phi_y + \phi_y^*\right)\delta\kappa_{xy}\right]_{x=-a}^{x=a} dy = 0 \tag{4.29}$$

Substitute the Eqs. (4.4), (4.6), (4.12) and (4.15) into Eq. (4.29), since $\delta \boldsymbol{f}$ is arbitrary, the coefficient of it should always be zero and so a set of algebraic equations for solving $\boldsymbol{f}$ can be obtained.

$$\boldsymbol{p}\boldsymbol{f} = \boldsymbol{q} \tag{4.30}$$

where $\boldsymbol{p}$ is the coefficient matrix of $\delta \boldsymbol{f}^T \boldsymbol{f}$ in $\int_{-b}^{b} \left[\phi_x \delta\kappa_y + \phi_y \delta\kappa_{xy} \right]_{x=-a}^{x=a} dy$ and $\boldsymbol{q}$ is the coefficient matrix of $\boldsymbol{f}$ in $-\left\{ \int_{-b}^{b} \left[\phi_x^* \delta\kappa_y + \phi_y^* \delta\kappa_{xy} \right]_{x=-a}^{x=a} dy \right\}$.

Solve the first k terms in Eq. (4.30) yields Value for $f_n, \overline{f}_n, f_{-n}, \overline{f}_{-n}$. Substitute those results of $f_n, \overline{f}_n, f_{-n}, \overline{f}_{-n}$, Eqs. (4.7) and (4.14) into Eq. (4.13), any point's value about w can be obtained. Others bending solutions such as bending moment and shear force can be derived by the relationships with the deflection. The larger is the k, the more accurate is the result.

4.4 Symplectic results and discussion

In order to test the stability and accuracy of the results, the convergence and comparison study are carried out in the following sections.

4.4.1 Convergence study

Convergence studies were conducted in which the value of k was varied from $k = 4$ to $k = 7$ as shown in table 4.3 to table 4.7.This convergence study showed that when $k = 4$, the results would suffice for the present problem. It should be pointed

out that the value of k is limited by the word length of a computer, equations would be found to be ill conditioned for k with large value. Also it can be observed that:

- Bending results at the points $(0,0),(0,b)$ converge to a specific value and keep stable.
- Bending results at the point $(a,0)$ oscillate around a specific value and the amplitude decreases as k increases. Theoretically speaking, when $k \to \infty$, the amplitude is equal to zero and the value at the point $(a,0)$ would be stable. The results are exact solution at $x = \pm a$ when $k \to \infty$. While in practical applications, we can only take the larger k in order to get more accurate results.
- The convergence velocity of deflection is larger than that of the bending moment. The reason is that bending moment is the higher order derivative of the deflection.
- When the aspect ratio a/b is larger, the bending results are more stable. That because the boundary condition at the y direction is fully satisfied while at x direction, as variational principle is employed, the results are approximate when $k \neq \infty$. So if the influence of the edge at y direction is larger, the results will be better.

Table 4.3 Convergence study of the bending results of CCCC plates (v=0.3)

$Dw(0,0)/16qb^4$				
a/b	$k=4$	$k=5$	$k=6$	$k=7$
1.0	0.00126541	0.00126535	0.00126533	0.00126532
1.2	0.00172495	0.00172490	0.00172488	0.00172487
1.5	0.00219658	0.00219654	0.00219653	0.00219653
1.7	0.00238207	0.00238204	0.00238203	0.00238203
2.0	0.00253298	0.00253296	0.00253296	0.00253296
$M_x(0,0)/4qb^2$				
a/b	$k=4$	$k=5$	$k=6$	$k=7$
1.0	-0.0229074	-0.0229061	-0.0229056	-0.0229054
1.2	-0.0228416	-0.0228410	-0.0228407	-0.0228406
1.5	-0.0202682	-0.0202681	-0.0202681	-0.0202681
1.7	-0.0182691	-0.0182692	-0.0182692	-0.0182692
2.0	-0.0158078	-0.0158080	-0.0158080	-0.0158080
$M_y(0,0)/4qb^2$				
a/b	$k=4$	$k=5$	$k=6$	$k=7$
1.0	-0.0229062	-0.0229056	-0.0229053	-0.0229052
1.2	-0.0299727	-0.0299721	-0.0299718	-0.0299717
1.5	-0.0367722	-0.0367717	-0.0367716	-0.0367715
1.7	-0.0392702	-0.0392699	-0.0392698	-0.0392697
2.0	-0.0411553	-0.0411551	-0.0411551	-0.0411550
$M_x(a,0)/4qb^2$				
a/b	$k=4$	$k=5$	$k=6$	$k=7$
1.0	0.0513861	0.0514693	0.0511766	0.0514619
1.2	0.0554235	0.0555660	0.0552392	0.0555399
1.5	0.0570233	0.0571909	0.0568527	0.0571568
1.7	0.0570964	0.0572658	0.0569277	0.0572311
2.0	0.0569846	0.0571528	0.0568162	0.0571186
$M_y(0,b)/4qb^2$				
a/b	$k=4$	$k=5$	$k=6$	$k=7$
1.0	0.0513387	0.0513356	0.0513345	0.0513341
1.2	0.0639010	0.0638991	0.0638984	0.0638981
1.5	0.0756602	0.0756592	0.0756589	0.0756587
1.7	0.0798405	0.0798399	0.0798397	0.0798396
2.0	0.0828666	0.0828663	0.0828662	0.0828661

Table 4.4 Convergence study of the bending results of CCCS plates (v=0.3)

$Dw(0,0)/16qb^4$				
a/b	$k=4$	$k=5$	$k=6$	$k=7$
1.0	0.00157048	0.00157048	0.00157048	0.00157047
1.2	0.00196902	0.00196901	0.00196901	0.00196901
1.5	0.00233584	0.00233583	0.00233583	0.00233582
1.7	0.00246964	0.00246964	0.00246964	0.00246964
2.0	0.00257192	0.00257191	0.00257191	0.00257191
$M_x(0,0)/4qb^2$				
a/b	$k=4$	$k=5$	$k=6$	$k=7$
1.0	-0.0236010	-0.0236004	-0.0236001	-0.0236000
1.2	-0.0222113	-0.0222110	-0.0222109	-0.0222108
1.5	-0.0190369	-0.0190368	-0.0190367	-0.0190367
1.7	-0.0171209	-0.0171208	-0.0171208	-0.0171208
2.0	-0.0149893	-0.0149893	-0.0149893	-0.0149893
$M_y(0,0)/4qb^2$				
a/b	$k=4$	$k=5$	$k=6$	$k=7$
1.0	-0.0277421	-0.0277420	-0.0277420	-0.02774190
1.2	-0.0336203	-0.0336201	-0.0336201	-0.03362008
1.5	-0.0386956	-0.0386955	-0.0386955	-0.03869545
1.7	-0.0404136	-0.0404135	-0.0404135	-0.04041343
2.0	-0.0416094	-0.0416093	-0.0416093	-0.04160929
$M_x(a,0)/4qb^2$				
a/b	$k=4$	$k=5$	$k=6$	$k=7$
1.0	0	-0.0000218518	0.0000223367	-0.0000183799
1.2	0	-0.0000218610	0.0000223310	-0.0000183914
1.5	0	-0.0000218382	0.0000223416	-0.0000183898
1.7	0	-0.0000218271	0.0000223471	-0.0000183873
2.0	0	-0.0000218200	0.0000223506	-0.0000184497
$M_y(0,b)/4qb^2$				
a/b	$k=4$	$k=5$	$k=6$	$k=7$
1.0	0.0600023	0.0600017	0.0600014	0.0600012
1.2	0.0703008	0.0703003	0.0703001	0.0703001
1.5	0.0789198	0.0789195	0.0789194	0.0789194
1.7	0.0817223	0.0817221	0.0817221	0.0817220
2.0	0.0835650	0.0835649	0.0835649	0.0835649

Table 4.5 Convergence study of the bending results of CCCF plates (v=0.3)

$Dw(0,0)/16qb^4$

a/b	$k=4$	$k=5$	$k=6$	$k=7$
1.0	0.00188952	0.00188969	0.00188981	0.00188990
1.2	0.00214069	0.00214075	0.00214081	0.00214086
1.5	0.00238490	0.00238489	0.00238490	0.00238491
1.7	0.00248137	0.00248134	0.00248133	0.00248133
2.0	0.00256166	0.00256163	0.00256162	0.00256161

$M_x(0,0)/4qb^2$

a/b	$k=4$	$k=5$	$k=6$	$k=7$
1.0	-0.0167664	-0.0167595	-0.0167560	-0.0167539
1.2	-0.0172184	-0.0172137	-0.0172112	-0.0172096
1.5	-0.0162716	-0.0162694	-0.0162681	-0.0162673
1.7	-0.0153723	-0.0153711	-0.0153703	-0.0153698
2.0	-0.0141956	-0.0141952	-0.0141949	-0.0141946

$M_y(0,0)/4qb^2$

a/b	$k=4$	$k=5$	$k=6$	$k=7$
1.0	-0.0313606	-0.0313623	-0.0313634	-0.0313644
1.2	-0.0353537	-0.0353540	-0.0353545	-0.0353549
1.5	-0.0389587	-0.0389582	-0.0389581	-0.0389581
1.7	-0.0402849	-0.0402843	-0.0402841	-0.0402840
2.0	-0.0413120	-0.0413115	-0.0413113	-0.0413112

$Dw(a,0)/16qb^4$

a/b	$k=4$	$k=5$	$k=6$	$k=7$
1.0	0.00294495	0.00294605	0.00294631	0.00294821
1.2	0.00295431	0.00295554	0.00295572	0.00295765
1.5	0.00293225	0.00293352	0.00293367	0.00293560
1.7	0.00292193	0.00292321	0.00292335	0.00292527
2.0	0.00291546	0.00291673	0.00291688	0.00291879

$M_x(a,0)/4qb^2$

a/b	$k=4$	$k=5$	$k=6$	$k=7$
1.0	-0.00318793	0.00270158	-0.00187105	0.00103806
1.2	-0.00322766	0.00269352	-0.00184004	0.000999317
1.5	-0.00321726	0.00266578	-0.00180908	0.000972200
1.7	-0.00320750	0.00265556	-0.00180071	0.000966472
2.0	-0.00291546	0.00264978	-0.00179687	0.000964393

$M_y(0,b)/4qb^2$

a/b	$k=4$	$k=5$	$k=6$	$k=7$
1.0	0.0657496	0.0657493	0.0657505	0.0657519
1.2	0.0727781	0.0727770	0.0727772	0.0727778
1.5	0.0790244	0.0790229	0.0790225	0.0790224
1.7	0.0812600	0.0812587	0.0812582	0.0812580
2.0	0.0829293	0.0829284	0.0829280	0.0829278

Table 4.6 Convergence study of the bending results of CSCF plates (v=0.3)

$Dw(0,0)/16qb^4$

a/b	$k=4$	$k=5$	$k=6$	$k=7$
1.0	0.00224491	0.00224514	0.00224528	0.00224539
1.2	0.00239438	0.00239449	0.00239456	0.00239461
1.5	0.00252378	0.00252379	0.00252381	0.00252382
1.7	0.00256853	0.00256852	0.00256852	0.00256853
2.0	0.00260051	0.00260049	0.00260048	0.00260048

$M_x(0,0)/4qb^2$

a/b	$k=4$	$k=5$	$k=6$	$k=7$
1.0	-0.0175192	-0.0175131	-0.0175099	-0.0175079
1.2	-0.0165766	-0.0165722	-0.0165698	-0.0165683
1.5	-0.0150505	-0.0150483	-0.0150470	-0.0150461
1.7	-0.0142320	-0.0142306	-0.0142298	-0.0142293
2.0	-0.0133793	-0.0133787	-0.0133784	-0.0133781

$M_y(0,0)/4qb^2$

a/b	$k=4$	$k=5$	$k=6$	$k=7$
1.0	-0.0369980	-0.0370004	-0.0370018	-0.0370029
1.2	-0.0391492	-0.0391501	-0.0391507	-0.0391512
1.5	-0.0408781	-0.0408780	-0.0408780	-0.0408781
1.7	-0.0414233	-0.0414229	-0.0414228	-0.0414228
2.0	-0.0417651	-0.0417647	-0.0417646	-0.0417645

$Dw(a,0)/16qb^4$

a/b	$k=4$	$k=5$	$k=6$	$k=7$
1.0	0.00297015	0.00297137	0.00297157	0.00297350
1.2	0.00294819	0.00294946	0.00294961	0.00295155
1.5	0.00292421	0.00292548	0.00292563	0.00292755
1.7	0.00291745	0.00291872	0.00291887	0.00292079
2.0	0.00291424	0.00291551	0.00291565	0.00291759

$M_x(a,0)/4qb^2$

a/b	$k=4$	$k=5$	$k=6$	$k=7$
1.0	-0.00324114	0.00271002	-0.00185416	0.001009700
1.2	-0.00323186	0.00268182	-0.00182232	0.000981468
1.5	-0.00321035	0.00265742	-0.00180163	0.000966705
1.7	-0.00320285	0.00265135	-0.00179759	0.000964571
2.0	-0.00319874	0.00264877	-0.00179625	0.000964467

$M_y(0,b)/4qb^2$

a/b	$k=4$	$k=5$	$k=6$	$k=7$
1.0	0.0758052	0.0758077	0.0758099	0.0758118
1.2	0.0794352	0.0794356	0.0794364	0.0794371
1.5	0.0822781	0.0822774	0.0822773	0.0822773
1.7	0.0831341	0.0831332	0.0831329	0.0831327
2.0	0.0836265	0.0836257	0.0836254	0.0836251

Table 4.7 Convergence study of the bending results of CFCF plates (v=0.3)

$Dw(0,0)/16qb^4$				
a/b	*k* = 4	*k* = 5	*k* = 6	*k* = 7
1.0	0.00255827	0.00255866	0.00255892	0.00255911
1.2	0.00256017	0.00256034	0.00256047	0.00256057
1.5	0.00257152	0.00257153	0.00257156	0.00257158
1.7	0.00257991	0.00257988	0.00257988	0.00257988
2.0	0.00259021	0.00259017	0.00259016	0.00259015
$M_x(0,0)/4qb^2$				
a/b	*k* = 4	*k* = 5	*k* = 6	*k* = 7
1.0	-0.0109747	-0.0109630	-0.0109570	-0.0109531
1.2	-0.0117270	-0.0117185	-0.0117139	-0.0117110
1.5	-0.0123190	-0.0123146	-0.0123121	-0.0123104
1.7	-0.0124935	-0.0124909	-0.0124894	-0.0124883
2.0	-0.0125867	-0.0125857	-0.0125851	-0.0125846
$M_y(0,0)/4qb^2$				
a/b	*k* = 4	*k* = 5	*k* = 6	*k* = 7
1.0	-0.0405929	-0.0405969	-0.0405996	-0.0406016
1.2	-0.0408188	-0.0408200	-0.0408212	-0.0408221
1.5	-0.0411269	-0.0411263	-0.0411263	-0.0411264
1.7	-0.0412911	-0.0412902	-0.0412899	-0.0412898
2.0	-0.0414674	-0.0414666	-0.0414662	-0.0414660
$Dw(a,0)/16qb^4$				
a/b	*k* = 4	*k* = 5	*k* = 6	*k* = 7
1.0	0.00290328	0.00290447	0.00290460	0.00290648
1.2	0.00291114	0.00291237	0.00291250	0.00291441
1.5	0.00291421	0.00291547	0.00291561	0.00291752
1.7	0.00291437	0.00291564	0.00291578	0.00291770
2.0	0.00291418	0.00291545	0.00291560	0.00291751
$M_x(a,0)/4qb^2$				
a/b	*k* = 4	*k* = 5	*k* = 6	*k* = 7
1.0	-0.00318191	0.00264123	-0.00179249	0.000964841
1.2	-0.00319264	0.00264735	-0.00179655	0.000966054
1.5	-0.00319775	0.00264926	-0.00179734	0.000965530
1.7	-0.00319835	0.00264920	-0.00179710	0.000965148
2.0	-0.00319830	0.00264894	-0.00179681	0.000961953
$M_y(0,b)/4qb^2$				
a/b	*k* = 4	*k* = 5	*k* = 6	*k* = 7
1.0	0.08152044	0.0815236	0.0815274	0.0815309
1.2	0.08181548	0.0818152	0.0818164	0.0818177
1.5	0.08236169	0.0823598	0.0823593	0.0823592
1.7	0.08266683	0.0826648	0.0826641	0.0826637
2.0	0.08299035	0.0829888	0.0829880	0.0829876

4.4.2 Comparison study

Table 4.8 compares the bending results obtained using the symplectic method with those of Timoshenko and Woinowsky-Krieger (1959) for CCCC plates. The bending results show excellent agreement. Table 4.9 to Table 4.13 compares the symplectic results with those obtained by finite software ABAQUS for the five cases mentioned in this Chapter (i.e. CCCC, CCCS, CCCF, CSCF and CFCF). It can be seen that there are big gaps between there two results for the bending moment at the edges. Take the results of Timoshenko and Woinowsky-Krieger (1959) as the reference; the ABAQUS® can not predict the bending moment of the plate at the edges accurately. The symplectic method has a wider application than the classical methods and more stable than the finite element method.

Table 4.8 Comparison study for CCCC plates under uniform load (v=0.3)

a/b		$Dw(0,0)/16qb^4$	$M_x(a,0)/4qb^2$	$M_y(0,b)/4qb^2$	$M_x(0,0)/4qb^2$	$M_y(0,0)/4qb^2$
1.0	Present	0.00127	0.0514	0.0513	-0.0229	-0.0229
	[1]	0.00126	0.0513	0.0513	-0.0231	-0.0231
1.1	Present	0.00151	0.0539	0.0581	-0.0231	-0.0267
	[1]	0.00150	0.0538	0.0581	-0.0231	-0.0264
1.2	Present	0.00173	0.0554	0.0639	-0.0228	-0.0300
	[1]	0.00172	0.0554	0.0639	-0.0228	-0.0299
1.3	Present	0.00191	0.0563	0.0687	-0.0222	-0.0327
	[1]	0.00191	0.0563	0.0687	-0.0222	-0.0327
1.4	Present	0.00207	0.0568	0.0726	-0.0213	-0.0350
	[1]	0.00207	0.0568	0.0726	-0.0212	-0.0349
1.5	Present	0.00220	0.0570	0.0757	-0.0203	-0.0368
	[1]	0.00220	0.0570	0.0757	-0.0203	-0.0368
1.6	Present	0.00230	0.0571	0.0780	-0.0193	-0.0382
	[1]	0.00230	0.0571	0.0780	-0.0193	-0.0381
1.7	Present	0.00238	0.0571	0.0798	-0.0183	-0.0393
	[1]	0.00238	0.0571	0.0799	-0.0182	-0.0392
1.8	Present	0.00245	0.0571	0.0812	-0.0174	-0.0401
	[1]	0.00245	0.0571	0.0812	-0.0174	-0.0401
1.9	Present	0.00250	0.0570	0.0822	-0.0165	-0.0407
	[1]	0.00249	0.0571	0.0822	-0.0165	-0.0407
2.0	Present	0.00253	0.0570	0.0829	-0.0158	-0.0412
	[1]	0.00254	0.0571	0.0829	-0.0158	-0.0412

[1]: Results of Timoshenko and Woinowsky-Krieger (1959)

Table 4.9 Comparison study for CCCC plates under uniform load (v=0.3)

a/b	1.0	1.2	1.5	1.7	2.0
$Dw(0,0)/16qb^4$					
Present	0.00127	0.00173	0.00220	0.00238	0.00253
FEM	0.00127	0.00173	0.00220	0.00238	0.00253
$M_x(0,0)/4qb^2$					
Present	-0.0229	-0.0228	-0.0203	-0.0183	-0.0158
FEM	-0.0229	-0.0228	-0.0202	-0.0182	-0.0158
$M_y(0,0)/4qb^2$					
Present	-0.0229	-0.0300	-0.0368	-0.0393	-0.0412
FEM	-0.0229	-0.0300	-0.0367	-0.0392	-0.0411
$M_x(a,0)/4qb^2$					
Present	0.0514	0.0554	0.0570	0.0571	0.0570
FEM	0.0471	0.0510	0.0514	0.0514	0.0525
$M_y(0,b)/4qb^2$					
Present	0.0513	0.0639	0.0757	0.0798	0.0829
FEM	0.0471	0.0591	0.0694	0.0735	0.0778

Table 4.10 Comparison study for CCCS plates under uniform load (v=0.3)

a/b	1.0	1.2	1.5	1.7	2.0
$Dw(0,0)/16qb^4$					
Present	0.00157	0.00197	0.00235	0.00247	0.00257
FEM	0.00157	0.00197	0.00234	0.00247	0.00257
$M_x(0,0)/4qb^2$					
Present	-0.0236	-0.0222	-0.0190	-0.0171	-0.0149
FEM	-0.0236	-0.0222	-0.0190	-0.0171	-0.0149
$M_y(0,0)/4qb^2$					
Present	-0.0277	-0.0336	-0.0387	-0.0404	-0.0416
FEM	-0.0277	-0.0336	-0.0386	-0.0403	-0.0415
$M_y(0,b)/4qb^2$					
Present	-0.0600	-0.0703	-0.0789	-0.0817	-0.0836
FEM	-0.0543	-0.0642	-0.0726	-0.0754	-0.0773

Table 4.11 Comparison study for CCCF plates under uniform load (v=0.3)

a/b	1.0	1.2	1.5	1.7	2.0
$Dw(0,0)/16qb^4$					
Present	0.00189	0.00214	0.00238	0.00248	0.00256
FEM	0.00189	0.00214	0.00238	0.00248	0.00256
$M_x(0,0)/4qb^2$					
Present	-0.0168	-0.0172	-0.0163	-0.0154	-0.0142
FEM	-0.0167	-0.0172	-0.0162	-0.0153	-0.0142
$M_y(0,0)/4qb^2$					
Present	-0.0314	-0.0354	-0.0390	-0.0403	-0.0413
FEM	-0.0313	-0.0353	-0.0389	-0.0402	-0.0412
$Dw(a,0)/16qb^4$					
Present	0.00294	0.00295	0.00293	0.00292	0.00292
FEM	0.00296	0.00296	0.00294	0.00293	0.00292
$M_x(a,0)/4qb^2$					
Present	-0.00319	-0.00323	-0.00322	-0.00320	-0.00292
FEM	-0.000218	-0.00081	-0.00076	-0.00075	-0.00075
$M_y(0,b)/4qb^2$					
Present	0.0657	0.0728	0.0790	0.0813	0.0829
FEM	0.0650	0.0692	0.0729	0.0751	0.0767

Table 4.12 Comparison study for CSCF plates under uniform load (v=0.3)

a/b	1.0	1.2	1.5	1.7	2.0
$Dw(0,0)/16qb^4$					
Present	0.00224	0.00239	0.00252	0.00257	0.00260
FEM	0.00225	0.00239	0.00252	0.00257	0.00260
$M_x(0,0)/4qb^2$					
Present	-0.0175	-0.0166	-0.0150	-0.0142	-0.0134
FEM	-0.0175	-0.0165	-0.0150	-0.0142	-0.0133
$M_y(0,0)/4qb^2$					
Present	-0.0370	-0.0391	-0.0409	-0.0414	-0.0418
FEM	-0.0370	-0.0391	-0.0408	-0.0413	-0.0416
$Dw(a,0)/16qb^4$					
Present	0.00297	0.00295	0.00292	0.00292	0.00291
FEM	0.00298	0.00295	0.00293	0.00292	0.00292
$M_x(a,0)/4qb^2$					
Present	-0.00324	-0.00323	-0.00321	-0.00320	-0.00320
FEM	-0.00083	-0.00078	-0.00075	-0.00075	-0.00075
$M_y(0,b)/4qb^2$					
Present	0.0758	0.0794	0.0823	0.0831	0.0836
FEM	0.0698	0.0733	0.0761	0.0769	0.0774

Table 4.13 Comparison study for CFCF plates under uniform load (v=0.3)

a/b	1.0	1.2	1.5	1.7	2.0
$Dw(0,0)/16qb^4$					
Present	0.00256	0.00256	0.00257	0.00258	0.00259
FEM	0.00256	0.00256	0.00257	0.00258	0.00259
$M_x(0,0)/4qb^2$					
Present	-0.0110	-0.0117	-0.0123	-0.0125	-0.0126
FEM	-0.0109	-0.0117	-0.0123	-0.0125	-0.0126
$M_y(0,0)/4qb^2$					
Present	-0.0406	-0.0408	-0.0411	-0.0412	-0.0415
FEM	-0.0406	-0.0407	-0.0410	-0.0412	-0.0416
$Dw(a,0)/16qb^4$					
Present	0.00290	0.00291	0.00291	0.00291	0.00291
FEM	0.00292	0.00292	0.00292	0.00292	0.00292
$M_x(a,0)/4qb^2$					
Present	-0.00318	-0.00319	-0.00320	-0.00320	-0.00320
FEM	-0.00058	-0.00058	-0.00075	-0.00075	-0.00058
$M_y(0,b)/4qb^2$					
Present	0.0815	0.0818	0.0824	0.0827	0.0830
FEM	0.0768	0.0770	0.0763	0.0765	0.0781

4.5 Closure

In this chapter, the symplectic solution for the plates with two opposite sides clamped is discussed. Variational principle is used to deal with the boundary condition. Convergence and comparison study are conducted to verify the stability and validity of the symplectic method. It can give the accurate results for the edges of the plates which can not be accurately predicted by finite element software. From the study we can conclude that the symplectic method can successfully solve the bending solutions of plates with two opposite sides clamped.

Chapter 5 Plates with Opposite Sides Unsymmetrical

5.1 Introduction

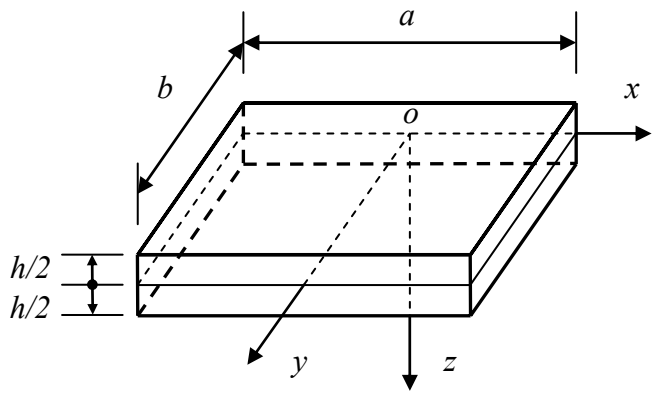

Fig. 5.1 Configuration and coordinate system of plates

Symplectic solution for plates with opposite sides unsymmetrical will be discussed in this chapter. The cases include: plates with one side simply supported and the opposite side clamped, plates with one side simply supported and the opposite side free and plates with one side clamped and the opposite side free. Without symmetry, more constants should be solved in the symplectic formulation. In this chapter, the eigenvalue, eigenvector, general solutions are newly developed by the current research study. Then the constant for the general solution will be solved from the boundary conditions at the x direction. Consequently, the exact

solutions are obtained. Fig.5.1 shows the configuration and coordinate system of plates which are discussed in this chapter.

5.2 Plates with one side simply supported and the opposite side clamped

In this section, the transcendental equation, eigenvalue, eigenvector and general solution for plates with one side simply supported and the opposite side clamped are derived. Based on that derivation, the bending solutions for four types of plates (CFSF, CSSF, CCSF and CSSC) will be solved.

5.2.1 Symplectic formulation

Consider a plate with one side simply supported and the opposite side clamped at $y=0$ and $y=b$, the boundary conditions are

$$\begin{aligned} &M_y\big|_{y=0}=0, \quad w\big|_{y=0}=0 \\ &\theta\big|_{y=b}=0, \quad w\big|_{y=b}=0 \end{aligned} \tag{5.1}$$

Knowing that $\theta=\dfrac{\partial w}{\partial y}$, $M_y=\dfrac{\partial \phi_x}{\partial x}$, $\kappa_x=\dfrac{1}{D}\dfrac{\partial \phi_y}{\partial y}-\nu\kappa_y=\dfrac{\partial^2 w}{\partial x^2}$ and $\kappa_{xy}=-\dfrac{\partial w^2}{\partial x \partial y}$, the boundary conditions in Eq. (5.1) can be replaced by

$$\begin{aligned} &\phi_x\big|_{y=0}=0, \quad \left.\frac{1}{D}\frac{\partial \phi_y}{\partial y}-\nu\kappa_y\right|_{y=0}=0 \\ &\kappa_{xy}\big|_{y=b}=0, \quad \left.\frac{1}{D}\frac{\partial \phi_y}{\partial y}-\nu\kappa_y\right|_{y=b}=0 \end{aligned} \tag{5.2}$$

For a zero eigenvalue, the eigen-solutions are all equal to zero. These are trivial solutions and they do not have physical interpretation. For nonzero eigenvalues, substituting the general eigen-solutions expressed by Eq.(2.39) into the homogeneous boundary conditions (5.2), and equating the determinant of coefficient matrix to zero yield the transcendental equation of nonzero eigenvalues for bending of simply supported plate on opposite sides along $y=0$ and $y=b$ as

$$\sin\left(2\mu b\right)=2\mu b \tag{5.3}$$

The corresponding basic eigenvector is

$$\psi_n=\begin{pmatrix}\phi_x\\ \phi_y\\ \kappa_y\\ \kappa_{xy}\end{pmatrix}=\begin{Bmatrix}-\left[\sin^2\left(\mu_n b\right)+\dfrac{1+\nu}{1-\nu}\right]\sin\left(\mu_n y\right)-\mu_n y\cos\left(\mu_n y\right)\\ \left[\dfrac{2}{1-\nu}-\sin^2\left(\mu_n b\right)\right]\cos\left(\mu_n y\right)+\mu_n y\sin\left(\mu_n y\right)\\ -\dfrac{\mu_n}{D\left(1-\nu\right)}\left\{\left[1+\sin^2\left(\mu_n b\right)\right]\sin\left(\mu_n y\right)+\mu_n y\cos\left(\mu_n y\right)\right\}\\ \dfrac{\mu_n}{D\left(1-\nu\right)}\left\{-\sin^2\left(\mu_n b\right)\cos\left(\mu_n y\right)+\mu_n y\sin\left(\mu_n y\right)\right\}\end{Bmatrix} \tag{5.4}$$

Then the solution to eigenvalue equation (2.32) is

$$\boldsymbol{v}_n=\exp(\mu_n x)\boldsymbol{\psi}_n \tag{5.5}$$

From the curvature-deflection relation (2.9), the deflection of plate can be expressed as

$$w_n=\frac{\exp(\mu_n x)}{D\mu_n\left(1-\upsilon\right)}\left\{-\cos^2\left(\mu_n b\right)\sin\left(\mu_n y\right)+\mu_n y\cos\left(\mu_n y\right)\right\} \tag{5.6}$$

The first several eigenvalues for a plate with Poisson's ratio ν=0.3 are listed in Table 5.1.

Based on the eigenvalues and eigenvectors, the general solution for a plate with one side simply supported and the opposite side clamped can be solved from the

expansion theorem. Thus, the analytical solution of the original problem can be obtained.

Table 5.1 Nonzero eigenvalue for plates with one side simply supported and the opposite side clamped (v=0.3)

N	1	2	3	4	5
Re($\mu_n b$)	π+0.6072	2 π+0.6668	3 π+0.6954	4 π+0.7109	5π+0.7219
Im($\mu_n b$)	1.3843	1.6761	1.8584	1.9916	2.0966

5.2.2 Symplectic treatment for the boundary

The formulation derived in Sec. 5.2.1 is valid for bending of a thin plate with one side simply supported and the opposite side clamped at $y = 0$ and $y = b$ and no restriction is imposed on the remaining two boundaries. Exact bending solutions for various examples of such plates are presented as follows.

5.2.2.1 Plates with two opposite sides free, one side simply supported and the opposite side clamed (CFSF)

Consider a plate with boundary conditions CFSF under a uniformly distributed load q .The expanded expression can be constructed from the eigen-solutions of nonzero eigenvalue (5.3-5.6) as

$$\boldsymbol{v} = \sum_{n=1}^{\infty} \left[f_n \boldsymbol{v}_n + \overline{f}_n \overline{\boldsymbol{v}}_n + f_{-n} \boldsymbol{v}_{-n} + \overline{f}_{-n} \overline{\boldsymbol{v}}_{-n} \right] \tag{5.7}$$

where $\boldsymbol{v}_n, \boldsymbol{v}_{-n}$ are the eigenvectors that correspond to the eigenvalue μ_n, which is listed in Table 5.1 and their respective symplectic adjoint eigenvalue $-\mu_n$, while $\overline{\boldsymbol{v}}_n, \overline{\boldsymbol{v}}_{-n}$ are the eigenvectors that correspond to the complex conjugate eigenvalues $\pm\mu_n$.

and the deflection of the plate is

$$w = w^* + \sum_{n=1}^{\infty}\left[f_n w_n + \overline{f}_n \overline{w}_n + f_{-n} w_{-n} + \overline{f}_{-n} \overline{w}_{-n} \right] \tag{5.8}$$

A particular solution caused by distributed load q in the domain is

$$w^* = \frac{q}{48D}\left(2y^4 - 3by^3 + b^3 y\right) \tag{5.9}$$

the corresponding bending moment and shear force are

$$\begin{aligned} &\kappa_x^* = \kappa_{xy}^* = 0, && \kappa_y^* = \frac{q}{8D}\left(4y^2 - 3by\right) \\ &\phi_x^* = 0, && \phi_y^* = \frac{q\nu}{48} y^2 \left(-9b + 8y\right) \\ &M_x^* = \frac{q\nu}{8}\left(4y^2 - 3by\right), && M_y^* = \frac{q}{8}\left(4y^2 - 3by\right) \end{aligned} \tag{5.10a-f}$$

Eqs.(5.7) to (5.10) are also applicable to the other cases of plates with one side simply supported and the opposite side clamped.

The boundary condition in x direction is

$$\phi_x\big|_{x=\pm\frac{a}{2}} = 0 \quad ; \qquad \phi_y\big|_{x=\pm\frac{a}{2}} = 0 \tag{5.11}$$

The variational formula for the boundary conditions at two ends $x = \pm\dfrac{a}{2}$ is

$$\int_0^b \left[\left(\phi_x + \phi_x^*\right)\delta\kappa_y + \left(\phi_y + \phi_y^*\right)\delta\kappa_{xy} \right]_{x=-\frac{a}{2}}^{x=\frac{a}{2}} dy = 0 \tag{5.12}$$

Substitute the Eqs. (5.4), (5.5), (5.7) and (5.10) into Eq. (5.12), since $\delta \boldsymbol{f}$ is arbitrary, the coefficient of it should always be zero and so a set of algebraic equations for solving $\boldsymbol{f}$ can be obtained.

$$\boldsymbol{p}\boldsymbol{f} = \boldsymbol{q} \tag{5.13}$$

where $\boldsymbol{p}$ is the coefficient matrix of $\delta \boldsymbol{f}^T \boldsymbol{f}$ in $\int_0^b \left[\phi_x \delta\kappa_y + \phi_y \delta\kappa_{xy} \right]_{x=-\frac{a}{2}}^{x=\frac{a}{2}} dy$ and $\boldsymbol{q}$ is the coefficient matrix of $\boldsymbol{f}$ in $-\left\{ \int_0^b \left[\phi_x^* \delta\kappa_y + \phi_y^* \delta\kappa_{xy} \right]_{x=-\frac{a}{2}}^{x=\frac{a}{2}} dy \right\}$.

Solve the first k terms in Eq. (5.13) yields the value for constants. Consequently, any point's value about w, M_x, M_y can be obtained. The larger is the k, the more accurate is the result.

5.2.2.2 Plates with two adjacent sides simply supported, one side clamped and one side free. (CSSF)

Consider a plate with boundary condition CSSF, under a uniformly distributed load q. The boundary condition in x direction is

$$\begin{aligned} \phi_y\big|_{x=-\frac{a}{2}} &= 0 \quad ; \qquad \kappa_y\big|_{x=-\frac{a}{2}} = 0 \\ \phi_x\big|_{x=\frac{a}{2}} &= 0 \quad ; \qquad \phi_y\big|_{x=\frac{a}{2}} = 0 \end{aligned} \tag{5.14}$$

The variational formula for the boundary conditions at two ends $x = \pm\frac{a}{2}$ is

$$\int_0^b \left[\left(\kappa_y + \kappa_y^* \right) \delta\phi_x + \left(\phi_y + \phi_y^* \right) \delta\kappa_{xy} \right]_{x=-\frac{a}{2}} dy + \int_0^b \left[\left(\phi_x + \phi_x^* \right) \delta\kappa_y + \left(\phi_y + \phi_y^* \right) \delta\kappa_{xy} \right]_{x=\frac{a}{2}} dy = 0 \tag{5.15}$$

Substitute the Eqs. (5.4), (5.5), (5.7) and (5.10) into Eq. (5.15), since $\delta \boldsymbol{f}$ is arbitrary, the coefficient of it should always be zero and so a set of algebraic equations for solving $\boldsymbol{f}$ can be obtained.

$$\boldsymbol{p}\boldsymbol{f} = \boldsymbol{q} \tag{5.16}$$

where $\boldsymbol{p}$ is the coefficient matrix of $\delta \boldsymbol{f}^T \boldsymbol{f}$ in the expression of $\int_0^b \left[\kappa_y \delta\phi_x + \phi_y \delta\kappa_{xy} \right]_{x=-\frac{a}{2}} dy + \int_0^b \left[\phi_x \delta\kappa_y + \phi_y \delta\kappa_{xy} \right]_{x=\frac{a}{2}} dy$ and $\boldsymbol{q}$ is the coefficient matrix of $\boldsymbol{f}$ in $-\left\{ \int_0^b \left[\kappa_y^* \delta\phi_x + \phi_y^* \delta\kappa_{xy} \right]_{x=-\frac{a}{2}} dy + \int_0^b \left[\phi_x^* \delta\kappa_y + \phi_y^* \delta\kappa_{xy} \right]_{x=\frac{a}{2}} dy \right\}$.

Solve the first k terms in Eq. (5.16) yields the value for constants. So any point's value about w, M_x, M_y can be obtained. The larger is the k, the more accurate is the result.

5.2.2.3 Plates with two adjacent sides clamped, one side simply supported and one side free. (CCSF)

Consider a plate with boundary conditions CCSF, under a uniformly distributed load q. The boundary condition in x direction is

$$\begin{aligned} \kappa_y \big|_{x=-\frac{a}{2}} = 0 \quad ; \quad \kappa_{xy} \big|_{x=-\frac{a}{2}} = 0 \\ \phi_x \big|_{x=\frac{a}{2}} = 0 \quad ; \quad \phi_y \big|_{x=\frac{a}{2}} = 0 \end{aligned} \tag{5.17}$$

In this case, the variational formula for the boundary conditions at two ends $x = \pm \frac{a}{2}$ is

$$\int_0^b \left[\left(\kappa_y + \kappa_y^* \right) \delta\phi_x + \left(\kappa_{xy} + \kappa_{xy}^* \right) \delta\phi_y \right]_{x=-\frac{a}{2}} dy + \int_0^b \left[\left(\phi_x + \phi_x^* \right) \delta\kappa_y + \left(\phi_y + \phi_y^* \right) \delta\kappa_{xy} \right]_{x=\frac{a}{2}} dy = 0 \tag{5.18}$$

Substitute the Eqs. (5.4), (5.5), (5.7) and (5.10) into Eq. (5.18), since $\delta \boldsymbol{f}$ is arbitrary, the coefficient of it should always be zero and so a set of algebraic equations for solving $\boldsymbol{f}$ can be obtained.

$$\boldsymbol{p}\boldsymbol{f} = \boldsymbol{q} \tag{5.19}$$

where $\boldsymbol{p}$ is the coefficient matrix of $\delta \boldsymbol{f}^T \boldsymbol{f}$ in expression $\int_0^b \left[\kappa_y \delta\phi_x + \kappa_{xy} \delta\phi_y \right]_{x=-\frac{a}{2}} dy$ $+\int_0^b \left[\phi_x \delta\kappa_y + \phi_y \delta\kappa_{xy} \right]_{x=\frac{a}{2}} dy$ and $\boldsymbol{q}$ is the coefficient matrix of $\boldsymbol{f}$ in $-\left\{ \int_0^b \left[\kappa_y^* \delta\phi_x + \kappa_{xy}^* \delta\phi_y \right]_{x=-\frac{a}{2}} dy + \int_0^b \left[\phi_x^* \delta\kappa_y + \phi_y^* \delta\kappa_{xy} \right]_{x=\frac{a}{2}} dy \right\}$.

Solve the first k terms in Eq. (5.19) yields the value for constants. So any point's value about w, M_x, M_y can be obtained.

5.2.2.4 Plates with two adjacent sides simply supported, others clamped. (CSSC)

Consider a plate with boundary condition CSSC, under a uniformly distributed load q, the boundary condition in x direction is

$$\begin{aligned} \kappa_y \big|_{x=-\frac{a}{2}} = 0 \quad ; \quad \kappa_{xy} \big|_{x=-\frac{a}{2}} = 0 \\ \phi_y \big|_{x=\frac{a}{2}} = 0 \quad ; \quad \kappa_y \big|_{x=\frac{a}{2}} = 0 \end{aligned} \tag{5.20}$$

The variational formula for the boundary conditions at two ends $x = \pm \frac{a}{2}$ is:

$$\int_0^b \left[\left(\kappa_y + \kappa_y^* \right) \delta\phi_x + \left(\kappa_{xy} + \kappa_{xy}^* \right) \delta\phi_y \right]_{x=-\frac{a}{2}} dy + \int_0^b \left[\left(\kappa_y + \kappa_y^* \right) \delta\phi_x + \left(\phi_y + \phi_y^* \right) \delta\kappa_{xy} \right]_{x=\frac{a}{2}} dy = 0 \tag{5.21}$$

Substitute the Eqs. (5.4), (5.5), (5.7) and (5.10) into Eq. (5.21), since $\delta \boldsymbol{f}$ is arbitrary, the coefficient of it should always be zero and so a set of algebraic equations for solving $\boldsymbol{f}$ can be obtained.

$$\boldsymbol{p}\boldsymbol{f} = \boldsymbol{q} \tag{5.22}$$

where $\boldsymbol{p}$ is the coefficient matrix of $\delta \boldsymbol{f}^T \boldsymbol{f}$ in $\int_0^b \left[\kappa_y \delta\phi_x + \kappa_{xy} \delta\phi_y \right]_{x=-\frac{a}{2}} dy$ $+\int_0^b \left[\kappa_y \delta\phi_x + \phi_y \delta\kappa_{xy} \right]_{x=\frac{a}{2}} dy$ and $\boldsymbol{q}$ is the coefficient matrix of $\boldsymbol{f}$ in $-\left\{ \int_0^b \left[\kappa_y^* \delta\phi_x + \kappa_{xy}^* \delta\phi_y \right]_{x=-\frac{a}{2}} dy + \int_0^b \left[\kappa_y^* \delta\phi_x + \phi_y^* \delta\kappa_{xy} \right]_{x=\frac{a}{2}} dy \right\}$.

Solve the first k terms in Eq. (5.22) yields the value for constants. So any point's value about w, M_x, M_y can be obtained.

5.3 Plates with one side simply supported and the opposite side free

In this section, the transcendental equation, eigenvalue, eigenvector and the general bending solutions for plates with one side simply supported and the opposite side free are derived. Based on that derivation, the bending solutions for two types of plates (SFFF and SSFF) will be solved.

5.3.1 Symplectic formulation

Consider a plate with one side simply supported and the opposite side free in the y direction, the boundary conditions are

$$\begin{aligned} M\big|_{y=0} &= 0, \quad w\big|_{y=0} = 0 \\ M\big|_{y=b} &= 0, \quad F_{Vy}\big|_{y=b} = 0 \end{aligned} \tag{5.23}$$

Knowing that $M_y = \dfrac{\partial \phi_x}{\partial x}$, $F_{Vy} = -\dfrac{\partial^2 \phi_y}{\partial x^2}$, and $\kappa_x = \dfrac{1}{D}\dfrac{\partial \phi_y}{\partial y} - \nu\kappa_y = \dfrac{\partial^2 w}{\partial x^2}$, the boundary conditions in Eq. (5.23) can be replaced by

$$\begin{aligned} \phi_x\big|_{y=0} &= a_1, \quad \frac{1}{D}\frac{\partial \phi_y}{\partial y} - \nu\kappa_y\bigg|_{y=0} = 0 \\ \phi_x\big|_{y=b} &= 0, \quad \phi_y\big|_{y=b} = 0 \end{aligned} \tag{5.24}$$

The unknown constant a_1 in the boundary conditions should be treated first because it is an inhomogeneous term.

For a_1 term, the following equation should be solved

$$\boldsymbol{H}\boldsymbol{\psi}_0 = 0 \tag{5.25}$$

with boundary conditions on two sides as

$$\begin{aligned} \phi_x\big|_{y=0} &= 1, \quad \frac{1}{D}\frac{\partial \phi_y}{\partial y} - \nu\kappa_y\bigg|_{y=0} = 0 \\ \phi_x\big|_{y=b} &= 0, \quad \phi_y\big|_{y=b} = 0 \end{aligned} \tag{5.26}$$

The solution is

$$\boldsymbol{\psi_0} = \left\{ -\frac{b-y}{b}, 0, 0, \frac{1}{2D(1-\nu)b} \right\}^{\mathrm{T}} \tag{5.27}$$

and the corresponding solution for Eq. (2.32) is

$$\boldsymbol{\nu}_0 = \boldsymbol{\psi}_0 \tag{5.28}$$

From the curvature-deflection relation, the deflection of the plate after integration is

$$w_0 = \frac{xy}{2bD(1-\nu)} \tag{5.29}$$

and the solution with homogeneous boundary conditions is

$$\begin{aligned} &\phi_x\big|_{y=0}=0, \quad \frac{1}{D}\frac{\partial\phi_y}{\partial y}-\nu\kappa_y\bigg|_{y=0}=0 \\ &\phi_x\big|_{y=b}=0, \quad \phi_y\big|_{y=b}=0 \end{aligned} \tag{5.30}$$

For a zero eigenvalue, the eigensolutions are all equal to zero. These are trivial solutions and they do not have physical interpretation. For nonzero eigenvalues, substituting the general eigensolutions that are expressed by Eq. (2.39) into the homogeneous boundary conditions (5.30) and equating the determinant of the coefficient matrix to zero yield the transcendental equation of nonzero eigenvalues for the bending of simply supported plate on opposite sides along $y=0$ and $y=b$ as

$$2\mu b(1-\nu)+(3+\nu)\sin(2\mu b)=0 \tag{5.31}$$

The corresponding basic eigenvector is

$$\psi_n=\begin{pmatrix}\phi_x\\ \phi_y\\ \kappa_y\\ \kappa_{xy}\end{pmatrix}=\begin{Bmatrix} -\dfrac{3+\nu}{1-\nu}\cos^2(\mu_n b)\sin(\mu_n y)-\mu_n y\cos(\mu_n y) \\ -\dfrac{3+\nu}{1-\nu}\sin^2(\mu_n b)\cos(\mu_n y)+\mu_n y\sin(\mu_n y) \\ \dfrac{\mu_n}{D(1-\nu)^2}\left\{\left[(3+\nu)\sin^2(\mu_n b)-3+\nu\right]\sin(\mu_n y)-(1-\nu)\mu_n y\cos(\mu_n y)\right\} \\ \dfrac{\mu_n}{D(1-\nu)^2}\left\{\left[(3+\nu)\sin^2(\mu_n b)-2\right]\cos(\mu_n y)+(1-\nu)\mu_n y\sin(\mu_n y)\right\} \end{Bmatrix} \tag{5.32}$$

Then, the solution to eigenvalue equation (2.32) is

$$\boldsymbol{v}_n=\exp(\mu_n x)\boldsymbol{\psi}_n \tag{5.33}$$

From the curvature-deflection relation, the deflection of the plate can be expressed as

$$w_n=\exp(\mu_n x)\left[\frac{1+\nu-(3+\nu)\sin^2(\mu_n b)}{D(1-\nu)^2\mu_n}\sin(\mu_n y)+\frac{y\cos(\mu_n y)}{D(1-\nu)}\right] \tag{5.34}$$

Similarly, the first several eigenvalues for a plate with Poisson's ratio ν = 0.3 are listed in Table 5.2.

Table 5.2 Nonzero eigenvalue for a thin plate with one side simply supported and the opposite side free (v=0.3)

N	1	2	3	4
Re($\mu_n b$)	0.5π+0.5690	0.5π+0.7863	1.5π+0.7100	4π+0.7109
Im($\mu_n b$)	0	0	0.7439	0.9865

Based on the eigenvalues and eigenvectors, the general solution for a plate with opposite sides clamped can be solved from the expansion theorem. Thus, the analytical solution of the original problem can be obtained.

5.3.2 Symplectic treatment for the boundary

The formulation derived in Sec. 5.3.1 is valid for bending of a thin plate with one side simply supported and the opposite side free at $y = 0$ and $y = b$ and no restriction is imposed on the remaining two boundaries. Exact bending solutions for various examples of such plates are presented as follows.

5.3.2.1 Plates with one side simply supported others free with support at the corner of two adjacent free sides. (SFFF)

Consider a plate with boundary conditions SFFF under a uniformly distributed load q . The expanded expression can be constructed from the eigensolutions of the nonzero eigenvalue (5.31-5.34) as

$$\boldsymbol{v} = \sum_{n=1}^{\infty} \left[f_n \boldsymbol{v}_n + \overline{f}_n \overline{\boldsymbol{v}}_n + f_{-n} \boldsymbol{v}_{-n} + \overline{f}_{-n} \overline{\boldsymbol{v}}_{-n} \right] \tag{5.35}$$

where $\boldsymbol{v}_n, \boldsymbol{v}_{-n}$ are the eigenvalues that correspond to the eigenvalue μ_n, which is listed in Table 5.2, and their respective symplectic adjoint eigenvalue $-\mu_n$, while $\overline{\boldsymbol{v}}_n, \overline{\boldsymbol{v}}_{-n}$ are the eigenvectors that correspond to the complex conjugate eigenvalues $\pm\mu_n$.

and the deflection of the plate is

$$w = w^* + \sum_{n=1}^{\infty}\left[f_n w_n + \overline{f}_n \overline{w}_n + f_{-n} w_{-n} + \overline{f}_{-n} \overline{w}_{-n} \right] + a_1 w_0 + c_1 x + c_2 y + c_3 \tag{5.36}$$

where the $c_1 x + c_2 y + c_3$ is the rigid body displacement.

As $w\big|_{y=a} = 0$, we can get

$$c_1 = c_3 = 0 \tag{5.37}$$

A particular solution that is caused by the distributed load q in the domain is

$$w^* = \frac{q}{24D(1-\nu)}\left[-3bx^2 y + \left(-2b + 3b\nu\right) y^3 + (1-\nu) y^4 \right] \tag{5.38}$$

and the corresponding bending moment and shear force are

$$M_x^* = \frac{qy}{4}\left[-b\left(1+3\nu\right) + 2\nu y \right], \qquad F_{Vx}^* = 0 \tag{5.39a,b}$$

Consequently,

$$\begin{aligned} \phi_y^* &= \int M_x^* dy \\ \phi_x^* &= \iint F_{Vx}^* dy dy \end{aligned} \tag{5.40a,b}$$

$$\begin{aligned} &\phi_x\big|_{y=0} = a_1, \quad \frac{1}{D}\frac{\partial \phi_y}{\partial y} - \nu\kappa_y\Big|_{y=0} = 0 \\ &\phi_x\big|_{y=b} = 0, \quad \phi_y\big|_{y=b} = 0 \end{aligned} \tag{5.41a,b}$$

Substitute the boundary condition (5.41a, b) into the expression (5.40a, b) and we can get

$$\phi_x^* = a_1\left(1-\frac{y}{b}\right)$$
$$\phi_y^* = \frac{1}{24}b^2 q\left(3b+5b\nu\right)+\frac{1}{24}qy^2\left[-3b\left(1+3\nu\right)+4\nu y\right] \tag{5.42a,b}$$

As $w\big|_{\left(-\frac{a}{2},b\right)} = w\big|_{\left(\frac{a}{2},b\right)} = 0$, a_1, c_2 can be expressed by $f_i, \overline{f}_i$ $(i=\pm1,\pm2,\cdots)$ which are the unknown constants that can be determined by the boundary conditions

$$\phi_x\big|_{x=\pm\frac{a}{2}} = \phi_y\big|_{x=\pm\frac{a}{2}} = 0 \tag{5.43}$$

In practical applications, it is necessary to solve only the first k terms in Eq. (5.35). Then, the variational formula for the boundary conditions at two ends $x=\pm\frac{a}{2}$ is

$$\int_0^b\left[\left(\phi_x+\phi_{x0}+\phi_x^*\right)\delta\kappa_y+\left(\phi_y+\phi_{y0}+\phi_y^*\right)\delta\kappa_{xy}\right]_{x=-\frac{a}{2}}^{x=\frac{a}{2}}dy = 0 \tag{5.44}$$

Substitute Eqs. (5.27) (5.32) (5.35) and (5.42) into Eq. (5.44). Because $\delta\boldsymbol{f}$ is arbitrary, its coefficient should always be zero, and a set of algebraic equations for solving $\boldsymbol{f}$ can be obtained.

$$\boldsymbol{p}\boldsymbol{f} = \boldsymbol{q} \tag{5.45}$$

where $\boldsymbol{p}$ is the coefficient matrix of $\delta\boldsymbol{f}^T\boldsymbol{f}$ in the expression of $\int_0^b\left[\left(\phi_x+\phi_{x0}\right)\delta\kappa_y+\left(\phi_y+\phi_{y0}\right)\delta\kappa_{xy}\right]_{x=-\frac{a}{2}}^{x=\frac{a}{2}}dy$, and $\boldsymbol{q}$ is the coefficient matrix of $\boldsymbol{f}$ in $-\int_0^b\left[\phi_x^*\delta\kappa_y+\phi_y^*\delta\kappa_{xy}\right]_{x=-\frac{a}{2}}^{x=\frac{a}{2}}dy$.

f_n, $\overline{f}_n$, f_{-n}, $\overline{f}_{-n}$ can be solved from Eq. (5.45).

Thus, the expression for w is

$$
\begin{aligned}
w = {} & \frac{q}{24D(1-\nu)}\left[-3bx^2y+\left(-2b+3b\nu\right)y^3+(1-\nu)y^4\right]+a_1\frac{xy}{2bD\left(1-\nu\right)}+c_2y \\
& \sum_{n=1}^{\infty}\left(f_n e^{\mu_n x}\left(\frac{1+\nu-\left(3+\nu\right)\sin^2\left(\mu_n b\right)}{D\left(1-\nu\right)^2\mu_n}\sin\left(\mu_n y\right)+\frac{y\cos\left(\mu_n y\right)}{D\left(1-\nu\right)}\right)+\right. \\
& \quad \overline{f}_n e^{\overline{\mu}_n x}\left(\frac{1+\nu-\left(3+\nu\right)\sin^2\left(\overline{\mu}_n b\right)}{D\left(1-\nu\right)^2\overline{\mu}_n}\sin\left(\overline{\mu}_n y\right)+\frac{y\cos\left(\overline{\mu}_n y\right)}{D\left(1-\nu\right)}\right)+ \\
& \quad f_{-n}e^{\mu_{-n}x}\left(\frac{1+\nu-\left(3+\nu\right)\sin^2\left(\mu_n b\right)}{D\left(1-\nu\right)^2\mu_n}\sin\left(\mu_n y\right)+\frac{y\cos\left(\mu_n y\right)}{D\left(1-\nu\right)}\right)+ \\
& \quad \left.\overline{f}_{-n}e^{\overline{\mu}_{-n}x}\left(\frac{1+\nu-\left(3+\nu\right)\sin^2\left(\overline{\mu}_n b\right)}{D\left(1-\nu\right)^2\overline{\mu}_n}\sin\left(\overline{\mu}_n y\right)+\frac{y\cos\left(\overline{\mu}_n y\right)}{D\left(1-\nu\right)}\right)\right.
\end{aligned}
\tag{5.46}
$$

where the constants can be solved with different value of k

The slope, shear force, bending moment, and twisting moment can be solved according to their relationship with deflection:

$$\theta_x = \frac{\partial w}{\partial x}, \quad \theta_y = \frac{\partial w}{\partial y} \tag{5.48a}$$

$$M_x = D\left(\kappa_x + \nu\kappa_y\right) = D\left(\frac{\partial^2 w}{\partial x^2}+\nu\frac{\partial^2 w}{\partial y^2}\right) \tag{5.48b}$$

$$M_y = D\left(\kappa_y + \nu\kappa_x\right) = D\left(\frac{\partial^2 w}{\partial y^2}+\nu\frac{\partial^2 w}{\partial x^2}\right) \tag{5.48c}$$

$$M_{xy} = D\left(1-\nu\right)\kappa_{xy} = -D\left(1-\nu\right)\frac{\partial^2 w}{\partial x\partial y} \tag{5.48d}$$

$$F_{Vx} = F_{Sx} - \frac{\partial M_{xy}}{\partial y} = \frac{\partial M_x}{\partial x} - \frac{2\partial M_{xy}}{\partial y} = D\left[\frac{\partial^3 w}{\partial x^3}+\left(2-\nu\right)\frac{\partial^3 w}{\partial y^2\partial x}\right] \tag{5.48e}$$

$$F_{Vy} = F_{Sy} - \frac{\partial M_{xy}}{\partial x} = \frac{\partial M_y}{\partial y} - \frac{2\partial M_{xy}}{\partial x} = D\left[\frac{\partial^3 w}{\partial y^3}+\left(2-\nu\right)\frac{\partial^3 w}{\partial x^2\partial y}\right] \tag{5.48f}$$

5.3.2.2 Plates with two adjacent sides simply supported others free (SSFF)

Consider a plate with boundary conditions SSFF under a uniformly distributed load q. The deflection of the plate is

$$w = w^* + \sum_{n=1}^{\infty}\left[f_n w_n + \overline{f}_n \overline{w}_n + f_{-n} w_{-n} + \overline{f}_{-n} \overline{w}_{-n} \right] + a_1 w_0 + c_1 x + c_2 y + c_3 \tag{5.49}$$

where the $c_1 x + c_2 y + c_3$ is the rigid body displacement.

As $w\big|_{y=0} = 0, \quad w\big|_{x=-\frac{a}{2}} = 0$, we can get

$$\begin{aligned} c_1 &= c_3 = 0 \\ c_2 &= a_1 \frac{a}{4bD(1-\nu)} \end{aligned} \tag{5.50a,b}$$

The variational formula for the boundary conditions at two ends $x = \pm\frac{a}{2}$ is

$$\int_0^b \left[\left(\kappa_y + \kappa_{y0} + \kappa_y^*\right)\delta\phi_x + \left(\phi_y + \phi_{y0} + \phi_y^*\right)\delta\kappa_{xy} \right]_{x=-\frac{a}{2}} dy + \int_0^b \left[\left(\phi_x + \phi_{x0} + \phi_x^*\right)\delta\kappa_y + \left(\phi_y + \phi_{y0} + \phi_y^*\right)\delta\kappa_{xy} \right]_{x=\frac{a}{2}} dy = 0 \tag{5.51}$$

Substitute Eqs. (5.27) (5.32) (5.35) and (5.42) into Eq. (5.44). Because $\delta \boldsymbol{f}$ is arbitrary, its coefficient should always be zero, and a set of algebraic equations for solving $\boldsymbol{f}$ can be obtained.

$$\boldsymbol{p}\boldsymbol{f} = \boldsymbol{q} \tag{5.52}$$

where $\boldsymbol{p}$ is the coefficient matrix of $\delta \boldsymbol{f}^T \boldsymbol{f}$ in the expression of $\int_0^b \left[\kappa_y \delta\phi_x + \phi_y \delta\kappa_{xy} \right]_{x=-\frac{a}{2}} dy + \int_0^b \left[\phi_x \delta\kappa_y + \phi_y \delta\kappa_{xy} \right]_{x=\frac{a}{2}} dy$, and $\boldsymbol{q}$ is the coefficient matrix of $\boldsymbol{f}$ in $-\left(\int_0^b \left[\kappa_y^* \delta\phi_x + \phi_y^* \delta\kappa_{xy} \right]_{x=-\frac{a}{2}} dy + \int_0^b \left[\phi_x^* \delta\kappa_y + \phi_y^* \delta\kappa_{xy} \right]_{x=\frac{a}{2}} dy \right)$.

f_n, $\overline{f}_n$, f_{-n}, $\overline{f}_{-n}$ can be solved from Eq. (5.52).

Thus, the expression for w is

$$
\begin{aligned}
w = {} & \frac{q}{24D(1-\nu)}\left[-3bx^2y+\left(-2b+3b\nu\right)y^3+(1-\nu)y^4\right]+a_1\frac{xy}{2bD\left(1-\nu\right)}+a_1\frac{a}{4bD\left(1-\nu\right)}y \\
& \sum_{n=1}^{\infty}\Bigg(f_n e^{\mu_n x}\left(\frac{1+\nu-\left(3+\nu\right)\sin^2\left(\mu_n b\right)}{D\left(1-\nu\right)^2\mu_n}\sin\left(\mu_n y\right)+\frac{y\cos\left(\mu_n y\right)}{D\left(1-\nu\right)}\right)+ \\
& \quad \overline{f}_n e^{\overline{\mu}_n x}\left(\frac{1+\nu-\left(3+\nu\right)\sin^2\left(\overline{\mu}_n b\right)}{D\left(1-\nu\right)^2\overline{\mu}_n}\sin\left(\overline{\mu}_n y\right)+\frac{y\cos\left(\overline{\mu}_n y\right)}{D\left(1-\nu\right)}\right)+ \\
& \quad f_{-n} e^{\mu_{-n} x}\left(\frac{1+\nu-\left(3+\nu\right)\sin^2\left(\mu_n b\right)}{D\left(1-\nu\right)^2\mu_n}\sin\left(\mu_n y\right)+\frac{y\cos\left(\mu_n y\right)}{D\left(1-\nu\right)}\right)+ \\
& \quad \overline{f}_{-n} e^{\overline{\mu}_{-n} x}\left(\frac{1+\nu-\left(3+\nu\right)\sin^2\left(\overline{\mu}_n b\right)}{D\left(1-\nu\right)^2\overline{\mu}_n}\sin\left(\overline{\mu}_n y\right)+\frac{y\cos\left(\overline{\mu}_n y\right)}{D\left(1-\nu\right)}\right)
\end{aligned}
\tag{5.53}
$$

where the constants can be solved with different value of k

The slope, shear force, bending moment, and twisting moment can be solved according to their relationship (5.48) with deflection.

5.4 Plates with one side clamped and the opposite side free

In this section, the transcendental equation, eigenvalue eigenvector and general bending solution for plates with one side clamped and the opposite side free are derived. Based on that derivation, the bending solutions for three types of plates (CFFF, CFFC and CFFS) will be solved.

5.4.1 Symplectic formulation

Consider a plate with one side clamped and the opposite side free in the y direction, the boundary conditions are

$$\begin{aligned} &\theta\big|_{y=0} = 0, \quad w\big|_{y=0} = 0 \\ &M\big|_{y=b} = 0, \quad F_{Vy}\big|_{y=b} = 0 \end{aligned} \tag{5.54}$$

Knowing that $\theta = \dfrac{\partial w}{\partial y}$, $M_y = \dfrac{\partial \phi_x}{\partial x}$, $\kappa_x = \dfrac{1}{D}\dfrac{\partial \phi_y}{\partial y} - \nu\kappa_y = \dfrac{\partial^2 w}{\partial x^2}$, and $\kappa_{xy} = -\dfrac{\partial w^2}{\partial x \partial y}$, the boundary conditions in Eq. (5.54) can be replaced by

$$\begin{aligned} &\kappa_{xy}\big|_{y=0} = 0, \quad \left.\frac{1}{D}\frac{\partial \phi_y}{\partial y} - \nu\kappa_y\right|_{y=0} = 0 \\ &\phi_x\big|_{y=b} = 0, \quad \phi_y\big|_{y=b} = 0 \end{aligned} \tag{5.55}$$

For a zero eigenvalue, the eigensolutions are all equal to zero. These are trivial solutions and they do not have physical interpretation. For nonzero eigenvalues, substituting the general eigensolutions that are expressed by Eq. (2.39) into the homogeneous boundary conditions (5.55) and equating the determinant of the coefficient matrix to zero yield the transcendental equation of nonzero eigenvalues for the bending of a simply supported plate on opposite sides along $y = 0$ and $y = b$ as

$$2\mu^2 b^2 (1-\nu)^2 + (\nu-1)(\nu+3)\cos(2\mu b) - \nu^2 - 2\nu - 5 = 0 \tag{5.56}$$

The corresponding basic eigenvector is

$$\psi_n = \left\{ \begin{array}{l} \frac{D}{\mu_n^2(1-\nu)^2}\left\{\cos(\mu_n y)\left[\cos(\mu_n b)\left(b\mu_n^2 y + b\mu_n^2\nu^2 y - 2\nu b\mu_n^2 y - 4\right) + \sin(\mu_n b)(2b + y + \nu y)\right] + \right. \\ \left. \sin(\mu_n y)\left[\mu_n(1-\nu)\cos(\mu_n b)(b + b\nu + 2y) + \sin(\mu_n b)\left(-1-\nu^2 + b\mu_n^2 y + b\mu_n^2\nu^2 y - 2\nu b\mu_n^2 y - 2\nu\right)\right]\right\} \\ \frac{D}{\mu_n^2(1-\nu)^2}\left\{\cos(\mu_n y)\left[\sin(\mu_n b)\left(b\mu_n^2 y + b\mu_n^2\nu^2 y - 2\nu b\mu_n^2 y + 2\right) + 2\cos(\mu_n b)\mu_n(\nu-1)(b-y)\right] + \right. \\ \left. \sin(\mu_n y)\left[\mu_n\left(\nu^2-1\right)\sin(\mu_n b)(b-y) - \cos(\mu_n b)\left(2 + b\mu_n^2 y + b\mu_n^2\nu^2 y - 2\nu b\mu_n^2 y + 2\nu\right)\right]\right\} \\ \frac{1}{\mu_n(1-\nu)^2}\left\{\cos(\mu_n y)\left[\cos(\mu_n b)\left(b\mu_n^2 y - \nu b\mu_n^2\nu^2 y - 4\right) - \mu_n\sin(\mu_n b)(2b - 2b\nu + y + \nu y)\right] + \right. \\ \left. \sin(\mu_n y)\left[\mu_n\cos(\mu_n b)(b - b\nu + 2y) - \sin(\mu_n b)\left(1 + \nu - b\mu_n^2 y + \nu b\mu_n^2 y\right)\right]\right\} \\ \frac{1}{\mu_n(1-\nu)^2}\left\{y\cos(\mu_n y)\left[\mu_n b\sin(\mu_n b)(1-\nu) + 2\mu_n\cos(\mu_n b)\right] + \right. \\ \left. \sin(\mu_n y)\left[\mu_n\sin(\mu_n b)(b - b\nu + y + \nu y) + \cos(\mu_n b)\left(2 + b\mu_n^2 y\nu - b\mu_n^2 y\right)\right]\right\} \end{array} \right\} \tag{5.57}$$

Then, the solution to eigenvalue equation (2.32) is

$$\boldsymbol{v}_n = \exp(\mu_n x)\boldsymbol{\psi}_n \tag{5.58}$$

From the curvature-deflection relation, the deflection of the plate can be expressed as

$$\begin{aligned} w_n = \frac{\exp(\mu_n x)}{\mu_n^3(1-\nu)^2}&\left\{\cos(\mu_n y)\left[\mu_n b y\cos(\mu_n b)(\nu-1) + \mu_n y(1+\nu)\sin(\mu_n b)\right] + \right. \\ &\left. \sin(\mu_n y)\left[\mu_n\cos(\mu_n b)(b - b\nu - 2y) + \sin(\mu_n b)\left(b\mu_n^2 y\nu - b\mu_n^2 y - \nu - 1\right)\right]\right\} \end{aligned} \tag{5.59}$$

Similarly, the first several eigenvalues for a plate with a Poisson's ratio ν = 0.3 are listed in Table 5.3.

Table 5.3 Nonzero eigenvalue for a plate with one side clamped and the opposite side free (ν=0.3)

N	1	2	3	4	5
$\mathrm{Re}(\overline{\mu}_n b)$	0.5π +1.13603	0.5π +0.45643	1.5π +1.25221	2.5π +1.32914	3.5π+1.370925
$\mathrm{Im}(\overline{\mu}_n b)$	0	0.35653	1.63374	2.09731	2.40263

Based on the eigenvalues and eigenvectors, the general solution for a plate with both opposite sides clamped can be solved from the expansion theorem. Thus, the analytical solution of the original problem can be obtained.

5.4.2 Symplectic treatment for the boundary

The formulation derived in Sec. 5.4.1 is valid for bending of a thin plate with one side clamped and the opposite side free at $y = 0$ and $y = b$ and no restriction is imposed on the remaining two boundaries. Exact bending solutions for various examples of such plates are presented as follows.

5.4.2.1 Plates with one side clamped and others free (CFFF)

Consider a plate with boundary conditions CFFF under a uniformly distributed load q . The expanded expression can be constructed from the eigensolutions of the nonzero eigenvalue (5.56-5.59) as

$$\boldsymbol{v} = \sum_{n=1}^{\infty} \left[f_n \boldsymbol{v}_n + \overline{f}_n \overline{\boldsymbol{v}}_n + f_{-n} \boldsymbol{v}_{-n} + \overline{f}_{-n} \overline{\boldsymbol{v}}_{-n} \right] \tag{5.60}$$

where $\boldsymbol{v}_n, \boldsymbol{v}_{-n}$ are the eigenvalues that correspond to the eigenvalue μ_n, which is listed in Table 5.3, and their respective symplectic adjoint eigenvalue $-\mu_n$, while $\overline{\boldsymbol{v}}_n, \overline{\boldsymbol{v}}_{-n}$ are the eigenvectors that correspond to the complex conjugate eigenvalues $\pm\mu_n$.

and the deflection of the plate is

$$w = w^* + \sum_{n=1}^{\infty} \left[f_n w_n + \overline{f}_n \overline{w}_n + f_{-n} w_{-n} + \overline{f}_{-n} \overline{w}_{-n} \right] \tag{5.61}$$

A particular solution that is caused by the distributed load q in the domain is

$$w^* = \frac{q}{24D}\left[y^4 - 4by^3 + 6b^2y^2 \right] \tag{5.62}$$

So,

$$\begin{aligned} \kappa_y^* &= \frac{q\left(y^2 - 2by + b^2\right)}{2D}, \qquad \kappa_{xy}^* = 0 \\ M_x^* &= \frac{q\nu\left(y^2 - 2by + b^2\right)}{2}, \qquad F_{Vx}^* = 0 \end{aligned} \tag{5.63a-d}$$

Consequently,

$$\begin{aligned} \phi_y^* &= \int M_x^* dy = c_1 + c_2 y \\ \phi_x^* &= \iint F_{Vx}^* dy dy = \frac{1}{6} q\nu\left(y^3 - 3by^2 + 3b^2 y\right) + c_3 \end{aligned} \tag{5.64a,b}$$

Substitute Eq. (5.64) into the boundary condition

$$\phi_x\big|_{y=b} = 0, \quad \phi_y\big|_{y=b} = 0 \tag{5.65a,b}$$

We can get $c_1 = 0, \qquad c_3 = 0$ (5.66a,b)

As $M_{xy}\Big|_{\left(-\frac{a}{2},b\right)} = M_{xy}\Big|_{\left(\frac{a}{2},b\right)} = 0$ (5.67)

c_2 can be expressed by $f_i, \overline{f}_i \ (i = \pm 1, \pm 2, \cdots)$ and $f_{-i}, \overline{f}_{-i} \ (i = \pm 1, \pm 2, \cdots)$, which are the unknown constants that can be determined by the boundary conditions

$$\begin{aligned} \phi_y\big|_{x=-\frac{a}{2}} &= 0 \quad ; \qquad \phi_y\big|_{x=-\frac{a}{2}} = 0 \\ \phi_x\big|_{x=\frac{a}{2}} &= 0 \quad ; \qquad \phi_y\big|_{x=\frac{a}{2}} = 0 \end{aligned} \tag{5.68a-d}$$

In practical applications, it is necessary to solve only the first k terms in Eq. (5.68). Then, the variational formula for the boundary conditions at two ends $x = \pm\frac{a}{2}$ is

$$\int_0^b \left[\left(\phi_x + \phi_x^*\right)\delta\kappa_y + \left(\phi_y + \phi_y^*\right)\delta\kappa_{xy} \right]_{x=-\frac{a}{2}}^{x=\frac{a}{2}} dy = 0 \tag{5.69}$$

Substitute Eqs. (5.64 a, b), (5.57) and (5.60) into Eq. (5.69). Because $\delta \boldsymbol{f}$ is arbitrary, its coefficient should always be zero, and a set of algebraic equations for solving $\boldsymbol{f}$ can be obtained.

$$\boldsymbol{p}\boldsymbol{f} = \boldsymbol{q} \tag{5.70}$$

where $\boldsymbol{p}$ is the coefficient matrix of $\delta \boldsymbol{f}^T \boldsymbol{f}$ in $\int_0^b \left[\phi_x \delta\kappa_y + \phi_y \delta\kappa_{xy} \right]_{x=-\frac{a}{2}}^{x=\frac{a}{2}} dy$, and $\boldsymbol{q}$ is the coefficient matrix of $\boldsymbol{f}$ in $-\int_0^b \left[\phi_x^* \delta\kappa_y + \phi_y^* \delta\kappa_{xy} \right]_{x=-\frac{a}{2}}^{x=\frac{a}{2}} dy$. f_n, $\overline{f}_n$, f_{-n}, $\overline{f}_{-n}$ can be solved from Eq. (5.70).

Thus, any point's value about deflection, moments, shear force etc. can be obtained.

5.4.2.2 Plates with two adjacent sides clamped and others free (CFFC)

Consider a plate with boundary conditions CFFC under a uniformly distributed load q. The variational formula for the boundary conditions at two ends $x = \pm \frac{a}{2}$ is

$$\int_0^b \left[\left(\kappa_y + \kappa_y^* \right) \delta\phi_x + \left(\kappa_{xy} + \kappa_{xy}^* \right) \delta\phi_y \right]_{x=\frac{a}{2}} dy + \int_0^b \left[\left(\phi_x + \phi_x^* \right) \delta\kappa_y + \left(\phi_y + \phi_y^* \right) \delta\kappa_{xy} \right]_{x=-\frac{a}{2}} dy = 0 \tag{5.71}$$

Substitute Eqs. (5.64), (5.57) and (5.60) into Eq. (5.71). Because $\delta \boldsymbol{f}$ is arbitrary, its coefficient should always be zero, and a set of algebraic equations for solving $\boldsymbol{f}$ can be obtained.

$$\boldsymbol{p}\boldsymbol{f} = \boldsymbol{q} \tag{5.72}$$

where $\boldsymbol{p}$ is the coefficient matrix of $\delta \boldsymbol{f}^T \boldsymbol{f}$ in the expression of $\int_0^b \left[\kappa_y \delta\phi_x + \kappa_{xy} \delta\phi_y \right]_{x=\frac{a}{2}} dy + \int_0^b \left[\phi_x \delta\kappa_y + \phi_y \delta\kappa_{xy} \right]_{x=-\frac{a}{2}} dy$, and $\boldsymbol{q}$ is the coefficient matrix of $\boldsymbol{f}$ in $-\left\{ \int_0^b \left[\kappa_y^* \delta\phi_x + \kappa_{xy}^* \delta\phi_y \right]_{x=\frac{a}{2}} dy + \int_0^b \left[\phi_x^* \delta\kappa_y + \phi_y^* \delta\kappa_{xy} \right]_{x=-\frac{a}{2}} dy \right\}$.

f_n, $\overline{f}_n$, f_{-n}, $\overline{f}_{-n}$ can be solved from Eq. (5.72).

Thus, any point's value about deflection, moments, shear force etc. can be obtained.

5.4.2.3 Plates with two adjacent sides free, one clamped and another simply supported (CFFS)

Consider a plate with boundary conditions CFFS under a uniformly distributed load q. The variational formula for the boundary conditions at two ends $x = \pm \frac{a}{2}$ is

$$\int_0^b \left[\left(\kappa_y + \kappa_y^* \right) \delta\phi_x + \left(\phi_y + \phi_y^* \right) \delta\kappa_{xy} \right]_{x=\frac{a}{2}} dy + \int_0^b \left[\left(\phi_x + \phi_x^* \right) \delta\kappa_y + \left(\phi_y + \phi_y^* \right) \delta\kappa_{xy} \right]_{x=-\frac{a}{2}} dy = 0 \tag{5.73}$$

Substitute Eqs. (5.64), (5.57) and (5.60) into Eq. (5.73). Because $\delta \boldsymbol{f}$ is arbitrary, its coefficient should always be zero, and a set of algebraic equations for solving $\boldsymbol{f}$ can be obtained.

$$\boldsymbol{p}\boldsymbol{f} = \boldsymbol{q} \tag{5.74}$$

where $\boldsymbol{p}$ is the coefficient matrix of $\delta \boldsymbol{f}^T \boldsymbol{f}$ in the expression of $\int_0^b \left[\kappa_y \delta\phi_x + \phi_y \delta\kappa_{xy} \right]_{x=\frac{a}{2}} dy + \int_0^b \left[\phi_x \delta\kappa_y + \phi_y \delta\kappa_{xy} \right]_{x=-\frac{a}{2}} dy$, and $\boldsymbol{q}$ is the coefficient matrix of $\boldsymbol{f}$ in $-\left(\int_0^b \left[\kappa_y^* \delta\phi_x + \phi_y^* \delta\kappa_{xy} \right]_{x=\frac{a}{2}} dy + \int_0^b \left[\phi_x^* \delta\kappa_y + \phi_y^* \delta\kappa_{xy} \right]_{x=-\frac{a}{2}} dy \right)$.

f_n, $\overline{f}_n$, f_{-n}, $\overline{f}_{-n}$ can be solved from Eq. (5.75).

Thus, any point's value about deflection, moments, shear force etc. can be obtained.

5.5 Symplectic results and discussion

In order to test the stability and accuracy of the results, the convergence and comparison study are carried out in the following sections.

5.5.1 Convergence study

Convergence studies were conducted for the three typical cases: CCSF, SFFF and CFFF. There are four accurate digits exist with present k.

- Bending results at the points $(0,0), (0,b)$ converge to a specific value and keep stable.
- Bending results at the point $(a,0)$ oscillate around a specific value and the amplitude decreases as k increases. Theoretical speaking, when $k \to \infty$, the amplitude is equal to zero and the value at the point $(a,0)$ would be stable. The results are exact solution at $x = \pm a$ when $k \to \infty$. While in practical applications,

we can only take the larger k in order to get more accurate results.

- The convergence velocity of deflection is larger than that of the bending moment. The reason is that bending moment is the higher order derivative of the deflection.

Table 5.4 Convergence study of the bending results of CCSF square plates (v=0.3)

k	$\frac{Dw(0,0)}{qb^4}$	$\frac{M_x(0,0)}{qb^2}$	$\frac{M_y(0,0)}{qb^2}$	$\frac{Dw(a,0)}{qb^4}$	$\frac{M_x(a,0)}{qb^2}$	$\frac{M_y(0,b)}{qb^2}$
5	0.00311222	-0.0210261	-0.0393057	0.00549978	0.00203550	0.0836366
6	0.00311248	-0.0210199	-0.0393079	0.00550702	0.00269898	0.0836392
7	0.00311265	-0.0210154	-0.0393095	0.00551045	0.000876824	0.0836390
8	0.00311289	-0.0210127	-0.0393117	0.00550930	-0.00228849	0.0836436
9	0.00311306	-0.0210106	-0.0393131	0.00551026	-0.00117354	0.0836463

Table 5.5 Convergence study of the bending results of SFFF square plates (v=0.3)

k	$\frac{Dw(0,0)}{qb^4}$	$\frac{M_x(0,0)}{qb^2}$	$\frac{M_y(0,0)}{qb^2}$	$\frac{Dw(a,0)}{qb^4}$	$\frac{M_x(a,0)}{qb^2}$	$\frac{M_y(0,b)}{qb^2}$
8	0.0183422	-0.0628230	-0.117991	0.0161677	0.000439161	0
9	0.0183427	-0.0628274	-0.117991	0.0161699	-0.000764133	0
10	0.0183429	-0.0628301	-0.117991	0.0161703	-0.000453306	0
11	0.0183431	-0.0628318	-0.117991	0.0161694	0.000252816	0
12	0.0183432	-0.0628328	-0.117991	0.0161694	0.000310253	0

Table 5.6 Convergence study of the bending results of CFFF square plates (v=0.3)

k	$\frac{Dw(0,0)}{qb^4}$	$\frac{M_x(0,0)}{qb^2}$	$\frac{M_y(0,0)}{qb^2}$	$\frac{Dw(a,0)}{qb^4}$	$\frac{M_x(a,0)}{qb^2}$	$\frac{M_y(0,b)}{qb^2}$
5	0.0457568	0.0233731	0.122524	0.0418150	0.00309627	0
6	0.0457792	0.0235098	0.122654	0.0438499	0.01920110	0
7	0.0457986	0.0235120	0.122633	0.0426580	0.00147105	0
8	0.0458063	0.0235744	0.122651	0.0433620	-0.0136182	0
9	0.0458152	0.0235712	0.122652	0.0430625	-0.00342534	0

5.5.2 Comparison study

Comparison studies ware conducted for the nine cases of two opposite sides unsymmetrical. Here, $k=12$ for the plates with one side simply supported and the opposite side clamped, $k=9$ for the plates with one side simply supported and the opposite side free and $k=10$ for the plates with one side clamped and the opposite side free. Results obtained by finite element software ABAQUS® are used as the reference. From the tables we can see that these two methods show agreement at the center of the plate and for the deflection results at edges. While there are big differences exist for the bending moment results on the edges. According to the study of Chapter Four, we can see that the bending moment results of ABAQUS® are not so reliable at the edges. While the results calculated by symplectic method are analytical results. That means if the results for deflection are accurate, the bending moment results are reliable too. That is one of the reasons to develop this symplectic method.

Table 5.7 Comparison study of the bending results of CFSF plates (v=0.3)

a/b		$\frac{Dw(0,0)}{qb^4}$	$\frac{M_x(0,0)}{qb^2}$	$\frac{M_y(0,0)}{qb^2}$	$\frac{Dw(a,0)}{qb^4}$	$\frac{M_x(a,0)}{qb^2}$	$\frac{M_y(0,b)}{qb^2}$
1.0	Present	0.00514513	-0.0149299	-0.0606922	0.00587623	-0.00139589	0.122326
	FEM	0.00514989	-0.0148251	-0.0606982	0.00589769	-0.00028091	0.119372
1.5	Present	0.00512980	-0.0177963	-0.0613378	0.00592151	-0.00140599	0.122867
	FEM	0.00513916	-0.0177547	-0.0613133	0.00594405	-0.00028366	0.119785
2.0	Present	0.00515877	-0.0186694	-0.0619073	0.00592824	-0.00140888	0.123915
	FEM	0.00515651	-0.0186396	-0.0618251	0.00594316	-0.00070056	0.117742

Table 5.8 Comparison study of the bending results of CSSF plates (v=0.3)

a/b		$\frac{Dw(0,0)}{qb^4}$	$\frac{M_x(0,0)}{qb^2}$	$\frac{M_y(0,0)}{qb^2}$	$\frac{Dw(a,0)}{qb^4}$	$\frac{M_x(a,0)}{qb^2}$	$\frac{M_y(0,b)}{qb^2}$
1.0	Present	0.00394477	-0.0245030	-0.0497547	0.00579330	-0.00129662	0.102789
	FEM	0.00395778	-0.0244863	-0.0498444	0.00582570	-0.00034102	-0.001613
1.5	Present	0.00469050	-0.0231240	-0.0578644	0.00593857	-0.00140127	0.117050
	FEM	0.00469230	-0.0230755	-0.0578057	0.00595013	-0.00094107	0.109460
2.0	Present	0.00501876	-0.0210757	-0.0610243	0.00593424	-0.00141011	0.122555
	FEM	0.00502052	-0.0210437	-0.0609780	0.00594935	-0.00070211	0.116367

Table 5.9 Comparison study of the bending results of CCSF plates (v=0.3)

a/b		$\frac{Dw(0,0)}{qb^4}$	$\frac{M_x(0,0)}{qb^2}$	$\frac{M_y(0,0)}{qb^2}$	$\frac{Dw(a,0)}{qb^4}$	$\frac{M_x(a,0)}{qb^2}$	$\frac{M_y(0,b)}{qb^2}$
1.0	Present	0.00311306	-0.0210106	-0.0393131	0.00551026	-0.00117354	0.0836463
	FEM	0.00311755	-0.0209464	-0.0393050	0.00553553	-0.00091042	-0.060001
1.5	Present	0.00425549	-0.0239969	-0.0531235	0.00591581	-0.00138291	0.108502
	FEM	0.00425625	-0.0239589	-0.0530566	0.00592858	-0.00097157	0.101160
2.0	Present	0.00482369	-0.0222927	-0.0591352	0.00593564	-0.00140874	0.119240
	FEM	0.00482513	-0.0227160	-0.0590858	0.00595103	-0.00070605	0.113084

Table 5.10 Comparison study of the bending results of CSSC plates (v=0.3)

a/b		$\frac{Dw(0,0)}{qb^4}$	$\frac{M_x(0,0)}{qb^2}$	$\frac{M_y(0,0)}{qb^2}$	$\frac{Dw(a,0)}{qb^4}$	$\frac{M_x(a,0)}{qb^2}$	$\frac{M_y(0,b)}{qb^2}$
1.0	Present	0.00210376	-0.0304356	-0.0304419	0	0.000059067	0.0677414
	FEM	0.00211650	-0.0304647	-0.0304647	0	0.0628475	0.0628475
1.5	Present	0.00382112	-0.0293279	-0.0497040	0	-0.000059126	0.102785
	FEM	0.00382839	-0.0293078	-0.0496963	0	0.0708816	0.0954292
2.0	Present	0.00468333	-0.0247049	-0.0582498	0	-0.000059143	0.117876
	FEM	0.00468876	-0.0248190	-0.0582361	0	0.0732346	0.111705

Table 5.11 Comparison study of the bending results of SFFF plates (v=0.3)

a/b		$\frac{Dw(0,0)}{qb^4}$	$\frac{M_x(0,0)}{qb^2}$	$\frac{M_y(0,0)}{qb^2}$	$\frac{Dw(a,0)}{qb^4}$	$\frac{M_x(a,0)}{qb^2}$	$\frac{M_y(0,b)}{qb^2}$
1.0	Present	0.0183432	-0.0628328	-0.117991	0.0161694	0.000310253	0
	FEM	0.0184004	-0.0627598	-0.117809	0.0162434	-0.00203794	-0.00354953
1.5	Present	0.0345363	-0.109420	-0.115019	0.0172407	0.000347014	0
	FEM	0.0346766	-0.109642	-0.114464	0.0173328	-0.00329853	-0.0046529
2.0	Present	0.0653221	-0.143575	-0.115081	0.0178460	0.000364395	0
	FEM	0.0656950	-0.144053	-0.144053	0.0179785	-0.00271469	-0.00364937

Table 5.12 Comparison study of the bending results of SSFF plates (v=0.3)

a/b		$\frac{Dw(0,0)}{qb^4}$	$\frac{M_x(0,0)}{qb^2}$	$\frac{M_y(0,0)}{qb^2}$	$\frac{Dw(a,0)}{qb^4}$	$\frac{M_x(a,0)}{qb^2}$	$\frac{M_y(0,b)}{qb^2}$
1.0	Present	0.0574272	-0.0726277	-0.0726660	0.103164	0.0129806	0
	FEM	0.0574812	-0.0726566	-0.0726566	0.103994	-0.00229530	-0.1170180
1.5	Present	0.122080	-0.1160561	-0.0901455	0.217966	0.0844290	0
	FEM	0.132158	-0.1172680	-0.0904814	0.218965	-0.00340663	-0.00376742
2.0	Present	0.242167	-0.148563	-0.108166	0.370055	0.0676151	0
	FEM	0.243285	-0.1493590	-0.1019280	0.377446	-0.00272257	-0.00329053

Table 5.13 Comparison study of the bending results of CFFF plates (v=0.3)

a/b		$\frac{Dw(0,0)}{qb^4}$	$\frac{M_x(0,0)}{qb^2}$	$\frac{M_y(0,0)}{qb^2}$	$\frac{Dw(a,0)}{qb^4}$	$\frac{M_x(a,0)}{qb^2}$	$\frac{M_y(0,b)}{qb^2}$
1.0	Present	0.0458152	0.0235712	0.122652	0.0430625	-0.00342534	0
	FEM	0.0488688	0.0236736	0.122743	0.0433140	0.000351953	0.000123811
1.5	Present	0.0455905	0.0328935	0.124424	0.0422505	-0.00339099	0
	FEM	0.0456150	0.0330393	0.124621	0.4249490	0.000486809	0
2.0	Present	0.0453249	0.0366866	0.126051	0.0418993	-0.00336099	0
	FEM	0.0453422	0.0367879	0.126206	0.0421594	0.000366066	0

Table 5.14 Comparison study of the bending results of CFFC plates (v=0.3)

a/b		$\frac{Dw(0,0)}{qb^4}$	$\frac{M_x(0,0)}{qb^2}$	$\frac{M_y(0,0)}{qb^2}$	$\frac{Dw(a,0)}{qb^4}$	$\frac{M_x(a,0)}{qb^2}$	$\frac{M_y(0,b)}{qb^2}$
1.0	Present	0.00848644	-0.000983401	-0.000983401	0	0.126438	-0.000239702
	FEM	0.00870892	-0.000970712	-0.000970712	0	0.125700	-0.000591268
1.5	Present	0.0175709	-0.0135355	0.0176510	0	0.144765	0
	FEM	0.0178437	-0.0123728	0.0192467	0	0.146090	-0.000364981
2.0	Present	0.0257712	-0.0116813	0.0405057	0	0.151061	0
	FEM	0.0259537	-0.0109917	0.0416148	0	0.152062	-0.000386133

Table 5.155 Comparison study of the bending results of CFFS plates (v=0.3)

a/b		$\frac{Dw(0,0)}{qb^4}$	$\frac{M_x(0,0)}{qb^2}$	$\frac{M_y(0,0)}{qb^2}$	$\frac{Dw(a,0)}{qb^4}$	$\frac{M_x(a,0)}{qb^2}$	$\frac{M_y(0,b)}{qb^2}$
1.0	Present	0.0175136	-0.0254412	0.00247198	0	-0.000025647	0
	FEM	0.0180620	-0.0243576	0.00471059	0	-0.00194925	-0.00141142
1.5	Present	0.0267191	-0.0188677	0.0341498	0	-0.000025205	0
	FEM	0.0270711	-0.0179363	0.0359883	0	-0.00243339	-0.00159184
2.0	Present	0.0331376	-0.0054811	0.0604170	0	-0.00002540	0
	FEM	0.0333390	-0.00488736	0.0616031	0	-0.00189829	-0.00097855

5.6 Closure

In this chapter, the symplectic solution for the plates with two opposite sides unsymmetrical is discussed. The transcendental equation, eigenvalue, eigenvector, general bending solution and exact bending results are solved for 9 boundary conditions. Convergence and comparison study are conducted and corresponding symplectic results are present for others' reference. It is concluded that the bending results solved by symplectic method are valid for the cases studied in this chapter.

Chapter 6 Corner Supported Plates

6.1 Introduction

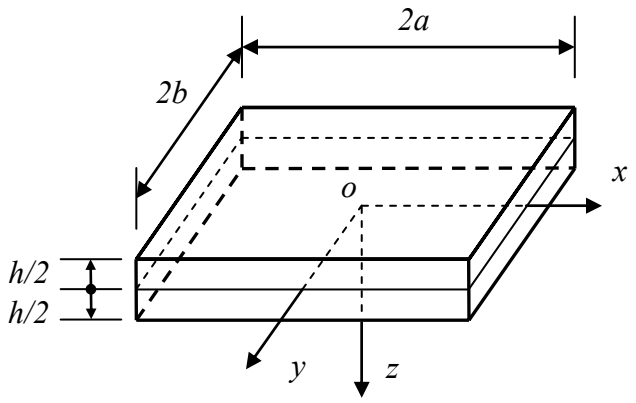

Fig. 6.1 Configuration and coordinate system of plates

This chapter presents the first ever exact solution for the bending problem of a free, rectangular thin plate supported at four corners. The problem has drawn great attention since the 1950s because of its vast engineering applications. The exact analysis employs a new symplectic elasticity approach that goes beyond the limitation of the classical plate bending analyses such as Timoshenko's method, Navier's solution, and Levy's solution. The latter (classical) methods are, in fact, proved to be special cases of this symplectic approach in the real eigenvalue regime. When plate bending problems enter the complex eigenvalue regime, such as plates without opposite sides simply supported, the classical methods fail to yield exact

solutions. The symplectic approach, however, does. The free boundaries with corner supports are dealt with using the variational principle. The expression of state vector has been formulated by Yao *et al*. (2007). Based on that formulation, exact analytical bending modes are then derived by the expansion of eigenfunctions. Fig.6.1 shows the configuration and coordinate system of plates which discussed in this chapter.

6.2 Symplectic formulation

The exact solution for bending of corner supported plates using a new symplectic approach is sought. For a plate with two opposite sides $y = \pm b$ free, the boundary conditions are

$$M_y\big|_{y=\pm b} = 0, \quad F_{Vy}\big|_{y=\pm b} = 0 \tag{6.1}$$

Knowing that

$$M_y = \frac{\partial \phi_x}{\partial x}, \quad F_{Vy} = -\frac{\partial^2 \phi_y}{\partial x^2} \tag{6.2}$$

we have

$$\phi_x = \int M_y dx + \tilde{a}_1 \qquad \phi_y = -\int\int F_{vy} dx + a_0 + a_2 x \tag{6.3}$$

The boundary conditions in Eq. (6.1) can be replaced by

$$\begin{aligned} &\phi_x\big|_{y=-b} = 0, && \phi_y\big|_{y=-b} = 0 \\ &\phi_x\big|_{y=b} = \tilde{a}_1 = a_1 - a_2 b, && \phi_y\big|_{y=b} = a_0 + a_2 x \end{aligned} \tag{6.4a, b}$$

and the unknown constants are $a_0, \tilde{a}_1, a_2$, where $\tilde{a}_1$ are expressed in two parts according to the null moment functions as

$$\phi_x = a_0 - a_2 y, \quad \phi_y = a_1 + a_2 x \tag{6.5}$$

These constants are inhomogeneous terms that must be solved. First, a_0 can be solved from the following equation

$$\boldsymbol{H}\psi_0^0 = 0 \tag{6.6}$$

with boundary conditions

$$\begin{aligned} \phi_x\big|_{y=-b} &= 0, \qquad \phi_y\big|_{y=-b} = 0 \\ \phi_x\big|_{y=b} &= 0, \qquad \phi_y\big|_{y=b} = 1 \end{aligned} \tag{6.7}$$

The solution is

$$\psi_0^0 = \left\{ 0, \frac{y+b}{2b}, \frac{-\nu}{2bD\left(1-\nu^2\right)}, 0 \right\}^T \tag{6.8}$$

The solution for the corresponding problem

$$\dot{\nu} = \boldsymbol{H}\nu \tag{6.9}$$

is

$$\nu_0^0 = \psi_0^0 \tag{6.10}$$

From the relation between the moment and the bending moment function

$$M_y = \frac{\partial \phi_x}{\partial x}, \qquad M_x = \frac{\partial \phi_y}{\partial y}, \qquad 2M_{xy} = \frac{\partial \phi_x}{\partial y} + \frac{\partial \phi_y}{\partial x} \tag{6.11}$$

the corresponding bending moments are

$$M_{x0}^0 = \frac{1}{2b}, \quad M_{y0}^0 = 0, \quad M_{xy0}^0 = 0 \tag{6.12}$$

From equations of equilibrium

$$\frac{\partial M_x}{\partial x} - \frac{\partial M_{xy}}{\partial y} - F_{sx} = 0, \qquad \frac{\partial M_y}{\partial y} - \frac{\partial M_{xy}}{\partial x} - F_{sy} = 0 \tag{6.13}$$

the shear forces are

$$F_{\boldsymbol{S}x0}^0 = 0, \quad F_{\boldsymbol{S}y0}^0 = 0 \tag{6.14}$$

Further, from the curvature-deflection relation

$$\kappa_x = \frac{\partial^2 w}{\partial x^2}, \quad \kappa_y = \frac{\partial^2 w}{\partial y^2}, \quad \kappa_{xy} = -\frac{\partial^2 w}{\partial x \partial y} \tag{6.15}$$

the deflection of the plate after integration is

$$w_0^0 = \frac{x^2 - \nu y^2}{4bD\left(1-\nu^2\right)} + \text{rigid body displacement} \tag{6.16}$$

The physical interpretation of v_0^0 is pure bending.

Next, the a_1 term can be solved from the following equation

$$\boldsymbol{H}\psi_0^1 = 0 \tag{6.17}$$

with boundary conditions

$$\begin{aligned} \phi_x\big|_{y=-b} &= 0, \qquad \phi_y\big|_{y=-b} = 0 \\ \phi_x\big|_{y=b} &= 1, \qquad \phi_y\big|_{y=b} = 0 \end{aligned} \tag{6.18}$$

The solution is

$$\psi_0^1 = \left\{ \frac{y+b}{2b}, 0, 0, \frac{1}{4bD\left(1-\nu\right)} \right\}^T \tag{6.19}$$

The corresponding solution for Eq. (6.9) is

$$\upsilon_0^1 = \psi_0^1 \tag{6.20}$$

From Eq. (6.11), the corresponding bending moments are

$$M_{x0}^1 = 0, \quad M_{y0}^1 = 0, \quad M_{xy0}^1 = \frac{1}{4b} \tag{6.21}$$

and from Eq. (6.13), the shear forces are

$$F_{\boldsymbol{S}x0}^1 = 0, \quad F_{\boldsymbol{S}y0}^1 = 0 \tag{6.22}$$

Further, from the curvature-deflection relation, the deflection of the plate after integration is

$$w_0^1 = -\frac{xy}{4bD\left(1-\nu\right)} + \text{rigid body displacement} \tag{6.23}$$

The physical interpretation of v_0^1 is pure torsion.

Finally, the a_2 term must be solved. As a_2 in the expression of ϕ_y in Eq. (6.4b) has a multiplier x, the solution corresponds to the next Jordan form of the inhomogeneous solution ψ_0^0 with respect to $\phi_y = 1$. Hence, the a_2 term can be solved from the following equation:

$$\boldsymbol{H}\psi_0^2 = \psi_0^0 \tag{6.24}$$

The coefficient of a_2 in the expression of ϕ_x in Eq. (6.4b) is $-b$, and its influence only exists in the boundary conditions of ψ_0^2. Hence, the boundary conditions on both opposite sides are

$$\begin{aligned} \phi_x\big|_{y=-b} &= 0, \qquad \phi_y\big|_{y=-b} = 0 \\ \phi_x\big|_{y=b} &= -b, \qquad \phi_y\big|_{y=b} = 0 \end{aligned} \tag{6.25}$$

The solution is

$$\psi_0^2 = \left\{ \frac{(1-\nu)\left(b^2 - y^2\right)}{4b(1+\nu)} - \frac{y+b}{2b}, 0, 0, \frac{\nu y}{2bD\left(1-\nu^2\right)}, 0 \right\}^T \tag{6.26}$$

and the corresponding solution for Eq. (6.9) is

$$v_0^2 = \psi_0^2 + x\psi_0^0 \tag{6.27}$$

From Eq. (6.11), the bending moments are

$$M_{x0}^2 = \frac{x}{2b}, \quad M_{y0}^2 = 0, \quad M_{xy0}^2 = \frac{\nu y}{2b(1+\nu)} \tag{6.28}$$

and from Eq. (6.13), the shear forces are

$$F_{sx0}^2 = \frac{1}{2b(1+\nu)}, \quad F_{sy0}^2 = 0 \tag{6.29}$$

Further, from the curvature-deflection relation, the deflection of the plate after integration is

$$w_0^2 = \frac{x^3 - 3\nu xy^2}{4bD\left(1-\nu^2\right)} + \text{rigid body displacement} \tag{6.30}$$

The physical interpretation of v_0^1 is constant shear bending in the direction of the x-axis.

After obtaining the three inhomogeneous particular solutions, we discuss the solutions that correspond to the homogeneous boundary conditions.

The homogeneous boundary conditions for a plate bending with both opposite sides free are

$$\phi_x\big|_{y=\pm b} = 0, \qquad \phi_y\big|_{y=\pm b} = 0 \tag{6.31}$$

Obviously, the eigensolutions that satisfy the eigenvalue equation

$$\boldsymbol{H}\psi\left(\boldsymbol{y}\right) = \mu\psi\left(\boldsymbol{y}\right) \tag{6.32}$$

and (2.39) are only eigensolutions of the nonzero eigenvalue. They can be divided into two sets, i.e., the symmetric and the antisymmetric solutions with respect to x.

Substituting solutions with only A and C terms in general solutions into the homogeneous boundary conditions (6.31) and equating the determinant of coefficient matrix to zero yield the transcendental equation of nonzero eigenvalues for symmetric plate deformation with both opposite sides free as

$$2\mu b\left(1-\nu\right) = \left(3+\nu\right)\sin\left(2\mu b\right) \tag{6.33}$$

Let eigenvalues μ_n be a solution to Eq. (6.33), and the corresponding eigensolution for symmetric deformation is

$$\psi_n = \begin{Bmatrix} -\dfrac{3+\nu}{1-\nu}\sin^2(\mu_n b)\cos(\mu_n y) + \mu_n y \sin(\mu_n y) \\ -\dfrac{3+\nu}{1-\nu}\cos^2(\mu_n b)\sin(\mu_n y) + \mu_n y \cos(\mu_n y) \\ \dfrac{\mu_n}{D(1-\nu)^2}\left\{\left[(3+\nu)\cos^2(\mu_n b) - 3 + \nu\right]\cos(\mu_n y) + (1-\nu)\mu_n y \sin(\mu_n y)\right\} \\ \dfrac{\mu_n}{D(1-\nu)^2}\left\{\left[2 - (3+\nu)\cos^2(\mu_n b)\right]\sin(\mu_n y) + (1-\nu)\mu_n y \cos(\mu_n y)\right\} \end{Bmatrix} \quad (6.34)$$

and the solution for the corresponding problem (6.9) is

$$v_n = \exp(\mu_n x)\psi_n \quad (6.35)$$

Further, from the curvature-deflection relation, the deflection of a plate after integration is

$$w_n = \exp(\mu_n x)\left\{\frac{1+\nu-(3+\nu)\cos^2(\mu_n b)}{D(1-\nu)^2\mu_n}\cos(\mu_n y) - \frac{y\sin(\mu_n y)}{D(1-\nu)}\right\} \quad (6.36)$$

The first several eigenvalues for a plate with a Poisson's ratio of $\nu = 0.3$ are listed in Table 6.1.

Table 6.1 Nonzero eigenvalue for symmetric deformation of thin plate with both opposite sides free (v=0.3)

N	1	2	3	4	5
Re($\mu_n b$)	1.2830	π +0.6973	2 π +0.7191	3 π +0.7313	4 π +0.7393
Im($\mu_n b$)	0	0.5446	0.8808	1.0730	1.2101

Based on the eigenvalues and eigenvectors, the general solution for a plate with both opposite sides free can be solved from the expansion theorem. Thus, the analytical solution of the original problem can be obtained.

6.3 Symplectic treatment for the boundary

A specific example for the bending of a corner-supported rectangular plate under a uniformly distributed load q is presented. As the problem is symmetric with respect to the x-axis, the expanded expression can be constructed only from the symmetric eigensolutions of the nonzero eigenvalue (6.33-6.35) as

$$\boldsymbol{v} = \sum_{n=1}^{\infty} \left[f_n \boldsymbol{v}_n + \overline{f}_n \overline{\boldsymbol{v}}_n + f_{-n} \boldsymbol{v}_{-n} + \overline{f}_{-n} \overline{\boldsymbol{v}}_{-n} \right] \tag{6.37}$$

where $\boldsymbol{v}_n, \boldsymbol{v}_{-n}$ are the eigenvalues that correspond to the eigenvalue μ_n, which is listed in Table 6.1, and their respective symplectic adjoint eigenvalue $-\mu_n$, while $\overline{\boldsymbol{v}}_n, \overline{\boldsymbol{v}}_{-n}$ are the eigenvectors that correspond to the complex conjugate eigenvalues $\pm\mu_n$.

and the deflection of the plate is

$$w = w^* + \sum_{n=1}^{\infty} \left[f_n w_n + \overline{f}_n \overline{w}_n + f_{-n} w_{-n} + \overline{f}_{-n} \overline{w}_{-n} \right] + c_0 w_0^{(0)} + c_1 w_0^{(1)} + c_2 w_0^{(2)} + c_3 x + c_4 y + c_5 \tag{6.38}$$

where $c_3 x + c_4 y + c_5$ is the rigid body displacement.

As the deflection shape of the plate is symmetric with respect to the x-axis and y-axis, no x^{2n-1}, y^{2n-1} exists in the expression.

Therefore, we can get

$$c_1 = c_2 = c_3 = c_4 = 0 \tag{6.39}$$

A particular solution that is caused by distributed load q in the domain is

$$w^* = \frac{q}{24D(1-\nu^2)} \left[x^4 - 12b^2(1-\nu)\nu y^2 - 6\nu x^2 y^2 + (2-\nu)\nu y^4 \right] \tag{6.40}$$

and the corresponding bending moment and shear force are

$$M_x^* = \frac{q}{2(1+\nu)}\left\{x^2 + \nu\left[-2b^2\nu + x^2 + (-1+\nu)y^2\right]\right\}, \qquad F_{Vx}^* = -\frac{q(-1+\nu)x}{1+\nu} \tag{6.41a,b}$$

Consequently,

$$\begin{aligned} \phi_y^* &= \int M_x^* dy = -\frac{qy\left[-6b^2\nu^2 + 3(1+\nu)x^2 + (-1+\nu)\nu y^2\right]}{6(1+\nu)} + p_0 \\ \phi_x^* &= \iint F_{Vx}^* dydy = -\frac{q(-1+\nu)xy^2}{2(1+\nu)} + p_1 x + p_2 \end{aligned} \tag{6.42a,b}$$

$$\begin{aligned} &\phi_x^*\big|_{y=-b} = 0, && \phi_y^*\big|_{y=-b} = 0 \\ &\phi_x^*\big|_{y=b} = c_2 - c_3 b = 0, && \phi_y^*\big|_{y=b} = c_1 + c_3 x = c_1 \end{aligned} \tag{6.43a-d}$$

Substitute the boundary condition (6.43) into the expression (6.42), and we can get

$$p_0 = p_2 = 0, \quad p_1 = -\frac{q(-1+\nu)x}{(1+\nu)} \tag{6.44a, b}$$

Substitute Eq. (6.44) into Eq. (6.42) and

$$\begin{aligned} \phi_y^* &= -\frac{qy\left[-6b^2\nu^2 + 3(1+\nu)x^2 + (-1+\nu)\nu y^2\right]}{6(1+\nu)} \\ \phi_x^* &= \frac{q(-1+\nu)(b-y)xy}{2(1+\nu)} \end{aligned} \tag{6.45a, b}$$

Substitute Eq. (6.45a) into Eq. (6.43b)， we can get

$$c_1 = \frac{b^3 q\nu(1+5\nu)}{3(1+\nu)} \tag{6.46}$$

$f_i, \overline{f}_i$ $(i = \pm 1, \pm 2, \cdots)$ are the unknown constants that can be determined by the boundary conditions $\phi_x = \phi_y = 0$ at two ends $x = \pm a$. In practical applications, it is necessary to solve only the first k terms in Eq. (6.37). Then, the variational formula for the boundary conditions at two ends $x = \pm a$ is

$$\int_{-b}^{b}\left[\left(\phi_x + \phi_x^*\right)\delta\kappa_y + \left(\phi_y + \phi_y^*\right)\delta\kappa_{xy}\right]_{x=-a}^{x=a} dy = 0 \tag{6.47}$$

Substitute Eqs. (6.34), (6.35), (6.37) and (6.45) into Eq. (6.47). Because $\delta \boldsymbol{f}$ is arbitrary, its coefficient should always be zero, and a set of algebraic equations for solving $\boldsymbol{f}$ can be obtained.

$$\boldsymbol{p}\boldsymbol{f} = \boldsymbol{q} \tag{6.48}$$

where $\boldsymbol{p}$ is the coefficient matrix of $\delta \boldsymbol{f}^T \boldsymbol{f}$ in $\int_{-b}^{b}\left[\phi_x \delta\kappa_y + \phi_y \delta\kappa_{xy}\right]_{x=-a}^{x=a} dy$, and $\boldsymbol{q}$ is the coefficient matrix of $\boldsymbol{f}$ in $-\int_{-b}^{b}\left[\phi_x^* \delta\kappa_y + \phi_y^* \delta\kappa_{xy}\right]_{x=-a}^{x=a} dy$. f_n, $\overline{f}_n$, f_{-n}, $\overline{f}_{-n}$ can be solved from Eq. (6.48).

Now, only one unknown constant exists in the expression of w, i.e., c_5, which can be solved by the boundary condition

$$w(a,b) = 0 \tag{6.49}$$

Thus, the expression for w is

$$\begin{aligned} w = {} & \frac{q}{24D(-1+\nu)(1+\nu)^2}\left\{-6a^2(1+\nu)\left(-x^2+\nu y^2\right)+2b^2\nu\left[-(1+5\nu)x^2-(-3+\nu)(2+\nu)y^2\right]+\right. \\ & \left.(1+\nu)\left[-x^4+6\nu x^2y^2+(-2+\nu)\nu y^4\right]\right\}+c_5+ \\ & \sum_{n=1}^{\infty}\left(f_n e^{\mu_n x}\left(\frac{\left[1+\nu-(3+\nu)\cos^2(\mu_n b)\right]\cos(\mu_n y)}{\mu_n D(1-\nu)^2}-\frac{y\sin(\mu_n y)}{D(1-\nu)}\right)+\right. \\ & \overline{f}_n e^{\overline{\mu}_n x}\left(\frac{\left[1+\nu-(3+\nu)\cos^2(\overline{\mu}_n b)\right]\cos(\overline{\mu}_n y)}{\overline{\mu}_n D(1-\nu)^2}-\frac{y\sin(\overline{\mu}_n y)}{D(1-\nu)}\right)+ \\ & f_{-n} e^{\mu_{-n} x}\left(\frac{\left[1+\nu-(3+\nu)\cos^2(\mu_{-n} b)\right]\cos(\mu_{-n} y)}{\mu_{-n} D(1-\nu)^2}-\frac{y\sin(\mu_{-n} y)}{D(1-\nu)}\right)+ \\ & \left.\overline{f}_{-n} e^{\overline{\mu}_{-n} x}\left(\frac{\left[1+\nu-(3+\nu)\cos^2(\overline{\mu}_{-n} b)\right]\cos(\overline{\mu}_{-n} y)}{\overline{\mu}_{-n} D(1-\nu)^2}-\frac{y\sin(\overline{\mu}_{-n} y)}{D(1-\nu)}\right)\right. \end{aligned} \tag{6.50}$$

The slope, shear force, bending moment, and twisting moment can be solved from the basic elasticity relationship.

6.4 Symplectic results and discussion

In order to test the stability and accuracy of the results, the convergence and comparison study are carried out in the following sections.

6.4.1 Convergence study

Table 6.2 presents a convergence study with k increasing from $k=7$ to $k=14$. Here, the quantities are expressed in dimensionless terms, for instance, the deflection is nondimensionalized as $Dw/16qa^4$. Here and after, Poisson's ratio $\nu=0.3$ is employed while any thickness ratio is not required because information on plate thickness is implicit within the dimensionless quantities through plate flexural rigidity $D\left(=Eh^3/12\left(1-\nu^2\right)\right)$ in which h is the plate thickness. In general, converged results are obtained for $k=14$ as observed in the table and, hence, all subsequent results are calculated using $k=14$.

It is clear that the bending of a corner-supported plate with uniform distributed loading has two planes of symmetry. The symmetric bending nature is further confirmed in Table 6.2, within the tolerance of k terms in some cases, it can be observed that:

$$\begin{array}{ccc} w(a,0)=w(0,b) & ; & \theta_x(a,0)=\theta_y(0,b) \\ M_x(a,0)=M_y(0,b) & ; & M_y(a,0)=M_x(0,b) \\ F_{Vx}(a,0)=F_{Vy}(0,b) & ; & F_{Vy}(a,0)=F_{Vx}(0,b) \end{array} .$$

It is also noticed that convergence of w, θ, M, F_V at points $(0,0)$ and $(0,b)$ is excellent while at point $(a,0)$, the values oscillate with decreasing amplitude about specific values as k increases. Theoretical speaking, absolute convergence is achieved for $k \to \infty$ and the boundary conditions are analytically fulfilled. In practice, a finite k is adopted while numerical convergence is assured.

The convergence rate decrease for quantities having higher derivatives of deflection. In general, the convergence rate for deflection is excellent and it becomes less convergent for slope, then moment and lastly shear force. The deteriorating convergence rate is because the slope is the first derivative of deflection, the moment is the second derivative of deflection and the shear force is the third derivative of the deflection. It can be concluded that the higher the derivative order, the poorer the convergence behavior.

Table 6.2 Convergence study of the bending results of FFFF plates (ν=0.3)

k	$\frac{Dw(0,0)}{16qb^4}$	$\frac{Dw(a,0)}{16qb^4}$	$\frac{Dw(0,b)}{16qb^4}$	$\frac{D}{8qb^3}\frac{\partial w}{\partial x}(a,0)$	$\frac{D}{8qb^3}\frac{\partial w}{\partial y}(0,b)$
7	0.0255066	0.0177477	0.0177471	-0.0195251	-0.0195234
8	0.0255066	0.0177472	0.0177472	-0.0195207	-0.0195234
9	0.0255065	0.0177474	0.0177472	-0.0195273	-0.0195233
10	0.0255065	0.0177474	0.0177472	-0.0195195	-0.0195232
11	0.0255065	0.0177474	0.0177473	-0.0195263	-0.0195231
12	0.0255065	0.0177474	0.0177473	-0.0195201	-0.0195230
13	0.0255065	0.0177474	0.0177473	-0.0195253	-0.0195230
14	0.0255065	0.0177474	0.0177473	-0.0195209	-0.0195229

k	$\frac{M_x(0,0)}{4qb^2}$	$\frac{M_y(0,0)}{4qb^2}$	$\frac{M_x(0,b)}{4qb^2}$	$\frac{M_y(a,0)}{4qb^2}$	$\frac{M_x(a,0)}{4qb^2}$
7	-0.111711	-0.111716	-0.150439	-0.151101	-0.000654977
8	-0.111711	-0.111714	-0.150439	-0.149999	0.000639537
9	-0.111711	-0.111713	-0.150439	-0.150725	-0.000588535
10	-0.111711	-0.111713	-0.150439	-0.150268	0.000496283
11	-0.111711	-0.111712	-0.150439	-0.150535	-0.000421168
12	-0.111711	-0.111712	-0.150439	-0.150400	0.000344437
13	-0.111711	-0.111712	-0.150439	-0.150441	-0.000284715
14	-0.111711	-0.111712	-0.150439	-0.150467	0.000225661

k	$\frac{M_y(0,b)}{4qb^2}$	$\frac{M_{xy}(0,0)}{4qb^2}$	$\frac{M_{xy}(a,0)}{4qb^2}$	$\frac{M_{xy}(0,b)}{4qb^2}$	$\frac{Q_x(a,0)}{2qb}$	$\frac{Q_y(0,b)}{2qb}$
7	0	0	0	0	-0.03893440	0
8	0	0	0	0	0.03247000	0
9	0	0	0	0	-0.02558350	0
10	0	0	0	0	0.01930580	0
11	0	0	0	0	-0.01383120	0
12	0	0	0	0	0.00916049	0
13	0	0	0	0	-0.00512306	0
14	0	0	0	0	0.00322078	0

6.4.2 Comparison study

Table 6.3 Comparison study of the bending results of FFFF plates (v=0.3)

Methods	[1]	[2]	[3]	[4]	[5]	[6]	[7]
$\frac{Dw(0,0)}{16qa^4}$	0.0249	0.0261	0.0256	—	0.0257	0.0256486	0.0255065
$\frac{Dw(-a,0)}{8qa^4}$	0.01705	0.0186	0.01793	—	0.01795	0.0179296	0.0177474
$\frac{M_x(0,0)}{4qa^2}$	0.1090	0.1104	0.1115	—	0.1115	0.111512	0.111711
$\frac{M_x(0,-a)}{4qa^2}$	0.1404	0.1542	0.1500	—	0.1499	0.149574	0.150439
$\frac{M_{xy}(-a,-0.6a)}{4qa^2}$	—	0.075	0.028	0.0003	0.0158	0.0422852	0.0634901
$\frac{M_{xy}(-0.6a,-0.6a)}{4qa^2}$	—	0.045	—	0.0418	0.0419	0.0419135	0.041317
$\frac{M_{xy}(-a,-a)}{4qa^2}$	—	—	—	—	—	0.0882664	0.122723*
$\frac{Q_x(-a,0)}{2qa^2}$	—	0.25	0.427	0.004	0.05	0.147769	0.00164927
$\frac{Q_x(-0.8a,0)}{2qa^2}$	—	0.2	—	0.1756	0.1754	0.175246	0.000272188

[1]: Galerkin method;

[2]: Lee and Ballesteros method;

[3]: Ritz method;

[4]: Modified Ritz method;

[5]: ABAQUS® from Wang *et al.* (2002);

[6]: Results by ABAQUS® from author;

[7]: Symplectic method.

In order to further substantiate the accuracy of symplectic approach, a comparison of results from various sources including Galerkin (1953), Lee and

Ballesteros (1960), the Ritz method and modified Ritz method (Wang et al, 2002), finite element solutions (Wang et al, 2002) and the symplectic solutions is presented in Table 3. In the present finite element simulation using ABAQUS, the plate thickness-to-width ratio is 0.01, the Poisson's ratio is $\nu = 0.3$ and a mesh of $100 \times 100 = 10000$ 4-node S4R doubly curved thin shell elements with reduced integration, hourglass control, finite membrane strains is constructed. In general, we observed excellent agreement for deflection and bending moment for results from all sources. The comparison for twisting moment shows mixed consistency with agreement at point $(-0.6a, -0.6a)$ and disagreement at points $(-a, -0.6a)$ and $(-a, -a)$. Apparently, the shear forces prediction from all sources are in absolute disagreement.

Without absolute agreement, one may argue that the accuracy of symplectic solutions is not justified. In this respect, we establish the reliability and accuracy of the symplectic approach via the following facts:

- From Tables 6.2, the bending moment and shear forces at free edges are zero which are, in fact, precisely the boundary conditions (6.46) and (6.62) that are imposed in the symplectic approach. However, it has long been recognized that the Ritz method and various FE methods are unable to satisfy the zero bending moment and zero shear force conditions at the free edges. Research on formulation of superior FEs satisfying natural boundary conditions are still going on.
- From static equilibrium of a corner-supported plate, the twisting moment at the corners is determined as $\left(M_{xy}/4qab\right)\Big|_{x=\pm a; y=\pm b} = 1/8$. The symplectic solution in Table 6.3 is 0.122723 which is very close to the exact equilibrium solution

where the slight difference is due to the number of terms employed in the computation. In this respect, the FE solution (=0.0882664) using ABAQUS is not accurate at all.

From the arguments above, there is strong ground to justify that the symplectic solutions presented in the tables are accurate solutions and could be referred as benchmarks for future reference.

For illustrative purposes, a set of contour and figures for deflection, bending moments, twisting moment and shear forces are presented in Figs. 6.2-6.37 respectively.

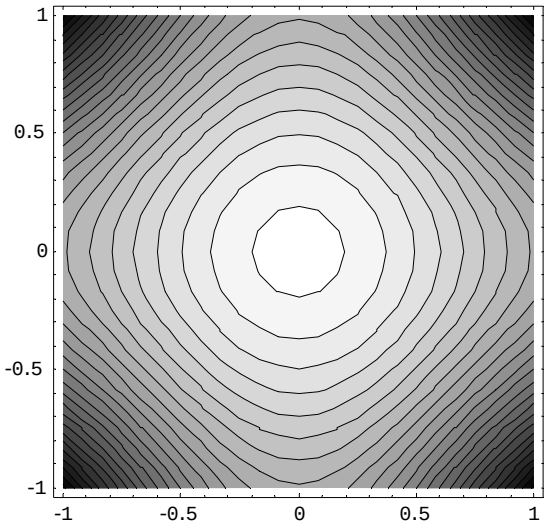

Fig. 6.2 Contour plot for the deflection of plate with a 1:1 aspect ratio

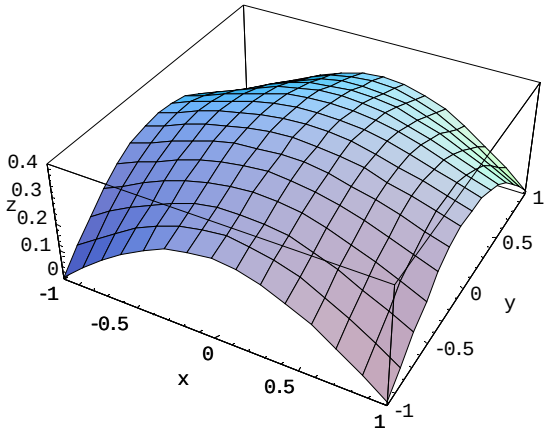

Fig. 6.3 3-D plot for the deflection of plate with a 1:1 aspect ratio

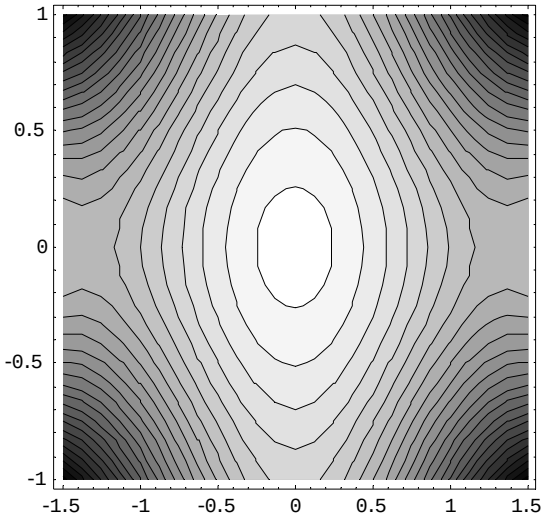

Fig. 6.4 Contour plot for the deflection of plate with a 1.5:1 aspect ratio

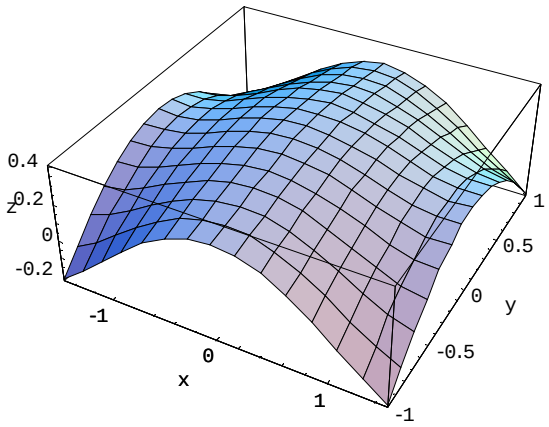

Fig. 6.5 3-D plot for the deflection of plate with a 1.5:1 aspect ratio

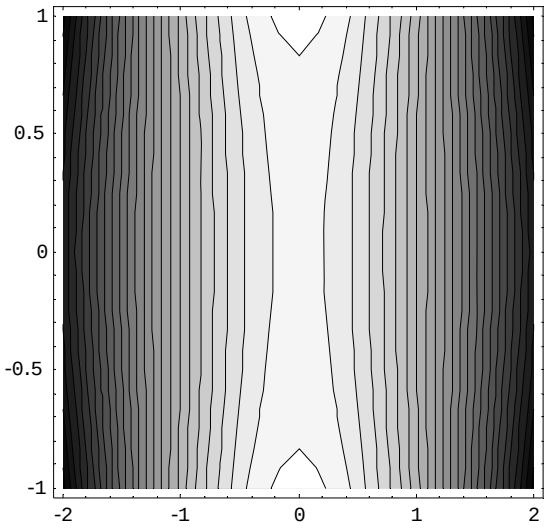

Fig. 6.6 Contour plot for the deflection of plate with a 2:1 aspect ratio

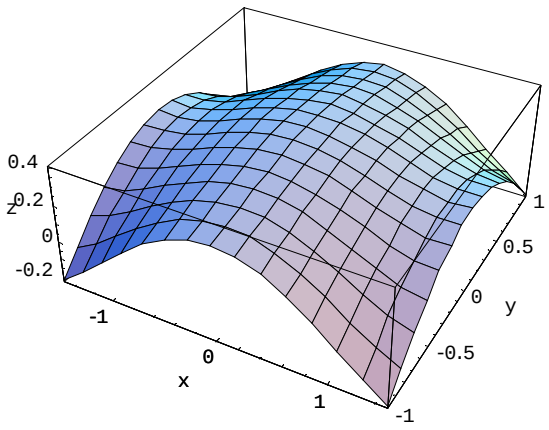

Fig. 6.7 3-D plot for the deflection of plate with a 2:1 aspect ratio

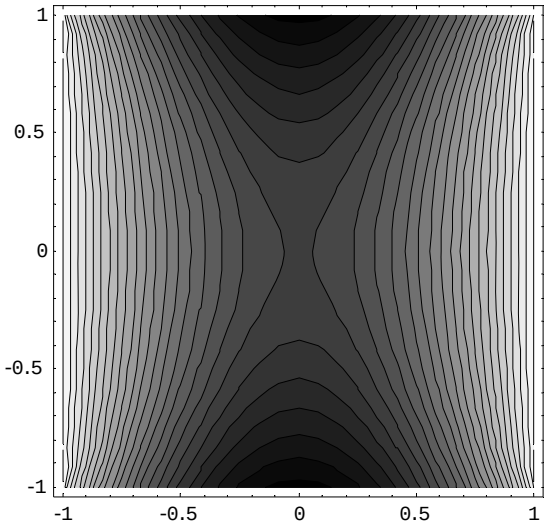

Fig. 6.8 Contour plot for the M_x of plate with a 1:1 aspect ratio

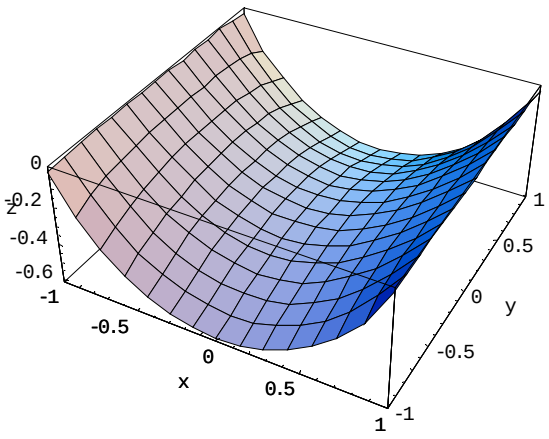

Fig. 6.9 3-D plot for the M_x of plate with with a 1:1 aspect ratio

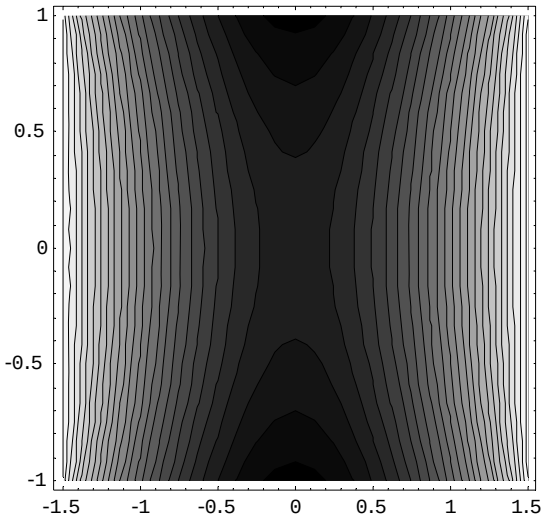

Fig. 6.10 Contour plot for the M_x of plate with a 1.5:1 aspect ratio

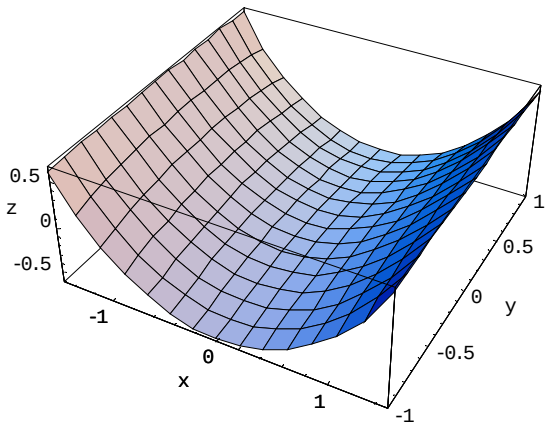

Fig. 6.11 3-D plot for the M_x of plate with a 1.5:1 aspect ratio

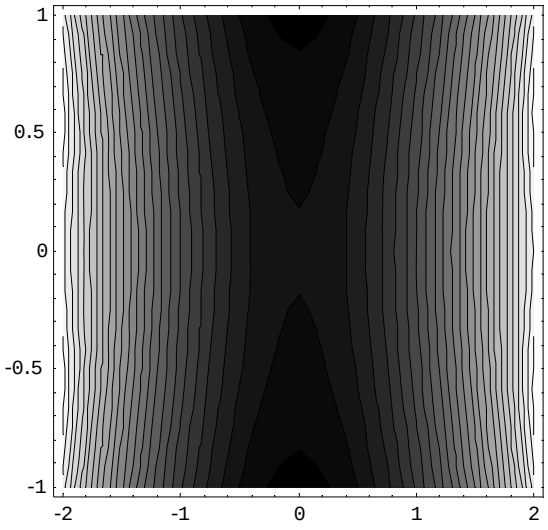

Fig. 6.12 Contour plot for the M_x of plate with a 2:1 aspect ratio

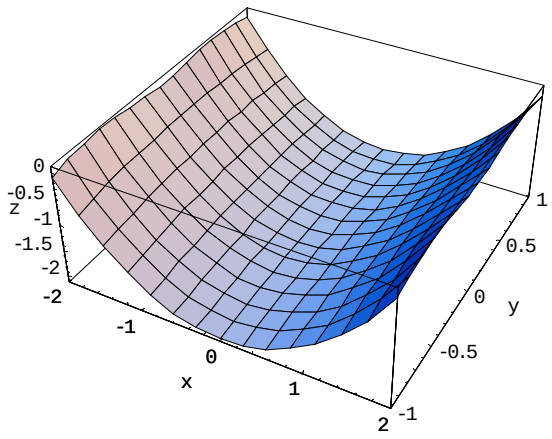

Fig. 6.13 3-D plot for the M_x of plate with a 2:1 aspect ratio

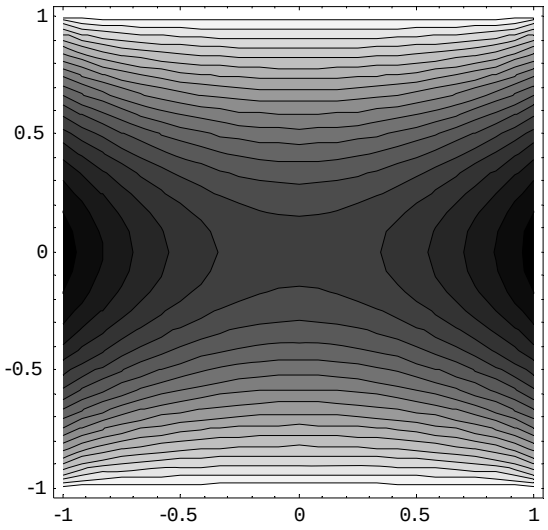

Fig. 6.14 Contour plot for the M_y of plate with a 1:1 aspect ratio

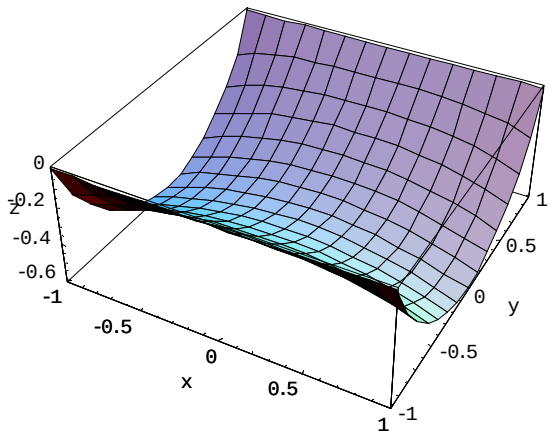

Fig. 6.15 3-D plot for the M_y of plate with a 1:1 aspect ratio

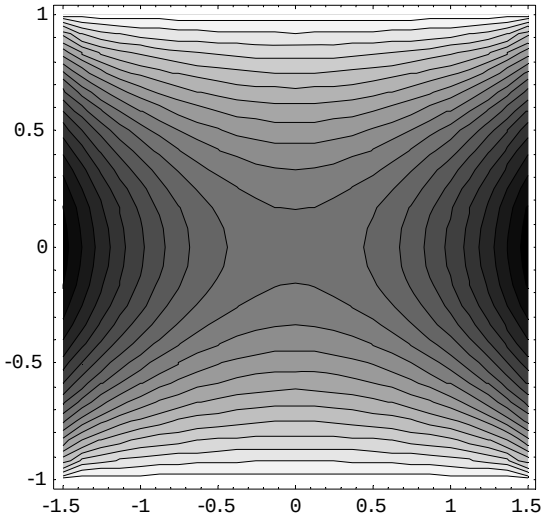

Fig. 6.16 Contour plot for the M_y of plate with a 1.5:1 aspect ratio

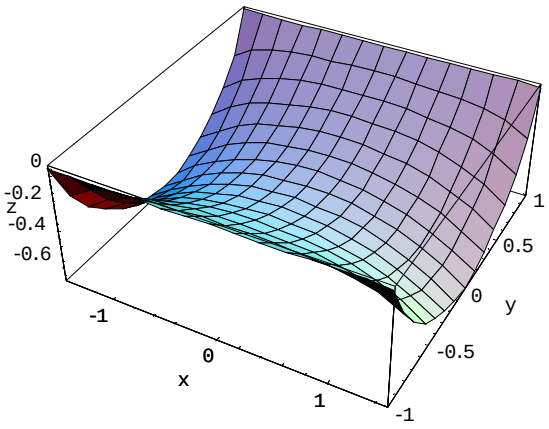

Fig. 6.17 3-D plot for the M_y of plate with a 1.5:1 aspect ratio

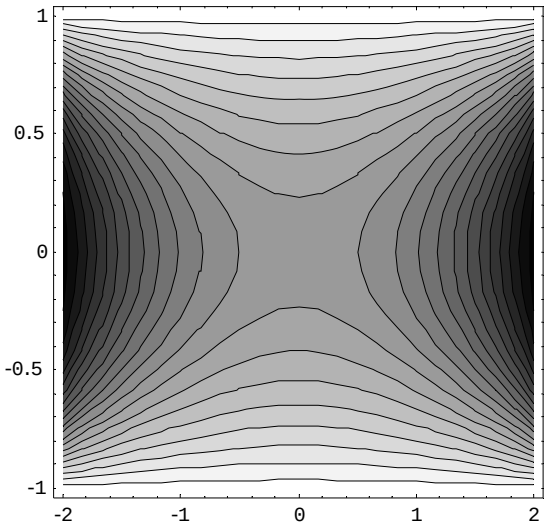

Fig. 6.18 Contour plot for the M_y of plate with a 2:1 aspect ratio

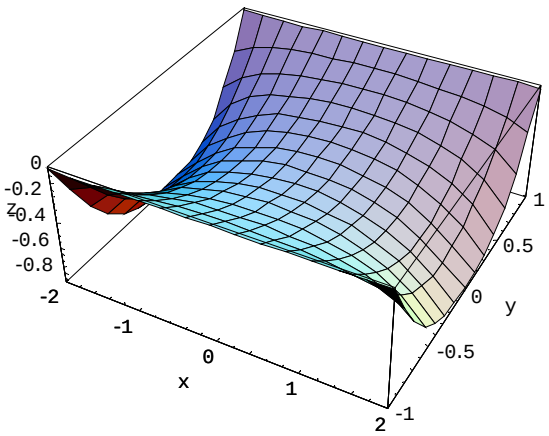

Fig. 6.19 3-D plot for the M_y of plate with a 2:1 aspect ratio

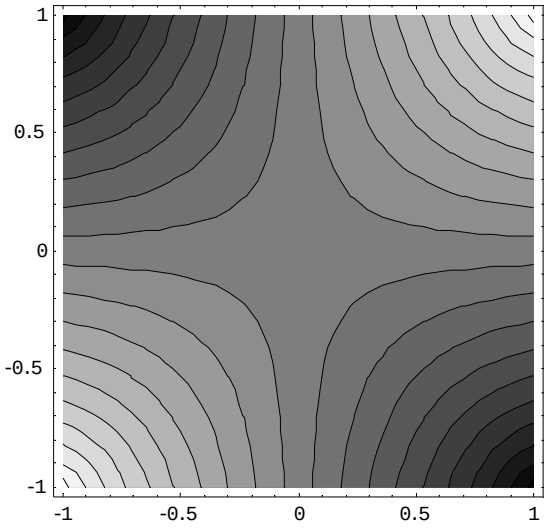

Fig. 6.20 Contour plot for the M_{xy} of plate with a 1:1 aspect ratio

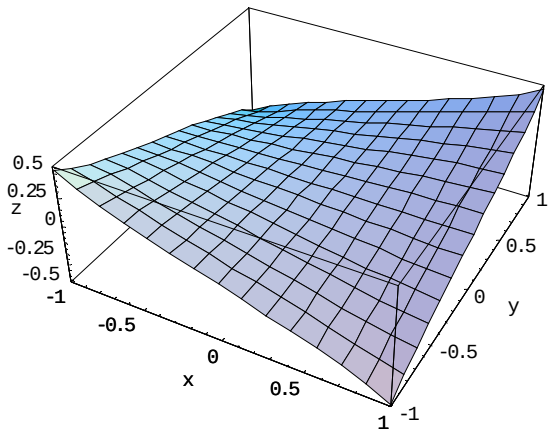

Fig. 6.21 3-D r plot for the M_{xy} of plate with a 1:1 aspect ratio

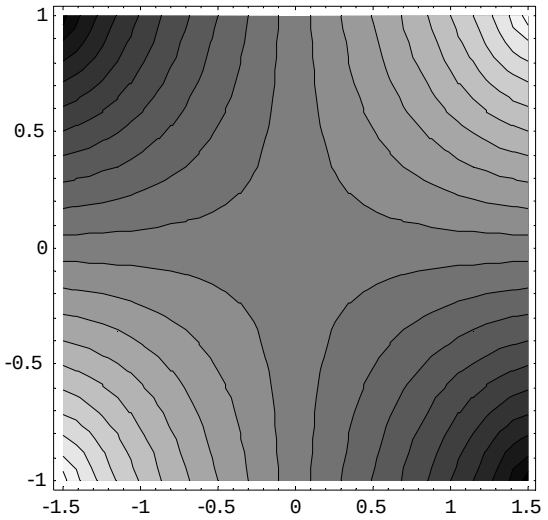

Fig. 6.22 Contour plot for the M_{xy} of plate with a 1.5:1 aspect ratio

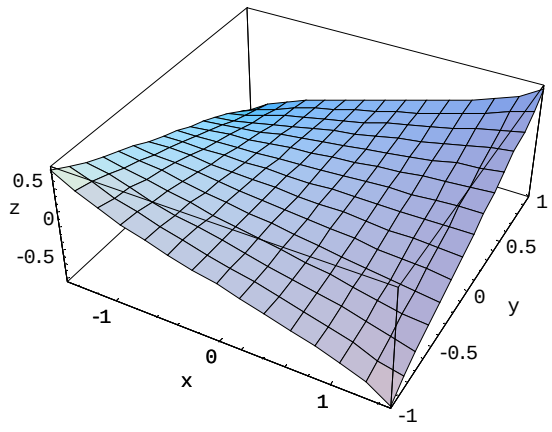

Fig. 6.23 3-D plot for the M_{xy} of plate with a 1.5:1 aspect ratio

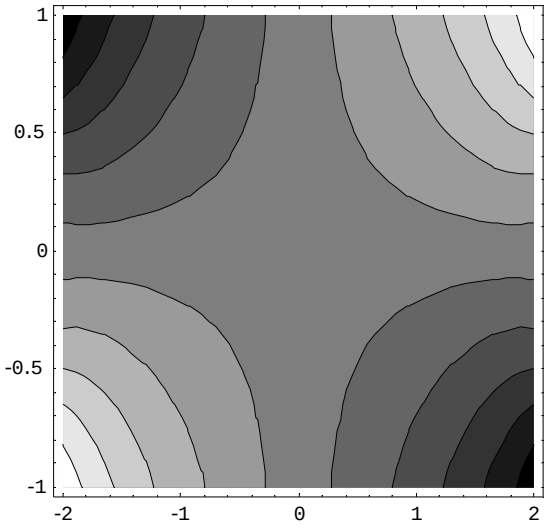

Fig. 6.24 Contour plot for the M_{xy} of plate with a 2:1 aspect ratio

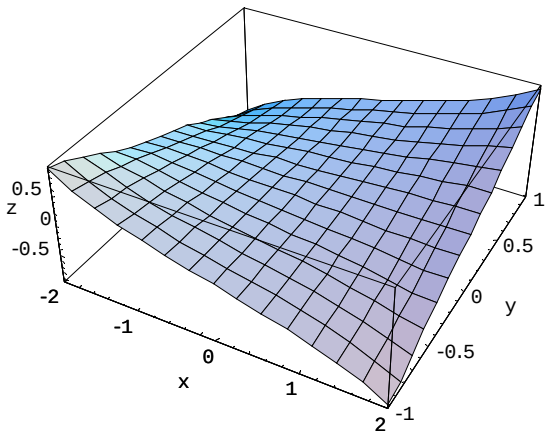

Fig. 6.25 3-D plot for the M_{xy} of plate with a 2:1 aspect ratio

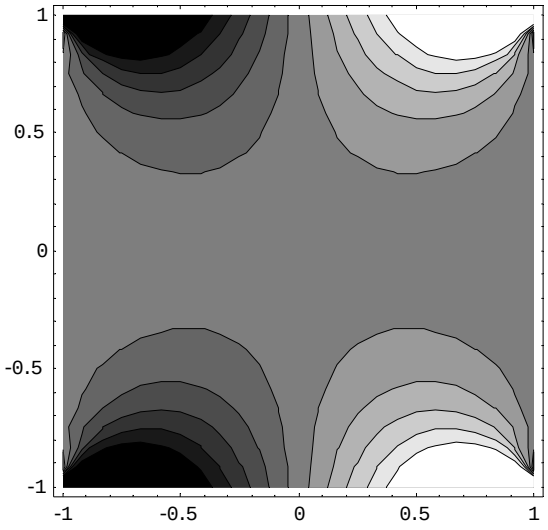

Fig. 6.26 Contour plot for the Q_x of plate with a 1:1 aspect ratio

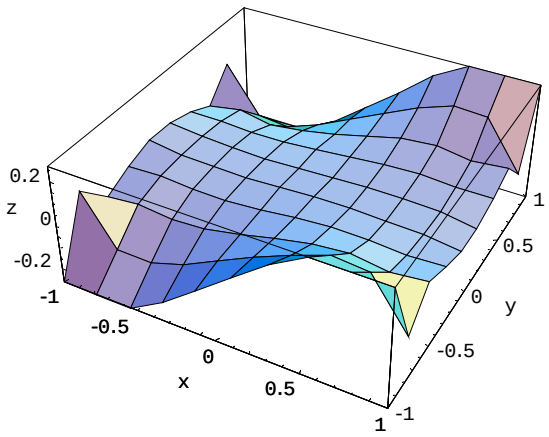

Fig. 6.27 3-D plot for the Q_x of plate with a 1:1 aspect ratio

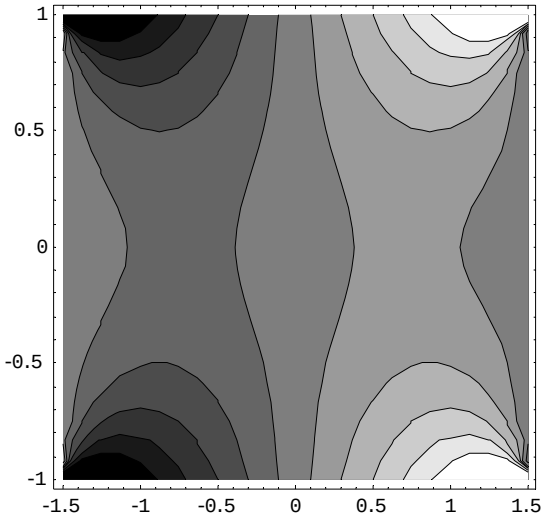

Fig. 6.28 Contour plot for the Q_x of plate with a 1.5:1 aspect ratio

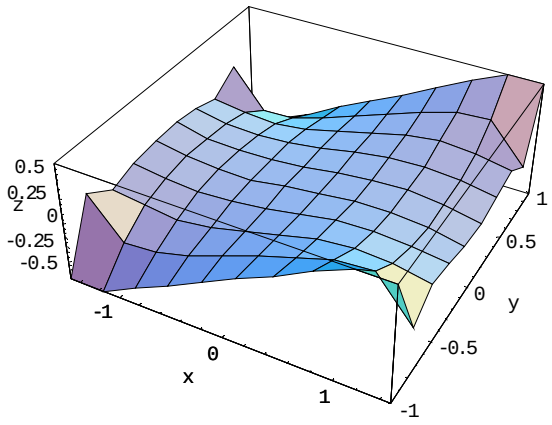

Fig. 6.29 3-D plot for the Q_x of plate with a 1.5:1 aspect ratio

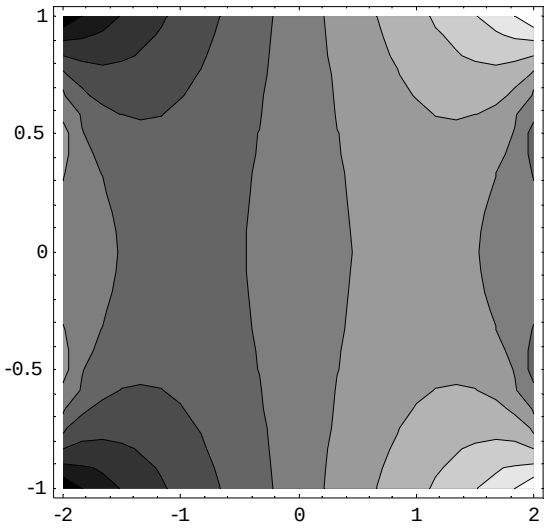

Fig. 6.30 Contour plot for the Q_x of plate with a 2:1 aspect ratio

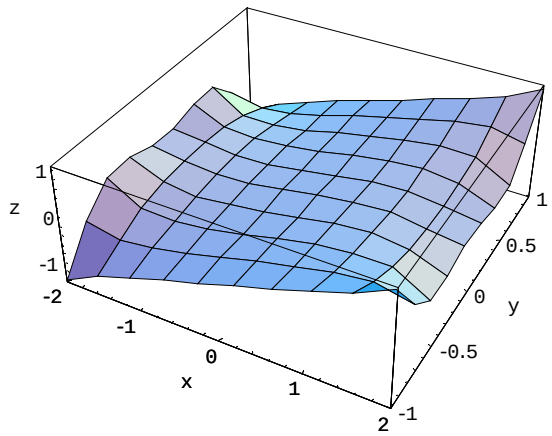

Fig. 6.31 3-D plot for the Q_x of plate with a 2:1 aspect ratio

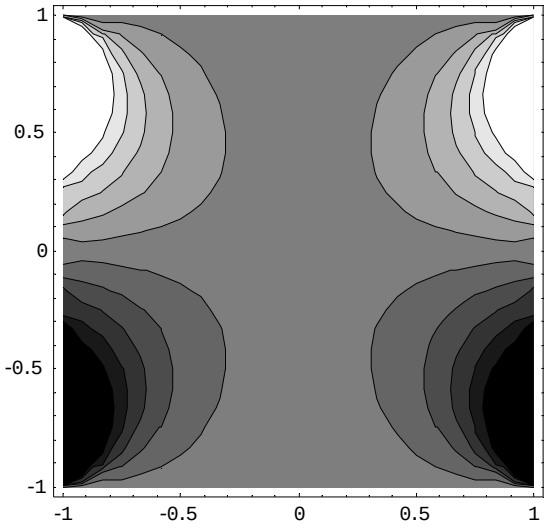

Fig. 6.32 Contour plot for the Q_y of plate with a 1:1 aspect ratio

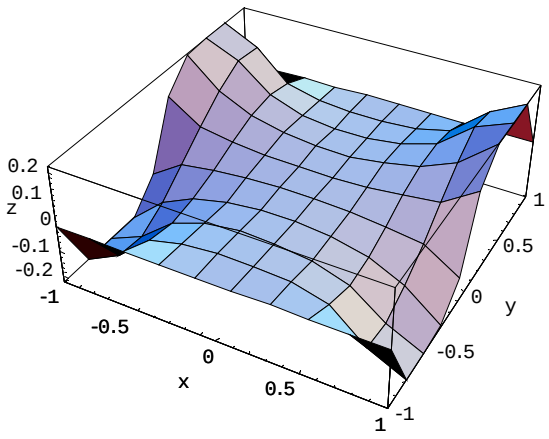

Fig. 6.33 3-D plot for the Q_y of plate with a 1:1 aspect ratio

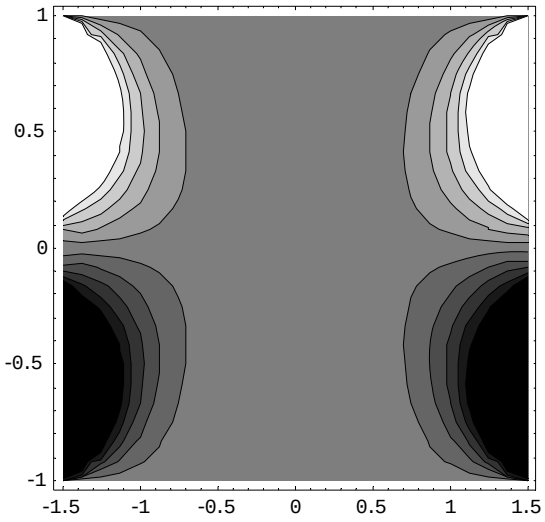

Fig. 6.34 Contour plot for the Q_y of plate with a 1.5:1 aspect ratio

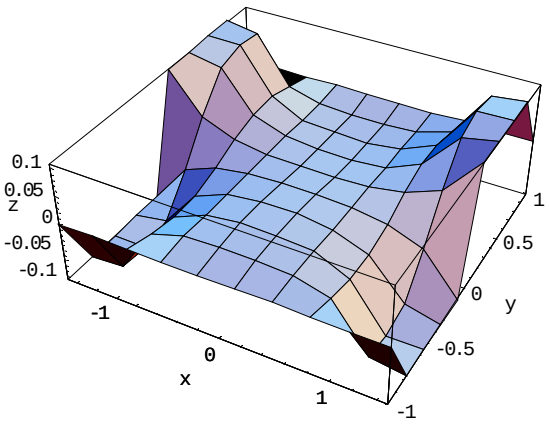

Fig. 6.35 3-D plot for the Q_y of plate with a 1.5:1 aspect ratio

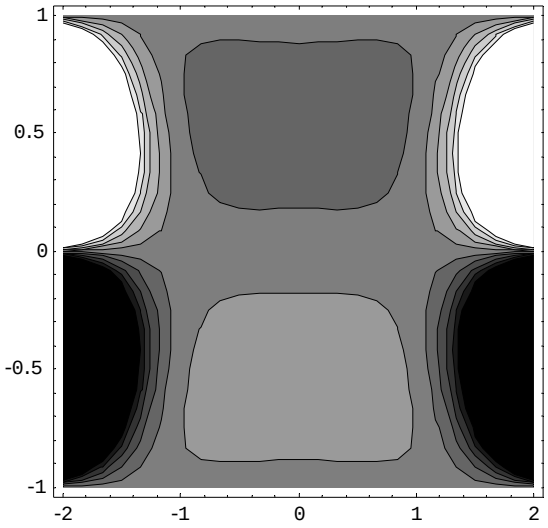

Fig. 6.36 Contour plot for the Q_y of plate with a 2:1 aspect ratio

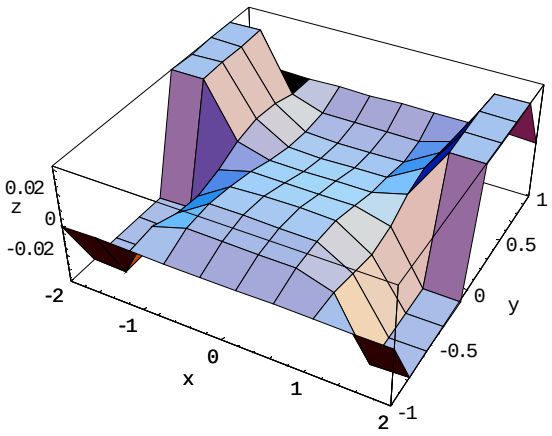

Fig. 6.37 3-D plot for the Q_y of plate with a 2:1 aspect ratio

6.5 Closure

Based on a new symplectic elasticity approach, this chapter presents benchmark analytical bending solutions for a corner-supported thin rectangular plate subject to a uniform distributed load. The approach trespasses an area of practical engineering interest beyond the ability of the classical methods such as Timoshenko's method, Navier method, Levy method and the approximate polynomial method of Lee and Ballesteros (1960). The variational principle is formulated in the symplectic geometry space and the zero bending moment and shear force boundary conditions at the free edges are satisfied. This problem has intrigued researchers for more than half a century in both analysis and numerical analysis including the finite element method because the satisfaction of natural boundary

conditions at the free edges has so far been unsuccessful. Furthermore, this symplectic approach also ensures the satisfaction of twisting moment condition at the support corners, which is again not satisfactory in other analytical and computational approaches. This part of the research has been published in the international journal (Lim *et al*., 2007 b).

Chapter 7 Conclusions and Recommendations

7.1 Conclusions

This thesis has presented a new breakthrough in applied mechanics in which a bottleneck previously prohibiting availability of exact solutions for bending of plates with arbitrary boundary conditions has been trespassed. It is based on a symplectic elasticity approach which has been used previously in quantum mechanics as well as relativity and other theoretical physics disciplines. The strain energy function in accordance with the Pro-Hellinger-Reissner variational principle is derived in a geometrical symplectic space. Using the essential Hamiltonian principle with Legendre's transformation, an eigenvalue is obtained and thus solved. It should be emphasized here that bending analysis here requires solving of an eigenvalue equation which is only required in vibration and buckling analyses in classical mechanics. The symplectic approach establishes the relationship between eigenvalue and bending. Unlike the traditional semi-inverse methods, no trial functions are required in the derivation process. The derivation procedure is identical to all cases. So it is applicable to plates without opposite sides simply supported and the analytical solutions for these cases are firstly founded. Analytical exact solutions for some cases with two opposite sides simply supported have been

presented and excellent agreement with established solutions has been illustrated in all cases. For other boundary conditions, variational principle is applied for the x-direction boundary treatment and the solution is exact in the sense that, although an infinite set of simultaneous equations must be solved for an exact answer, results can be obtained to any desired degree of accuracy by successive truncations of the infinite set.

Although this approach has solved the plate bending problems successfully, the limitation for application of the method exists. For instance, this approach is only applicable to the linear problems. Separation of variables in the Hamiltonian system is required before solve the nonlinear problems. In addition, energy dissertation is not allowed in the Hamiltonian system. A damping factor should be added in the Hamiltonian system to simulate this condition.

7.2 Recommendations

The following are some suggestions for further research of the present method:

- For plates with other types of loading conditions, such as non-uniform load and point load, the derivation procedure is similar. Only the particular solution is different to present the corresponding loading cases.
- For plates with other support conditions, only the expressions for the boundary conditions are different from the cases discussed in the thesis. So the exact solutions for other types of support conditions can be easily solved.
- The problems of other shapes plate which have not been addressed in this thesis can also be solved by the present approach by only little modifications of the current program. The circular sector plate has been derived in the book of Yao, *et.al*. (2007) by imposing the polar coordinates. Other shapes of plates can also be derived in the similar way.
- By introducing the shear deformation factor, it can be used to solve the thick plate bending problems.
- With a good treatment of the anisotropic property of composite plate, the bending results of this type of plates can be solved by this symplectic method.

The symplectic method is not limited to bending problems; further exact solutions for vibration, buckling and wave propagation in plates can also be obtained based on a similar symplectic approach. The extension will be explored in due course.

References

Argyris, J. N., Kelsey, S., and Kamel, H. (1964). Matrix methods for structural analysis, In: Matrix Methods of Structural analysis (ed. Fraeijs de Veubeke), Pergamon Press, Oxford.

Banerjee, P. K. and Butterfield, R. (1981). Boundary Element Methods in Engineering Science, McGraw-Hill, New York.

Barton, M. V. (1948). Finite Difference Equations for the Analysis of Thin Rectangular Plates with Combinations of Fixed and Free edges, Defense Research lab

Bergsträsser, M. (1928). Forschungsarb., 302, Berlin.

Boobnoff, I. G. (1902). On the stresses in a ship's bottom plating due to water pressure, Trans. Inst. Naval. Archit., 44: 15–52.

Boobnoff, I. G. (1914). Theory of Structure of Ships, St. Petersburg., 2:545.

Brebbia, C. A., Telles, J. C. F. and Wrobel, L. C. (1984). Boundary Element Techniques, Theory and Application in Engineering, Springer-Verlag, Berlin.

Chang F. V. (1979). Bending of Rectangular Cantilever Plate (with a concentrated load at the free edge), Journal of Tsing-hua University, 19 (2).

Chang F. V. (1980). Bending of Uniformly Cantilever Rectangular Plates, Journal of Applied Mathematics and Mechanics, 1 (3).

Courant, R. (1943). Variational Methods for the solution of problems of equilibrium and vibration, Bulletin of the American Mathematical Society, 49: 1-23.

De Gosson, M. A. (2001). The Principles of Newtonian and Quantum Mechanics, World Scientific Publishing.

Estanave, E. (1900). Thèses, Paris.

Evans, T. H. (1939). Tables of moments and deflections for a rectangular plate fixed on all edges and carrying a uniformly distributed load, Journal of Applied Mechanics, 61:7–10.

Feng, K. (1985). On difference scheme and symplectic geometry, In K. Feng, ed. Proc. Beijing Symp Differential Geometry and Diifferential Equations, Beijing, Science Press: 42-58.

Feng, K. (1986a). Difference schemes for Hamiltonian formalism and symplectic geometry, J. Computational Mathematics, 4(3): 279-289.

Feng, K. (1986b). Symplectic geometry and numerical methods in fluid dynamics, Proc. 10th International Conference on Numerical Methods on Fluid Dynamics, Beijing, 1986; Lecture Notes in Physics, 264: 1-7, Berlin, Springer Verlag.

Feng, K., Qin, M. Z. (1991). Hamilton Algorithm for Hamiltonian Dynamical Systems, Progress in Natural Science, 1(2): 105–116.

Finlayson, B. A. (1972). The Method of Weighted Residuals and Variational Principles, Academic Press, New York.

Funk, P. and Berger, E. (1950). Federhofer-Girkmann-Fest-schrift, Vienna, 199.

Galerkin, B. G. (1915 a). Series-Solutions of some cases of equilibrium of elastic beams and plates, Vestn Inshenernov, 1: 987-903 (in Russian).

Galerkin, B. G. (1915 b). Rectangular plates supported by edges, Izv. S-Peter politekh. Inst. 24 (1): 219–282, also In: Collected Papers, (1953). Moscow: Acad. Sci. SSSR, 2: 3–42, (in Russian).

Galerkin, B. G. (1953). Collected papers, Moscow, 2:15.

Gallagher, R. H. (1975). Finite Element Analysis, Prentice-Hill, Englewood Cliffs, New Jersey.

Girkmann, K. and Tungl, E. (1953). Osterr. Bauzeitschrift, 8:47.

Grinberg, G. A. (1951). On the solution of the plane problem of the theory of elasticity and of the problem of bending of a thin plate with clamped contour, Dokl. Akad. Nauk SSSR 76:661–664, (in Russian). (English abstract in: Mathl Rev. (1952) 13:184.)

Happel, H. (1914). Ű ber das Gleichgewicht rechteckiger Platten, Nachr. K. Ges.Wiss. Göttingen. Math.Phys. Kl.: 37–62.

Hartmann, F. (1991). Static analysis of plates, In: boundary Element Analysis of Plates and Shells (ed. D.W. Beskos), Springer-Verlag, berlin:1-35.

Hencky, H. (1913). Der Spannungszustand in rechteckigen Platten (Dissertation), Oldenbourg, München.

Holl, D. L. (1937). Cantilever Plate with Concentrated Edge Load, Journal of Applied Mechanics, 4.

Huang, M. K., and Conway, H. D. (1952). Bending of a Uniformly Loaded Rectangular Plate with two Adjacent Edges Clamped the others either simply supported or Free, Journal of Applied Mechanics: 451-460.

Hughes, T. J. R. (1987). Finite Element Analysis, Prentice-Hill, Englewood Cliffs, New Jersey.

Hutchinson, J. R. (1991). Analysis of plates and shells by boundary collocations. In: Boundary element Analysis of Plates and Shells (ed. D. E.Beskos), Springer-Verlag, Berlin:341-368.

Inglis, C. E. (1925). Stresses in rectangular plates clamped at their edges and loaded with a uniformly distributed pressure, Trans. Instn nav. Archit. 67: 147–165.

Jaramillo, T. J. (1950). Deflection and Moments to a Concentrated Load and Cantilever Plate of Infinite Length, Journal of Applied Mechanics, 17: 67–72.

Johnson, D. (1987). Plate bending by a boundary point method, Computers & Structures, 26(4):673-680.

Kauderer, M. (1994). Symplectic Matrices, First Order Systems and Special Relativity, World Scientific Publishing.

Kitipornchai, S., Xiang, Y., Liew, K. M. (1994). Vibration analysis of corner supported Mindlin plates of arbitrary shape using the Lagrange multiplier method, J Sound Vibrations, 173(4):457–70.

Koialovich, B. M. (1902). On one partial differential equation of the fourth order (Doctor Dissertation).St. Petersburg University Press, St. Petersburg, (in Russian). (German abstract (1902) in Jb Fortschr. Math., 33: 367–368.)

Kolodziej, J. A. (1987). Review of application of boundary collocation method in mechanics of continuum media, Solid Mechanics Archives, 12:187-231.

Koszul, J., Zou, Y. (1986). Theory of Symplectic Geometry，Beijing: Science Press. (in Chinese)

Krauth,W., Staudacher, M. (2000). Yang-Mills integrals for orthogonal, symplectic and exceptional groups, Nuclear Physics B, 584(1-2): 641-655.

Krishnasamy, G., Schmerr, L. W., Rudolphi, T. J., and Rizzo, F. L. (1990). Hypersingular boundary integral equations: some applications in acoustic and elastic wave scattering, Journal of Applied Mechanics, 57: 404-414.

Laws, B. C. (1937). Phil. Mag., 24: 1072.

Lax, P., Feng, K. (1993). SIAM News, 26(11).

Lee, S. L., Ballesteros, P. A. (1960). Uniformly loaded rectangular plate supported at the corners, Int J Mech Sci, 2:206–11.

Leissa, A. W., and Niedenfuhr, F. W. (1962 a), A study of the cantilevered Square Plate Subjected to a uniform loading, Journal of the Aero/ Space Sciences, 29 (2).

Leissa, A. W., and Niedenfuhr, F. W. (1962 b). Bending of a square plate with two adjacent Edges Free and the others Clamped or simply supported, AIAA Journal, 1 (1).

Leitz, H. (1917). Berechnung der eingespannten rechteckigen Platte, Z.Math. Phys. 64: 262–272.

Lévy, M. (1899). Memoires sur la theories des plaques planes, J Math Pures Appl, 3:219.

Lively, R. K., and Birchall, P. C. (1956). Analysis of a loaded Cantilever plate by finite difference methods, Royal Aircraft establishment Tech. Note M.S.26, Farnsborough.

Lim, C. W., Cui, S., and Yao, W.(2007 a) On new symplectic elasticity approach for exact bending solutions of rectangular thin plates with two opposite sides simply supported, International Journal of Solids and Structures, 44(16): 5396-5411.

Lim, C. W., Yao, W., and Cui, S. (2007 b) Benchmark symplectic solutions for bending of corner-supported rectangular thin plates, IES Journal A: Civil and Structural Engineering, (accepted)

MacNeal, R. H. (1951). The Solution of Elastic Plate Problems by Electrical Analogies, Journal of Applied Mechanics: 59-67.

March, H. W. (1925). The deflection of a rectangular plate fixed at the edges, Trans. Am. Math. Soc. 27:307–317.

Marcus, H. (1932). Dic Theorie elastischer Gewebe und ihre Anwendung auf die berechnung biegsamer platten, Springer,Berlin:173

Meleshko, V. V. (1997). Bending of an Elastic Rectangular Clamped Plate: Exact Versus 'Engineering' Solutions, Journal of Elasticity 48: 1–50.

Nádai, A. (1922). Z. angew. Math. Mech. 2:1.

Nádai, A. (1925). Elastische Platten, Berlin.

Nash,W. A. (1952). Several Approximate Analysis of the Bending of a Rectangular Cantilever Plate by Uniform Normal Pressure, Journal of Applied Mechanics: 33-36.

Navier, C. L. M. N. (1823). Bulletin des Science de la Societe Philomarhique de Paris.

Newmark, N. M. and Lepper, H. A. (1839). Univ. Illinois Bull., 36(84).

Pan, H. H. (1961). Note on the uniformly loaded rectangular plate supported at the corners, Int J Mech Sci, 3:313–5.

Papkovitch, P. F. (1941). Theory of structural design of ships, Leningrad (in Russian).

Plass, H .J., Games Jr. J. H. and Newson C. D. (1962). Application of Reissner's Variational Principle to Cantilever plate Deflection and Vibration Problems, Journal of Applied Mechanics, 29 (1)

Qin, M. Z. (1990). Symplectic geometry and computing Hamiltonian mechanics, Mechanics and Practice, 12(6): 1–20. (in Chinese)

Ritz, W. (1909). Theorie der transversalschwingungen einer quadratischen plattemit freien randern, Ann Phys, 28: 737-786.

Salvadori, M. G. and Baron, M. L. (1967). Numerical Methods in Engineering, Prentice-Hall, Englewood Cliffs, New Jersey.

Sezawa, K. (1923). The stress on rectangular plates, Engineering 116: 188–191.

Shanmugam, N. E., Huang, R., Yu, C. H. and Lee, S. L. (1988). Uniformly loaded rhombic orthotropic plates supported at corners, Comput. Struct., 30(5):1037–45.

Shanmugam, N. E., Huang, R, Yu, C. H. and Lee, S. L. (1989). Corner supported isosceles triangular plates, Comput. Struct., 32(5):963–72.

Shu T. K. and Shih T. T. (1957). Variational Principle of Elastic Thin Plates and its application, Journal of the Peking Aeronautics Institute.

Szilard, R. (1974). Theory and analysis of plates, Classical and Numerical Methods, Prentice-Hall, Englewood Cliffs, New Jersey.

Timoshenko, S.P. and Woinowsky-Krieger, S. (1959). Theory of plates and shells, 2nd ed. New York: McGraw-Hill: 218.

Tottenham, H. (1979). The boundary element method for plates and shells, In: Developments in Boundary Element Methods-1 (des PK Banerjee and R Butterfield), Applied Science Publishers, London: 173-207.

Turner, M. J., Clough, R. W., Martin, H. C., and Topp, L. J. (1956) Stiffness and deflection analysis of complex structures, J Aeronaut Sci, 23(9):805-823.

Ventsel, E. S. (1997). An indirect boundary element method for plate bending analysis, Int J Numer Meth Eng, 9: 1597-1611.

Wang, C. M., Wang, Y. C. and Reddy, J.N. (2002). Problems and remedy for the Ritz method in determining stress resultants of corner supported rectangular plates, Comput. Struct., 80: 245-254.

Wang, P. Ch. (1969). Numerical and Matrix Methods in Structural Mechanics, John Wiley and Sons, New York.

Washizu, K. (1968). Variational Methods in Elasticity and Plasticity, Pergamon Press, oxford.

Weinstein and Rock, D. H. (1944). On the bending of a clamped plate, Quart. Appl.

Weyl, H. (1939). The Classical Groups, Their Invariants and Representations, Princeton University Press.

Yao, W., Xu, C. (2001). A restudy of the paradox on an Elastic wedge based on the Hamiltonian system, ASME Journal of Applied Mechanics, 68(4): 678-681.

Yao, W., Yang, H. (2001). Hamiltonian system based Saint Venant solutions for multi-layered composite plane anisotropic plates, International Journal of Solids and structures, 38(32): 5807-5817.

Yao, W., Zhong, W., Lim, C. W. (2007). Symplectic Elasticity, World Scientific Publishing, in press.

Yeh, Gordon, C. K. (1954). Bending of a rectangular Plate on an Elastic Foundation with Two Adjacent edges Fixed and the Others Free, Proceedings of the second U. S. national Congress of applied mechanics: 375-380.

Young, D. (1940). Analysis of clamped rectangular plates, Journal of Applied Mechanics, 62:139-142.

Zhong, W. (1991). Plane elasticity problem in strip domain and Hamiltonian system, Journal of Dalian University of Technology, 31(4): 373-384. (in Chinese)

Zhong, W. (1992). On the reciprocal theorem and adjoint symplectic orthogonal relation, Acta Mechanica Sinica, 24(4): 432-437. (in Chinese)

Zhong, W. and Yao, W. (1997). New Solution System for Plate Bending — Force Method Hamiltonian System and Its Application, Modern Maths and Mechanics (MMM-VII), Shanghai: Shanghai University Press, 121-129.

Zienkiewicz, O. (1977). The Finite Element Method, McGraw-Hill, London.

List of Publications

Journal Papers

[1] Lim, C. W., Yao, W., and **Cui, S.** (2007). Benchmark symplectic solutions for bending of corner-supported rectangular thin plates, IES Journal A: Civil and Structural Engineering, (accepted)

[2] Lim, C. W., **Cui, S.,** and Yao, W. (2007). On new symplectic elasticity approach for exact bending solutions of rectangular thin plates with two opposite sides simply supported, International Journal of Solids and Structures, 44(16): 5396-5411.

Conference Papers

[1] Lim, C. W., **Cui, S.** (2007). Symplectic elasticity approach for free vibration of rectangular thin plates**,** the 12th Asia-Pacific Vibration Conference, 6-9 August, Hokkaido University, Sapporo, Japan.

[2] Lim, C.W., **Cui, S.** and Leung, A.Y.T. (2006). Symplectic elasticity approach for thin plate bending, The Second International Conference on Dynamics, Vibration and Control (ICDVC-2006), Paper W19, edited by Q. Lu, 23-26 August, Beijing, China.